Effects of nanomolar copper on water plants - comparison of biochemical and biophysical mechanisms of deficiency and sublethal toxicity under environmentally relevant conditions

Dissertation submitted for the degree of Doctor of Natural Sciences

Presented by

George Thomas

at the

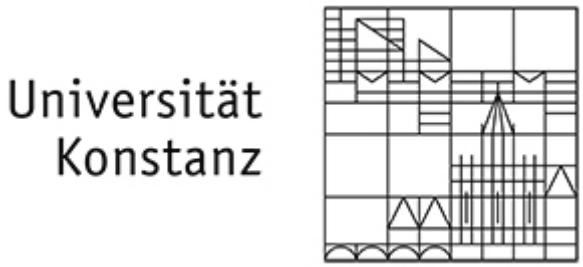

Department of Biology

Faculty of Sciences

Date of the oral examination: 21.02.2014
First supervisor: Prof. Dr. Hendrik Küpper
Second supervisor: Prof. Dr. Eva Freisinger

Table of contents

Summary

The thesis is a comprehensive study of the effects of nanomolar Cu (from deficiency, through optimal to toxicity) on *Ceratophyllum demersum* L. under environmentally relevant conditions. The thesis also deals with an investigation of the contribution of Cd and Ni toxicity to the almost complete absence of macrophytes in lake Ammelshain and in soft and hard water in general.

Effects of nanomolar heavy metal stress on Ceratophyllum demersum L.

The plant responses to Cu stress during six weeks of treatment were studied under high light (HL) and low light (LL) conditions. Growth was optimal in the range of 10-20 nM Cu. In HL, damage to the PSII RC was the first target of Cu toxicity, followed by damage to the regulation of heat dissipation (NPQ). Then electron transport through PSII was inhibited, followed by decrease in chlorophyll concentration. In LL, damage to the light harvesting complex (LHC) was associated with replacement of Mg by Cu in the chlorophyll of the LHCII. This caused a denaturation of the LHCII trimers to monomers, which likely further decreased the NPQ. Cu was mainly stored in the vein at all concentrations. But at toxic levels, Cu was additionally sequestered to the epidermis and mesophyll until export from vein was inhibited at highest Cu. This was accompanied with Zn uptake inhibition. Only the highest Cu concentrations led to elevated phytochelatin levels. We also found that the induction of phytochelatins is not proportional to metal concentration, but has a specific threshold for each phytochelatin species.

During Cu deficiency in HL conditions, a complete stop of growth was observed at “0” nM Cu after six weeks. Electron flow through PSII decreased from the second week, followed by pigment decrease and an increase in NPQ. The lack of high affinity Cu transporters resulted in a release of Cu from the plants below 10 nM Cu supply. A re-distribution of Zn was observed in the plant tissues at “0” nM Cu. In LL conditions, the deficiency stress was not as strong as for HL. The lack of electron transport through the PSII at deficient Cu was most likely caused by limited Cu loading of plastocyanin. Further, a reduction in the pigments added to the decrease in photosynthesis, resulting in reduced starch formation and oxygen production.

Effects of Cd and Ni toxicity to Ceratophyllum demersum L.

An investigation was performed on an oligotrophic lake to study whether heavy metal concentrations were responsible for the nearly complete lack of submerged macrophytes in the lake. Individually nontoxic cadmium (3 nM) and slightly toxic nickel (300 nM) concentrations became highly toxic when applied together in soft water. This kind of synergistic heavy metal toxicity may have a greater effect on the ecosystems than estimated so far. Phosphate limitation, which is a well-known problem in freshwater habitats, further enhanced the toxicity in soft water. Since the high water hardness in the lake limited the toxicity of these metal concentrations, the macrophytic growth inhibition in this lake might have additional reasons.

Zusammenfassung

Diese Doktorarbeit befasst sich ausführlich mit der Untersuchung von Einflüssen nanomolaren Kupfers (vom Mangel über Optimalbedingungen bis hin zur Toxizität) bei der aquatischen Modellpflanze *Ceratophyllum demersum* L. unter umweltrelevanten Bedingungen. Des Weiteren beschäftigt sich diese Forschungsarbeit mit dem Einfluss von Cd und Ni-Toxizität auf die nahezu vollständige Abwesenheit von Makrophyten im Ammelsheimer See, sowie in hartem und weichem Wasser allgemein.

Einflussvon nanomolarem Schwermetall Stress auf Ceratophyllumdemersum L.

Die Reaktion von Pflanzen auf Cu-Stress wurde anhand von sechswöchigen Versuchen unter Starklicht- und Schwachlichtbedingungen untersucht. Dabei zeigte sich ein optimales Wachstum in Anwesenheit von 10-20 nM Cu. Unter Starklichtbedingungen wurde anfangs das PSII RC durch die Cu-Toxizität beschädigt, was sich als Nächstes in einer beeinträchtigten Regulation der Wärmeabgabe (Nicht-Photochemischen Fluoreszenzlöschung, NPQ) zeigte. Anschließend erfolgte eine Inhibition des Elektronentransportes durch das PSII gefolgt von einer Abnahme der Chlorophyllkonzentration. Unter Schwachlichtbedingungen wurde eine Schädigung des Lichtsammelkomplexes (LHC) festgestellt, welche mit einem Austausch von Mg durch Cu in den Chlorophyllen des LHCII einherging. Dies führte wiederum zur Denaturierung von LHCII-Trimeren zu Monomeren, welche schließlich eine verminderte Wärmeabfuhr (NPQ) zur Folge hatte. Cu jeglicher Konzentrationen wurde hauptsächlich im Leitbündel der Pflanzen gespeichert. Unter toxischen Bedingungen wurde Cu jedoch zusätzlich an die Epidermis und das Mesophyll transportiert, bis der Export von Cu aus dem Leitbündel bei der höchsten Cu-Konzentration gehemmt wurde. Dieser Ablauf trat zusammen mit einer Inhibition der Zn-Aufnahme auf. Nur die höchsten Cu-Konzentrationen zogen eine erhöhte Phytochelatinmenge nach sich. Der Anstieg der Phytochelatinkonzentration erfolgte dabei nicht proportional zur vorliegenden Melallkonzentration. Vielmehr gab es einen spezifischen Schwellenwert für jede Phytochelatinart.

Während des Kupfermangels unter Starklichtbedingungen konnte ein vollständiger Wachstumsstopp nach sechs Wochen bei 0 nM Cu festgestellt werden. Ab der zweiten Woche nahm der Elektronenfluss durch das PSII ab, gefolgt von einer Pigmentabnahme und einem Anstieg in NPQ. Das Fehlen hoch affiner Cu-Transporter resultierte in der Freisetzung von

Cu derjenigen Pflanzen, die unterhalb einer 10 nM Cu-Versorgung lagen. Bei Kupfermangel (0 nM Cu) wurde eine Neuverteilung von Zn im Pflanzengewebe beobachtet. Unter Schwachlichtbedingungen war der Stress aufgrund des Cu-Mangels nicht so stark ausgeprägt wie bei Starklicht. Der geringe Elektronentransport durch das PSII unter Cu-Abwesenheit resultierte vermutlich aus dem Fehlen des kupferhaltigen Elektronenüberträgers Plastocyanin. Des Weiteren führte eine Abnahme im Pigmentgehalt zusätzlich zur Photosyntheseabnahme zu verminderter Stärkebildung und Sauerstoffproduktion.

Einfluss von Cd- und Ni- Toxizität auf Ceratophyllumdemersum L.

Erhöhte Konzentration verschiedener Schwermetalle waren vermutlich für das fast vollständige Fehlen von aquatischen Makrophyten in einem oligotrophen See verantwortlich. Während nicht toxische Konzentrationen von Cadmium (3 nM) und leicht toxische von Nickel (300 nM) einzeln eingesetzt kaum Stresssymptome in den Pflanzen hervorriefen, hatten sie einen enorm toxischen Einfluss, sobald sie zusammen in weichem Wasser (geringe Calcium- und Magnesiumkonzentrationen) vorlagen. Da die Toxizität dieser Metallkonzentrationen aufgrund einer hohen Wasserhärte des Sees verringert wurde, könnte das gehemmte Makrophytenwachstum in diesem See auch weitere Gründe haben. Die Phosphatlimitierung, welche ein bekanntes Problem bei Frischwasserhabitaten darstellt, bewirkte eine verstärkte Toxizität in weichem Wasser. Allerdings zeigen die Ergebnisse dieser Studie, dass diese Art von synergistischer Schwermetallvergiftung einen größeren Einfluss auf das Ökosystem haben könnte, als bisher vermutet wurde.

1. General Introduction

1.1 State of the art

Heavy metals including copper, iron, zinc, molybdenum, nickel, and others belonging to the first and second row of the transition metals in the periodic table of elements, are plant micronutrients and are necessary for various metabolic processes in both prokaryotes and eukaryotes. They are important to maintain proper growth and functioning of the plant even though they are only required in small quantities. Some of the micronutrients including copper (Cu) have a narrow beneficial range for a plant's proper growth and development, which means that they become toxic after exceeding a particular concentration in the plant. Since they are essential nutrients, the plant shows deficient effects when they are below their beneficial range. Therefore, the proper physiological functioning of the plants can only take place with proper availability, acquisition, homeostasis or distribution of these elements within the plants and are therefore prime targets of research. From the pioneering work of Sommer (1931) and Lipman and McKinney (1931) copper ($3d^{10}4s^1$ or $3d^9 4s^2$) is known to be an essential micronutrient. Because of its multiple oxidation state existence in vivo, either as reduced Cu^+ ($3d^{10}$) or as an oxidised Cu^{2+} ($3d^9$) state, it has a major role in the biological system (Solomon et al., 1992, 1996). Since Cu^+ with its affinity for thiol and thioether groups (as in cysteine or methionine), and Cu^{2+} with its preferable coordination to oxygen or imidazole nitrogen groups (as in aspartic and glutamic acid, or histidine respectively) can participate in a wide spectrum of interactions with proteins to drive diverse structures and biochemical reactions (Festa and Thiele, 2011). In the plant system, most functions of copper as a plant nutrient are based on the participation of enzymatically bound copper in redox reactions (Marschner, 1995). At least 30 copper containing enzymes are known to be redox catalysts (e.g. cytochrome oxidase) or dioxygen carriers (e.g. hemocyanin, Weser et al., 1979). According to Marschner (1995), Cu functions as the active centre in various enzymes and mainly is required in six locations of a plant, namely the cytosol, the endoplasmic reticulum (ER), the mitochondria's inner membrane, the chloroplasts' stroma, the thylakoid lumen and the apoplast. An important role of copper is in the electron transport chain between the photosynthetic reaction centres, where the transfer of electrons takes place through the blue copper protein plastocyanin, the most abundant Cu protein in the green tissue (Yamasaki et al., 2008). Cu (in the +1 oxidation state) act as a cofactor for various enzymes, where it

binds as a ligand to small molecules like O_2, as in the case of Cu/Zn superoxide dismutase (SOD) that are involved in the oxidative stress response. Apart from plastocyanin and Cu/Zn SOD, more than 32 related proteins (blue copper proteins) with unknown function have been identified in Arabidopsis (Nerissian et al., 1998). Cu is a cofactor of a large number of oxidases including mitochondrial cytochrome c oxidase, amine oxidase, multicopper oxidases such as ascorbate oxidase, laccases, polyphenol oxidase, etc. (Yruela, 2009). Involvement of Cu in the synthesis of a molybdenum cofactor (Kuper et al., 2004), have been proposed which would link Cu metabolism with nitrogen assimilation and phytochrome biosynthesis (Mendel, 2005). Cu plays an important role at the cellular level in the cell wall metabolism, oxidative phosphorylation, iron mobilization and signalling (see review Yruela, 2005).

In natural waters, the concentration of Cu is usually less than 2 ppb (Baccini, 1985; Moore and Ramamoorthy, 1984) and 20-30 ppm in non-contaminated soils and sediments (Nriagu, 1979; Salomons and Forstner, 1984). Copper levels in the water column of lakes are comparatively low because of the natural purification processes (chemical complexations, precipitation, adsorption) by which Cu is removed by sediments in the water (Forster and Wittmann, 1979). Cu concentration reach 500-2000 ppb in polluted conditions, where copper levels in soil and water increase as a result of anthropogenic activities including the release of Cu rich pig and poultry slurries into the environment, mining (Lopez and Lee, 1977), industrial (metal plating, steelworks, refineries) and domestic waste emissions, application of fertilizers, sewage sludge, and pesticides including algicides and fungicides which have been intensively used especially in vineyards (Yamamoto et al., 1985; Komárek et al., 2010). This results in the creation of copper toxicity for plants living in such environments (Moore and Ramamoorthy, 1984). Plants have been classified as indicators, excluders and hyperaccumulators based on their shoot uptake of heavy metals including Cu (Küpper and Kroneck, 2005) and so there are marked differences between plant species in their response to Cu toxicity.

The inhibition of photosynthesis, especially of the light reactions, is the greatest damage in photosynthetic organisms caused by most heavy metals including copper (Küpper and Kroneck, 2005). The formation of heavy metal substituted chlorophylls ([hms]-Chls: substitution of Mg^{2+} in the chlorophyll (Chl) molecule by heavy metal ions) within the reaction centres and light harvesting complexes (LHCs) was observed to be a reason for the inhibition under environmentally relevant conditions (Küpper et al. 1996, 1998, 2002). The mode of substitution, however, strongly depends on the irradiance. Low irradiance with a dark

phase, termed as shade reaction, results in the Cu substitution of Mg^{2+} in Chl molecules bound to the light harvesting complex II (LHC II). In the case of high irradiance, termed as sun reaction, the LHC II Chls are inaccessible to substitution and instead damage occurs in the PSII reaction centre (Cedeno-Maldonado et al., 1972; Küpper et al., 1998, 2002, 2009). Because of their less stable singlet excited state and lower tendency to bind axial ligands, [hms]-Chls are unsuitable for photosynthesis (Küpper et al., 2006). Malfunctioning of the photosynthetic apparatus as a result of copper toxicity, including interference with the biosynthesis of pigments and proteins in photosynthetic membranes (Lidon and Henriques, 1991), degradation of the grana stacking and the stroma lamellae, increase in the number and size of plastoglobuli, decrease in the lipid content and change in the fatty acid composition of the thylakoid memrabes (Sandmann and Böger 1980; Luna et al. 1994) resulting in the alteration in the PSII membrane fluidity (Lidon and Henriques, 1991; Yruela 2009), would divert the absorbed light energy towards different processes. This can result in the formation of reactive oxygen species (ROS), causing oxidative damage within the plant (Pinto et al., 2003). A copper excess may also impair cellular transport processes and induce deficiency of essential ions (Frausto da Silva and Williams, 2001; Dudev and Lim, 2013).

Plants try to evolve certain mechanisms to control and respond to the uptake and accumulation of nutrients, where these metals get chelated by particular ligands. These include the Metallothioneins (MTs), which are cysteine rich peptides encoded, by a family of genes and Phytochelatins (PCs), which are enzymatically synthesised cysteine rich peptides. These ligands form complexes with metals, and are most likely transported into and stored in the vacuole to avoid interference in the plant's physiology (Cobbett and Goldsbrough, 2002).

Cu deficiency is often observed in plants growing on soils with either low concentrations of total inherent copper, e.g. calcareous soils or ferrallitic and ferruginous coarse textured soils, as well as soils with high organic matter where copper gets complexed with organic substances, or soils with high nitrogen availability (Alloway and Tills, 1984).

The sensitivity to copper deficiency varies among species. Deficiency symptoms include decreased growth rate, chlorosis, curling of leaf margins and decreased fruit formation (Marschner, 1995). There is a decrease of the PSII activity in Cu deficient chloroplasts as plastocyanin cannot function without copper as its active site. Changes in the chloroplasts' thylakoid membranes and further decrease in the pigments (chlorophyll and carotenoids) have been reported (Droppa et al., 1987). Damage to the photosynthetic apparatus will divert the absorbed light energy towards different processes, finally resulting in oxidative stress. There

are some enzymes showing limited or no activity at all if copper is missing. This is true for the copper and zinc dependent superoxide dismutase (Marschner, 1995; Küpper and Kroneck, 2005), diamine oxidase (DAO), ascorbate oxidase (AO) polyphenol oxidase and *Cyt* c oxidase (Lonergan et al., 1982). Cu-deficient plants try to substitute Cu-proteins with proteins of similar or overlapping functions but with different central ions (Puig et al., 2007).

1.2 Aims and objectives of the thesis

The main aim of this project was to investigate various biochemical and biophysical mechanisms involved in a plant's response to environmentally relevant Cu conditions ranging from deficiency via optimal to toxic Cu concentrations.

We used the model plant *Ceratophyllum demersum* L., an aquatic submerged macrophyte which is sensitive to heavy metal stress. Since this plant has no roots, all required nutrients are taken up over a large shoot surface area, which makes this species sensitive to heavy metal stress (from earlier studies Mishra et al., 2008, 2009, Andresen et al., 2013, Thomas et al., 2013). Further, *Ceratophyllum demersum* L. is active during summer and dormant in winter. Remaining close to the surface within the summer season, this plant forms turions, buds that sink to the bottom of the water (limited by light, temperature or both), as mechanism to survive the winter conditions (Best, 1977). Since these model plants contain trace metals such as cadmium and lead in their tissue, they can be used as a measure of lake pollution (Stankovic et al., 2000).

Earlier studies on Cu, Cd and Ni toxicity were performed under artificial laboratory conditions and in a state of acute toxicity, i.e. rather short incubation time of hours to several days using high µM or even mM concentrations (Tsay et al., 1995, Baryla et al., 2000, Thomas et al., 2013) that are far above the range of highly polluted environments (Moore and Ramamoorthy, 1984). These conditions have the disadvantage of leading to unspecific inhibition, which will be further explained in the forthcoming chapters. Going for chelating agents in studies to create a specific metal deficiency bears the danger of reducing the bioavailability of other metals too, and thus leading to an unspecific metal deficiency, e.g. in the case of EDTA that is used for iron chelation. Moreover, unnatural light conditions were used in older studies (continuous strong light or rectangular switch-on – switch-off), which cannot be regarded as an environmental condition (Cedeno- Maldonado et al., 1972). Further,

earlier studies as explained in the introduction (Küpper et al. 1998, 2002, 2009) have shown a strong dependence on irradiance to play a major role during Cu toxicity, especially on the mode of Chl substitution. Thus, it remained unknown which of the inhibition mechanism(s) as a result of the metal stress are actually relevant in the environment. Furthermore, the interdependence of these inhibition mechanisms and their thresholds of occurrence have not been explained till now.

Heavy metals like Cd are important environmental pollutants. They are considered non essential and toxic to most organisms and so induce different stress effects on the plant as compared to Cu (Gill and Tuteja, 2011). The synthesis of phytocheltins (PCs) is one major strategy of heavy metal detoxification. We examined the different PC species which were induced in response to Cd and Cu treatments in the plant.

An investigation was also performed on an oligotrophic lake, to study the effect of the synergistic heavy metal toxicity on the ecosystems and if this was the reason behind the complete lack of submerged macrophytes in the lake.

2. Publications in peer reviewed journals and manuscripts

2.1. Effects of nanomolar copper on water plants - comparison of biochemical and biophysical mechanisms of deficiency and sublethal toxicity under environmentally relevant conditions.

George Thomas[a], Hans-Joachim Stärk[b], Gerd Wellenreuther[c], Bryan C. Dickinson[d], and Hendrik Küpper[a,e]*

a) Universität Konstanz, Mathematisch-Naturwissenschaftliche Sektion, Fachbereich Biologie, D-78457 Konstanz, Germany.

b) UFZ – Helmholtz Centre for Environmental Research, Department of Analytical Chemistry, Permoserstr. 15, D-04318 Leipzig, Germany.

c) HASYLAB at DESY, Notkestr. 85, 22603 Hamburg, Germany.

d) Harvard University, Department of Chemistry and Chemical Biology, 12 Oxford St., Cambridge, MA 02138, Massachusetts, USA.

e) University of South Bohemia, Faculty of Biological Sciences and Institute of Physical Biology, Branišovská 31, CZ-370 05 České Budejovice, Czech Republic

published in Aquatic Toxicology (2013) 140-141: 27-36.

Abstract

Toxicity and deficiency of essential trace elements like Cu are major global problems. Here, environmentally relevant sub-micromolar concentrations of Cu (supplied as $CuSO_4$) and simulations of natural light- and temperature cycles were applied to the aquatic macrophyte *Ceratophyllum demersum*. Growth was optimal at 10 nM Cu, while PSII activity (F_v/F_m) was maximal around 2 nM Cu. Damage to the PSII reaction centre was the first target of Cu toxicity, followed by disturbed regulation of heat dissipation (NPQ). Only after that, electron transport through PSII (Φ_{PSII}) was inhibited, and finally chlorophylls decreased. Copper accumulation in the plants was stable until 10 nM Cu in solution, but strongly increased at higher concentrations. The vein was the main storage site for Cu up to physiological concentrations (10 nM). At toxic levels it was also sequestered to the epidermis and mesophyll until export from the vein became inhibited, accompanied by inhibition of Zn uptake. Copper deficiency led to a complete stop of growth at "0" nM Cu after 6 weeks. This was accompanied by high starch accumulation although electron flow through PSII (Φ_{PSII}) decreased from 2 weeks, followed by decrease in pigments and increase of non photochemical quenching (NPQ). Release of Cu from the plants below 10 nM Cu supply in the nutrient solution indicated lack of high-affinity Cu transporters, and on the tissue level copper deficiency led to a re-distribution of zinc.

Keywords: biophysics of photosynthesis, *Ceratophyllum demersum*, chlorophyll fluorescence kinetics, copper deficiency, heavy metal stress, μXRF.

1. Introduction

Plant micronutrients include the heavy metals copper, iron, molybdenum, nickel and zinc belonging to the first and second row transition-elements. The availability, acquisition and distribution of these elements within the plants are prime targets of research as they have a major role in the proper physiological functioning of plants.

One of the major heavy metals which have been studied is copper. Copper has a particularly narrow beneficial range for the growth and development of the plant and becomes toxic after a particular concentration and causes deficiency effects on the plants when below the beneficial range. It has a major role in the physiology of plants mainly because of its multiple oxidation state existence *in vivo*, Cu^{+} and Cu^{2+}. Its role as a micronutrient has been known in plants since a long time (Sommer, 1931; Lipman and McKinney, 1931). Copper is mainly required at least in six locations in a plant cell which includes the cytosol, the endoplasmic reticulum (ER), the inner membrane of the mitochondria, the stroma of the chloroplast, the thylakoid lumen and the apoplast (Marschner, 1995), because of its function as the active centre of various enzymes. Copper plays an important role in photosynthetic electron transport, where the transfer of electrons takes place through plastocyanin (the most abundant Cu proteins in green tissue (Yamasaki et al., 2008)), which gets reduced and oxidized as the electron is transferred from the cytochrome b_6f complex to the PSI reaction centre. Another important function of the Cu (in the +1 oxidation state) is to bind to small molecules like O_2 as a ligand. Thus these ions act as a cofactor for various enzymes like Cu/Zn superoxide dismutase (SOD), cytochrome c oxidase, etc (Küpper and Kroneck, 2005)

The concentration of Cu is less than 32 nM in natural waters (Baccini, 1985) but these values reach up to 32 µM in polluted conditions, resulting in the creation of copper toxicity for plants living in such environments (Moore and Ramamoorthy, 1984). The increase of copper levels in the environment is mainly a result of anthropogenic activities, which include the industrial (metal plating, steelworks, refineries) and domestic waste emissions, application of fertilizers, sewage sludge, and pesticides (Yamamoto et al., 1985; Zhang et al., 2003).

The greatest damage caused by copper in photosynthetic organisms results from the inhibition of photosynthesis, mainly of the light reactions (review by Küpper and Kroneck, 2005). Here the substitution of Mg^{2+} in the chlorophyll (Chl) molecule by heavy metal ions leading to the formation of a heavy metal substituted chlorophylls ([hms]-Chls) (Küpper et al., 1996, 2002) is an important mechanism of damage at environmentally relevant Cu concentrations. [Hms]-Chls are unsuitable for photosynthesis unlike [Mg]-Chls, because of

their less stable singlet excited state and lower tendency to bind axial ligands (Küpper et al., 2006). The excited energy from these altered chlorophylls may be accidentally transferred to oxygen resulting in the production of singlet oxygen, one of the reactive oxygen species (ROS), which causes oxidative damage (Pinto et al., 2003). Potential participation of Cu in Fenton reaction would also result in ROS production (Halliwell and Gutteridge, 1984), although it has never been shown to be relevant *in vivo*. A degradation of the grana stacking, the stroma lamellae, increase in the number and size of the plastoglobuli and alteration in the PSII membrane fluidity was found as indirect effects of the Cu toxicity (Quartacci et al., 2000), which would further decrease the activity of the photosystems (Lidon and Henriques, 1991; Ouzounidou et al., 1992). Excess Cu is also known to induce deficiency of essential ions (Mn^{2+}, Zn^{2+}, etc) as there is a competition between the various heavy metals according to the Irving-William series (Frausto da Silva and Williams, 2001).

Cu deficiency changes the chloroplast's thylakoid membranes (Droppa *et al*., 1987), decreases the pigments (chlorophyll and carotenoids) and affects the PSII activity. Like in the case of toxicity, damage to the photosynthetic apparatus will divert absorbed light energy towards different processes, finally resulting in oxidative stress. When there is deficiency in Cu there is no proper functioning of Cu/Zn SOD, causing further rise of oxidative stress (Marschner, 1995; Küpper and Kroneck, 2005). Further, Cu-deficient plants substitute Cu-proteins with proteins of similar or overlapping function but different central ion (Puig et al., 2007).

Most of the Cu toxicity studies were carried out at higher (up to 500 µM) Cu concentrations (Tsay et al., 1995, Baryla et al., 2000), which are much above the range of even the most polluted environments (Moore and Ramamoorthy, 1984). This causes a decrease in the specificity of any inhibition - as soon as all high-affinity binding sites are saturated with Cu, further Cu will bind to low-affinity binding sites that would not be a target of copper binding at environmentally relevant toxic Cu concentrations. Additionally, in earlier studies chelating agents were used to achieve Cu deficiency, which bind to other heavy metals (incl. essential nutrients) and reduce their bioavailability. Moreover, un-natural light conditions, which includes continuous light or rectangular switch-on – switch-off, were used in the older studies although it is known that for the extent and symptoms of the heavy metal induced damage light intensity and dark phase are important (e.g. Cedeno-Maldonado et al., 1972; Küpper et al., 1996, 2002). Because of these reasons, it remained unknown which of the mechanism(s) of inhibition by copper toxicity are actually relevant in environmentally

relevant conditions. Further, even though all the mechanisms stated above have been studied, an interdependence of these mechanisms has not been explained till now.

Thus, the kinetic pattern and the concentration thresholds of the occurrence of different damage mechanisms were the main focus of the current paper. We used the model plant *Ceratophyllum demersum* L., which is an aquatic submerged macrophyte sensitive to heavy metal stress. Since it has no roots, all nutrients are taken up over a large surface area of the entire shoot. Because of its ability to grow without a solid substrate it has been used for environment control and life support system studies in space through the successful spaceflight projects of CEBAS / Aquarack (Blüm et al., 1994) and the currently undergoing OMEGAHAB-B1 projects of the DLR.

2. Material and Methods

2.1 Plant material and cultivation

The submerged, rootless macrophyte *Ceratophyllum demersum* L. was used for the experiments. Plants were cultivated in an optimized nutrient solution for submerged macrophytes and water plants (SMNS, Table S1, pH 7.8). Since 2005 the strain was continuously cultivated in hydroponic cultures under 12 h day/12 h night light conditions with two FLUORA® fluorescent and two warm white fluorescent tubes (Osram, München, Germany) and a temperature cycle from 18°C at 6 a.m., over 20°C at 9 a.m., to a maximum of 22°C at 3 p.m., back over 20°C at 9 p.m. to 18°C again at 6 a.m.. The high light culture unit had a slightly different set up with “daylight” fluorescent tubes (Dulux L 55 W / 12 950, Osram, München, Germany), 12 h sinusoidal light cycle with maximal irradiances at 500-650µE inside the media and 12 h night. The temperature was 19°C at 6 a.m., 21.5 at 9 a.m., 24 at 3 p.m., 23 at 9 p.m. and 19 at 6 a.m.

For each copper treatment (“0”, 0.5, 1, 2, 5, 10, 20, 50, 100, 200 nM prepared by $CuSO_4$) around 2 g of plants were placed into an aquarium containing 2 l of continuously aerated medium to secure a low biomass to water volume ratio. A continuous exchange of nutrient solution (flow rate 0.5 $l.day^{-1}$) was set up to ensure that the metal uptake into the plants was limited only by the concentration, but not by the amount of nutrient solution available. The increase in growth was measured at the end of each week after the plants were

cleaned. The experiment was carried out for 6 weeks at the end of which the plants were harvested. Young tissues being 4 cm from the apex and 2 cm from the apex of side branches, old tissues 8 cm from the stem end and the rest of the side branches were separated. Remaining SMNS was removed by shaking, the plants were frozen in liquid nitrogen and stored at -80°C until further analyses.

2.2 Photosynthesis biophysics

To study the physiological changes in the plants induced by heavy metals, two-dimensional (imaging) microscopic measurements using the Chl fluorescence kinetic microscope (Küpper et al., 2007a) were performed. One leaf from the 5th nodium, counted from the apex of the plant, was fixed in the measuring chamber with the help of cellophane. There was a continuous flow of the culture medium (but without micronutrients as they caused background in peroxide measurements) in the chamber (Küpper et al., 2008) that was used for the kinetics measurement. An area (approximate size of 1.1x1.1 µm) just before the last leaf branching point was measured. A detailed description of the microscope and the used protocols can be found in Küpper et al., 2007a; all photosynthetic parameters analysed in the current study are explained and referenced in Tab. S2. Values are given as means of five different experiments with two technical replicates each.

2.3 Determination of pigment content

Pigments were extracted from the leaves frozen every week and also from the harvested plant material. Samples were lyophilized and ground with sand and a few grains of Bis-Tris (Sigma-Aldrich, St Louis, MO, USA). Extraction of pigments was performed in 1 ml 100% acetone at 4°C overnight. Acetone is the ideal solvent for this task as it prevents artefacts (e.g. allomerisation) that occur in alcoholic solvents (reviewed e.g. by Küpper et al., 2006), and solubility of pigments in 100% acetone is not limiting up to 50 mg plant DW per ml (Küpper et al., 2007b). In the current work, complete extraction of pigments was furthermore confirmed by the white pellet after centrifuging the extracts. Spectra of pigment extracts were measured with the UV/VIS/NIR absorption spectrophotometer Lambda750 (Perkin-Elmer, Waltham, MA, USA) at a spectral bandwidth of 0.5 nm, 0.5 nm sampling interval and recording from 330 to 750 nm. Pigment composition was analyzed using the Gauss-Peak-

Spectra method (Küpper et al., 2007b) with an updated pigment database. Values are given as means of five different experiments.

2.4 Imaging hydrogen peroxide (H_2O_2)

Peroxyfluor-2 (PF2, Dickinson et al., 2010), a H_2O_2-specific fluorescent indicator based on a boronate deprotection mechanism (Chang et al., 2004; Lippert et al., 2011), was used to detect intracellular hydrogen peroxide (H_2O_2) production released by the plant. One leaf from the 5th nodium counted from the apex of the plant was incubated in 100 µM PF2 in 0.5 ml of SMNS (without micronutrients, Küpper et al., 2008) for 30 min in the dark. Destaining was done in darkness in 15 ml SMNS after 30 min, then the leaf was placed in the measuring chamber of the FKM. After every measurement the media was replaced, and all tubes were washed with ddH_2O. The H_2O_2-specific fluorescence was measured in the FKM using a filter set from AHF (Tübingen, Germany) with an excitation filter 420-500 nm (AHF F42-468), dichroic mirror 505 nm (AHF F71-302) and 520-550 nm emission filter (AHF F47-535). Flashes of blue supersaturating light were given at increasing signal integration times (20 µs up to 20 ms). For each sample, the integration time that led to the highest signal intensity without saturating the camera was chosen for quantitative analysis to avoid noise at too short exposure times and oversaturation of the camera at too long exposure times. Hundreds of single pictures were taken and averaged for each exposure time to reduce noise. Background for each exposure time was subtracted automatically via a measurement without light. Images of the measurement were analysed with the FKM software and the fluorescent signal was re-calculated to one integration time according to an empirical calibration of exposure times vs. signal intensity. Values are given as means of three different experiments.

2.5 Starch quantification

The amount of accumulated starch in the harvested plant samples after 6 weeks of treatment were analysed using the Total starch assay kit (AOAC Method 996.11 and AACC Method 76.13; Megazyme, Wicklow, Ireland) with a protocol that was optimized for our demands. 5 mg of lyophilized and ground samples were washed with 0.5 ml of 80% ethanol, incubated for 5 min at 85°C, and washed again. 0.2 ml of 2 M KOH were added, mixed properly and incubated on ice or at 4°C for at least one hour during which the samples had to be stirred continuously. 0.8 ml Na-acetate buffer (1.2 M, pH 3.8) were added, immediately followed by

10 µl each of α-amylase and amyloglucosidase while the sample was stirred. The samples were heated to 50°C for 30 min and vortexed 3 times in between. From each sample and each D-glucose standard (0, 0.01, 0.05, 0.25, 0.5 and 1 mg ml^{-1}) duplicate aliquots of 20 µl were treated with 600 µl of the GOPOD reagent provided in the kit and incubated for 20 min at 50°C. The measurement was done against the reagent blank at 510 nm using the spectrophotometer Lambda750 (Perkin-Elmer, Waltham, MA, USA). Values are given as means of four different experiments.

2.6 Elemental analyses of medium and digested plant samples

5-10 mg of lyophylized plant samples were digested in 250 µl nitric-perchloric acid mixture (85:15% v/v of concentrated acids) for 30 min at room temperature and gradually heated up to a maximum of 195°C until all liquid was vaporized. The remaining ashes were re-dissolved in 0.5 ml 5% HCl, gradually heating to 80°C. The samples were allowed to cool and then the volume was filled to 1.5 ml with ddH_2O before analyzing the components (Zhao et al., 1994, amounts scaled down) using the Atomic Absorption Spectrometer (GBC 932 AA). Element concentrations of the media from the aquaria and barrels were analysed using an inductively coupled plasma sector field mass spectrometer ICP-sfMS (Element XR, Thermo Fisher Scientific, Waltham, MA, USA). Prior to analysis, ICP-MS parameters were optimized every day and samples were diluted to 1:20. The calibration was verified using the following reference materials: SLRS-5 (River Water Reference Material for Trace Metals, NRCC), SPSSW1 (Surface Water Level 1, Spectra Pure Standards) and SRM 1643e (Trace Elements in Water, NIST). Rhodium (4 µg L^{-1}) was added to all samples for internal standardization. Values are given as means of four different experiments.

2.7 Elemental distribution studies of the frozen samples with µXRF

For sample preparation, capillaries (1 mm diameter, 0.1 mm wall; Hilgenberg GmbH, Malsfeld, Germany) were cut to 27 mm length and filled with water. The leaf was inserted into the water filled capillary with caution to avoid any damage to the leaf and fixed on a custom made sample holder. For calibration, we prepared a multielement standard containing 3 mM each of Na_3AsO_4, $CdCl_2$, $CrCl_3$, $CuCl_2$, NaFe(III)-EDTA, $NiCl_2$, $ZnCl_2$ in 20% glycerol and 5% HCl, dilutions were prepared with aqueous solutions of 20% glycerol + 5% HCl and filled into the same capillaries as used for the leaves. The capillaries containing

standards or leaves were shock-frozen in supercooled isopentane (-140^{0}C), submerged and stored in liquid nitrogen until the analysis. To limit beam damage and to prevent re-distribution of elements that would occur if samples thawed, throughout the measurement the sample was cooled in a cryostream to about 100 K (Cryocool LN3; Cryoindustries of America, Manchester, New Hampshire, USA). All µ-XRF measurements were done at beamline L of the synchrotron DORIS at the Deutsches Elektronen-Synchrotron (DESY, Hamburg, Germany). X-rays created in a bending magnet were monochromatized using a multilayer monochromator at 10.2 keV with a bandpass of approximately 2.3%. Focussing was achieved using a single-bounce capillary to approximately 10 µm spotsize in both horizontal and vertical dimension. µ-XRF tomography was done approx. 3 mm from the tip of the leaf with step size of 5 µm and a dwell time of 0.8 s per step. Ninety-one linescans were measured, with the sample being rotated by 2°, yielding a 180° tomogram. Two fluorescence detectors (Vortex-60 EX / Vortex-90 EX; SII Nanotechnology USA Inc., Northridge, California, USA) were used under 90° and 270° with respect to the incident beam to maximize detected fluorescence counts from the sample while minimizing background caused e.g. by elastic scattering due to the polarized nature of the synchrotron radiation. The detected µ-XRF spectra were fitted using PyMca (Solé et al., 2007). The fluorescence line areas were then normalized to 100 mA Doris current, the resulting sonograms were tomographically reconstructed with XRDUA (De Nolf and Janssens, 2010) using the maximum likelihood expectation maximization ("MLEM") algorithm. Absolute concentrations were obtained using the tomographic reconstruction of the multielement-standard measured in the identical geometry. Finally, the mean intensity of the 5% pixels with lowest intensities caused by stray radiation or reconstruction artefacts were subtracted from the data as background.

2.8 Statistics

Two-way analysis of variance (ANOVA) was done in SigmaPlot 11 (SPSS Science, USA) at significance level of $P < 0.05$ for all the data analysed, except for starch and metal analysis where one-way ANOVA was performed. If significant effects were found, post-hoc comparisons were performed with the Duncan's multiple range test (DMRT). In the manuscript, *NS indicates test results that were not significant at $P < 0.05$.

3. Results

The experiments in this study successfully covered the range of responses to copper from deficiency via optimal growth to lethal toxicity. Furthermore, the long (compared to almost all earlier studies) duration of these experiments, six weeks, combined with 10 different copper concentrations, allowed for analysis of threshold concentrations and time sequences. In this way it was possible to establish a sequence of events leading to optimal or suboptimal growth, as presented in detail below. The results have been shown as 2D graphs in the figures and their line graphs in the supplement.

3.1 Visible symptoms

The beneficial range of Cu in plants was between 10 nM and 30 nM while 10 nM Cu had the maximum growth, which was statistically significant when compared to the deficient and toxic copper concentrations used in the experiment ($P = 0.006$) Here the plants looked healthy with green leaves and strong meristems with sprouting from the tips (Fig. 1c) At the higher concentrations, plants were growing at the same rate till the end of the first week, except for the 200 nM Cu treatment that showed a growth reduction even from the first week. The plants at 200 nM and 100 nM copper showed visible stress (toxicity) symptoms from the fifth week, which included decrease of leaf size, fragile stem, loss of leaves from the bottom of the stem and bleaching of pigments (chlorosis). Finally a negative growth rate was registered, which indicated a stoppage of growth at the sixth week (Fig. 1d). Deficiency was observed from the second week mainly at "0" nM Cu with a reduction in the growth rate (Fig. 1a). The unhealthy symptoms as observed in the toxic concentrations were registered here due to the deficiency of Cu from 5 nM Cu in the fourth week. The growth rate was negative in the sixth week at "0" nM Cu when the plants almost died (Fig. 1b).

3.2 Photosynthetic parameters

Fluorescence kinetic analysis was used as a tool to identify changes in photosynthetic light reactions. For readers not familiar with them, all photosynthetic parameters analysed in the current study are explained and referenced in Tab. S2. While the colour maps allow for best judgement of the truly two-dimensional trends (Fig. 2b), for showing about error bars we added the same data as line graphs to the supplement (Fig. S5). The maximal fluorescence in dark-adapted samples (F_m) had a significant decreasing trend towards the final weeks of

treatment towards the toxic Cu concentration, starting from the second week ($P < 0.001$) (Fig. 2b). The photosynthetic quantum efficiency of PSII reaction centre in dark adapted state (measured as F_v/F_m) was maximal at 10 nM Cu for most of the experiments, but had higher values around 2 nM copper at the end of the experiment ($P =< 0.001$) (Fig. 2a). There was a further decrease towards the higher Cu concentrations from the fourth week.

The photochemical activity of PSII in actinic light (ΦPSII, also called "photochemical quenching", a parameter related to electron flow through PSII, Genty et al., 1989) generally was optimal around 10 nM Cu. When measured at the start of illumination (ΦPSII i1), it decreased from the second week mainly at the deficient Cu concentrations compared to optimal Cu (with reference to growth). A decrease of ΦPSII was found from the second week in the highest Cu concentrations with the lowest values in the sixth week (Fig. 2a). Similar trends were observed also after longer time of illumination ($P = 0.033$) (ΦPSII i6: Fig. 2b). After actinic light was switched off, the recovery of PSII to the dark relaxed state was measured both at the start (ΦPSII r1: Fig. 2e) and end (ΦPSII r5: Fig. 2f) of the recovery time. These parameters were optimal at low copper including the deficient concentrations (<10 nM), and only decreased at higher Cu concentrations (>10 nM), starting in the second week. ($P =< 0.033$)

The non-photochemical quenching (NPQ = regulation of exciton dissipation as heat, measured as $(F_m-F_m')/F_m$) at the end of the light phase (NPQi6) gave noisy results, but had an increase towards the sixth week from “0”nM to optimal Cu (around 10 nM) but not at the higher concentrations (Fig. 2g). In the end of the dark phase, however, there was an increasing trend in the toxic Cu concentrations ($P = 0.009$)(Fig. 2h).

3.3 Pigment composition

The pigments were extracted from the FKM-measured leaves in each week and also from the harvested young and old plant tissue after the sixth week. Chlorophyll a content steadily decreased from deficient via optimal to toxic Cu in the younger tissues (Fig. 3a, c), and this slope increased with longer exposure to the different copper concentrations ($P = 0.003$) (Fig. 3a). In the older parts of the plant, in contrast, Chl a+b were minimal around optimal Cu, and strongly increased towards toxic concentrations. The decrease in the Chl a/b ratio in young leaves (Fig. 3d) was mainly because of the decrease in Chl a from the fourth week

from 50 nM towards higher Cu concentration. Chl b showed a decrease only from the fifth week mainly at toxic Cu concentrations (Fig. 3b).

3.4 Hydrogen peroxide production

Higher hydrogen peroxide was measured because of many reports of oxidative stress during copper toxicity stress in plants. In the current study, however, it was detected in the plants treated with copper deficient conditions mainly in the 2 nM Cu treatment at the sixth week when compared to the leaf at the start of the treatment (Fig. S3a). Increased hydrogen peroxide production in response to actinic irradiation was recorded in the dye test with the control plant (Fig. S3b).

3.5 Starch accumulation

Starch accumulation was analysed because it shows a longer-term balance between photosynthetic energy production and physiological energy consumption. Harvested plants at deficient Cu concentrations had higher starch than those at optimal Cu, while starch accumulation decreased towards toxic Cu. The younger parts of the plant had higher starch content compared to the old (Fig. 4a).

3.6 Heavy metal accumulation

Metal accumulation was measured after six weeks of treatment. The Cu concentration in the plants was stable until 10 nM Cu^{2+} (NS at $P < 0.05$) in the nutrient solution, after which there was a significantly strong accumulation of Cu in the young ($P =< 0.001$) and old ($P = 0.013$) tissues with the increase of Cu in the media The highest Cu accumulation was around 400 ppm at the 200 nM Cu concentration. The young tissues had slightly more metal accumulation compared to the old tissues (Fig. 4b).

3.7 Metal distribution in leaves

The metal distribution studies were performed by µXRF on frozen-hydrated young mature leaves after two and four weeks of Cu treatment (Fig. 5). At deficient and optimal copper supply, Cu was mainly localized in the vein. Copper deficiency did not anyhow alter the copper distribution pattern, but lowered the tissue concentrations (Fig. 5g and Fig. 5c). In

contrast, at toxic Cu after two weeks there was sequestration of Cu from veins towards the mesophyll and epidermis, with copper concentrations in the epidermis reaching about half of the concentration in the vein (Fig. 5i). Longer treatment did not further increase the epidermal copper accumulation, but only Cu accumulation in the vein (compare Fig. 5i and Fig. 5k). Zn content of the leaves was reduced by increasing copper (compare scales of Fig. 5b-f-j and Fig. 5d-h-l). Copper deficiency did not only increase Zn accumulation in the leaves, but also changed the compartmentation pattern of Zn. While at optimal and toxic Cu, Zn was rather homogeneously distributed throughout the leaves, at deficient copper supply the additionally accumulated Zn was sequestered to the epidermis.

4. Discussion

This study systematically investigated the response of the aquatic model plant *C. demersum* towards deficient, optimal and toxic copper concentrations with a large array of methods, establishing time and concentration thresholds of different previously proposed damage mechanisms, yielding new insights into the sequence of events and interdependence of mechanisms that ultimately lead to either optimal growth, or inhibition by deficiency or toxicity.

The maximum growth was observed from the 1st week at 10 nM Cu, which was same Cu concentration as used for the stock culture. In Lake Constance (Bodensee) the Cu concentration was recorded as 17.3 nM (Zweckverband Bodensee-Wasserversorgung, http://www.zvbwv.de/). The shifting of the maximum growth towards higher concentrations towards the sixth week shows that after acclimation Cu concentrations that are initially slightly toxic can be optimal for long-term growth.

4.1 Copper deficiency

Cu limitation was significant below 5 nM in the growth pattern from the fourth week of treatment, which further decreased towards the sixth week while deficiency was attained for “0” nM Cu already from the second week. This suggests that the plants utilize an internal reserve of Cu for their normal functions during the initial weeks, after which deficiency occurs, affecting growth. This agreed with the Cu distribution studies performed during the

fourth week, where Cu accumulation in the vein was reduced as compared to the second week. Measurements of copper in the aquaria vs. copper in the storage barrels (with controls of all possible sources of copper contamination sources) furthermore showed that in the first weeks the plants even release copper out of their tissues into the nutrient solution if the Cu^{2+} concentration in the nutrient solution is below 10 nM (Fig. S2b). This indicates that *C. demersum* does not have copper transporters suitable to achieve an active uptake below this threshold concentration.

In Cu-deficient conditions electron flow between the photosystems became limiting. $\Phi_{PSII}i1$ and $\Phi_{PSII}i6$ decreased at deficient copper, while no inhibition of the photochemical yield of PSII by copper deficiency was found before (F_v/F_m) or after the actinic light period ($\Phi_{PSII}r1$, $\Phi_{PSII}r5$)(Fig. 2). This agreed to earlier study, which showed that Cu deficiency hampering the plastocyanin formation in turn reduces the electron transport from PSII to PSI (Baszynski et al., 1978).

Studies on *Arabidopsis* suggested that during deficiency, the plants tried to acclimate by downregulation of SOD that requires Cu. In this way, Cu could be made available to plastocyanin, which is required by the plant for the photo-autotrophic growth (Abdel-Ghany and Pilon, 2008). This down-regulation of SOD might lead to stress by accumulation of superoxide. But in our deficiency conditions, mainly at 2 nM Cu treatment, there was no considerable increase in superoxide observed (data not shown). However, a substantial increase in peroxides was observed at this concentration (Fig. S3a) indicating that superoxide would have been formed and dismutated into peroxides either by increased activity of SOD or by induction of Zn SOD. This agreed with the Zn distribution results from the µXRF, which demonstrated an increased accumulation of Zn at deficient Cu (Fig. 5b). A somewhat similar response to Cu deficiency was observed in earlier studies, where the Fe-SOD gene was strongly induced in *Arabidopsis* when Cu-SOD gene was downregulated (Abdel-Ghany et al., 2005). However, the "0" nM Cu treatment plants in our experiment had a negative growth rate and secondary effects which would have ultimately led to death.

4.2 Copper toxicity

The plants were able to tolerate up to a threshold level of 10 nM Cu in the nutrient solution, when they had an internal Cu concentration of around 20 ppm (Fig. 4b). At higher copper concentrations, i.e. already directly above the optimum Cu concentration, accumulation of Cu

in the plant increased, which was observed together with a reduction in growth. This indicates that above this concentration an overloading of copper efflux systems caused the loss of control over the intracellular copper. The toxicity thresholds vary between plant species, but the inhibitory effects were visible when mature leaf tissue Cu concentration was above 20 ppm in various studies (Gupta, 1979; Stevenson, 1986). The over-accumulation of Cu above the normal physiological conditions was also observed in the metal distribution studies (Fig. 5), which revealed a two phase response to Cu toxicity by the plants. They initially sequestered the excess Cu from the veins to the mesophyll and epidermis as a defence mechanism during the second week. But after four weeks there was further accumulation in the veins, while Zn nutrition of the surrounding tissue became inhibited along with this response. These alterations strongly indicate that in this second phase, micronutrient export from the veins breaks down, further accelerating damage to the leaves, finally resulting in the death of the plant.

The decrease in starch towards the higher Cu concentrations (Fig 4a) indicated that malfunctioning of photosynthesis contributed to the reduction in growth. The higher photosynthesis at optimal Cu concentration as observed from the F_v/F_m, Φ_{PSII} and NPQ compared to higher Cu at the sixth week further supported the higher starch production at optimal Cu concentrations, mainly in the young parts of the plants. Towards toxic copper concentrations, starch accumulation continuously declined. Further, we found copper accumulating more in the younger than in the older parts of the plant (Fig. 4b). This stronger uptake in metabolically more active parts of the plant (as shown by the generally higher starch contents in young compared to old tissues) indicates that copper was actively taken up even at the toxic 200 nM treatment.

High light conditions as used in the current study resemble summer conditions, where *C. demersum* floats at the surface of lakes. Studies show that plants respond to Cu stress differently in high and low irradiance of light resembling the sun and shade reaction which damages the photosynthesis process (Küpper et al., 1996). However, only in young tissues (which were also used for the measurements of photosynthesis biophysics) a decline in chlorophyll concentrations was found at toxic Cu as it is typically observed in the "sun reaction" type of damage. In old tissues, an increase of chlorophylls was found at toxic Cu, indicating a retardation of pigment degradation in senescent tissues. Less maximal Chl fluorescence yield (measured in young tissues) towards the later weeks of treatment corresponded to the decrease in the pigment concentration, which caused decrease in light

harvesting in young leaves. A greater F_m decrease than F_0 led to a decrease in F_v/F_m values in the high copper concentrations, showing a decreased maximal photochemical quantum yield of PSIIRC in dark-adapted state. A reason for this could be the insertion of Cu into the Phe a of the PSII reaction centre, rendering it non-functional as it happens in the "sun reaction" described earlier (Küpper et al., 1996, 2002).

F_v/F_m had the highest value around 2 nM copper (Fig. 2a) while optimal growth was found between 10 and 50 nM (Fig. 1a), showing that in *C. demersum* photosynthesis is more sensitive to copper toxicity than other parts or metabolism that limit growth. The opposite was found in a study on the diatom *Nitzschia closterium*, where Cu toxicity (0.47 µM) for 72 hrs inhibited the growth but not photosynthesis (Lumsden and Florence, 1983). This indicates that the optimal Cu required is different for individual physiological processes, and that the relative copper requirement and tolerance of these processes is at least in some cases different for higher plants vs. Diatoms (which are unicellular organisms).

The decreasing trend in Φ_{PSII} towards toxic Cu concentrations could be a consequence of the inhibition of the PSII reaction centre already discussed, or involve an additional blockage of the electron transport afterwards. The correlation with the decreasing F_v/F_m (where the electron transport beyond the PSIIRC is not relevant) shows that in the case of copper toxicity (in contrast to copper deficiency) the decrease of Φ_{PSII} is mainly a consequence of the inhibition of the PSIIRC. But the stronger decrease of the Φ_{PSII} compared to the F_v/F_m indicates a secondary inhibition target apart from the PSII reaction centres. According to earlier studies (Küpper et al., 2009), this could be an inactivation of the electron transfer after PSII or inhibition of the water splitting complex.

Earlier studies showed an increase in reactive oxygen species (ROS) in response to Cu toxicity (review e.g. by Pinto et al., 2003). However, to our knowledge in all studies reported so far higher copper concentrations were used than in our study. This difference shows again how different responses to environmentally relevant but still toxic heavy metal concentrations can be from responses to concentrations chosen in studies to induce a fast effect. The decrease of peroxide (ROS) production in our experiment at toxic concentrations when compared to deficient Cu conditions (Fig. S3b) could be due to the activation of various antioxidative enzymes including superoxide dismutase (SOD) and ascorbate peroxidase (APX) which quench the ROS (Srivastava et al., 2006)

The NPQ values in the dark phase were higher towards the higher Cu concentrations (Fig. 2h), which agrees with the decrease in Φ_{PSII} as there is more quenching as heat or by

other non photochemical ways. Since the values of the NPQ remain unaffected (at the level of the optimally growing plants) by toxic copper concentrations for a longer period than the photochemical activities (F_v/F_m, Φ_{PSII}), it can be concluded that PSII-mediated photochemistry is more vulnerable to Cu toxicity than the regulation of non-photochemical dissipation of excess energy.

From the time dependent studies a sequence of events, an interdependence and thresholds for various mechanisms of copper deficiency and toxicity stress can be concluded. At the toxic Cu concentrations, in young leaves the decrease in the F_m and F_v/F_m from the end of the second week was associated with the decrease in the chlorophyll and other pigments. The localization studies showed a re-distribution of Cu from veins towards mesophyll, where copper obviously inhibited photosynthesis by inhibiting PSIIRC and by hampering light harvesting. This led to decreased growth rate. However, at this point the plants still tried to defend themselves by sequestering copper to the epidermis. At the end of the fourth week, a further reduction in chlorophylls accompanied inhibition of electron transport after PSII, in addition to the persisting PSIIRC inhibition. At this point, there was higher accumulation of Cu in veins, indicating an inhibition of transport mechanisms responsible for sequestration e.g. into the epidermis. At the same time, Zn uptake became inhibited. The toxicity was more pronounced towards the sixth week when all the fluorescence parameters were drastically reduced. The toxicity stress symptoms became visible by bare eye, with a negative growth rate especially at 200 nM Cu. This treatment led to highest copper accumulation, and lowest starch content especially in the older tissues due to the lack of photosynthesis.

Towards the deficient Cu concentrations, the distribution studies showed that the plants were unable to re-distribute copper in order to make best use of it. Still most of the Cu remained in the vein, although inhibition of light-acclimated electron flow (while PSIIRC was fully functional) clearly showed that lack of plastocyanin became limiting for photosynthesis. Growth rate was reduced from 5 nM Cu after four weeks and the deficiency symptoms were becoming prominent when the reserve Cu was used up by the plants, as observed from the distribution studies at 0 nM Cu. At that time, there was reduction in the pigment content, which affected light harvesting and photosynthesis after the fifth week, which affected the growth rate and ultimately caused the death of the plant.

5. Conclusion

Growth of the plant was optimal at 10 nM Cu, while PSII activity (F_v/F_m) was maximal around 2 nM Cu. The main storage site for Cu up to physiological concentrations was in the vein.

At toxic copper concentrations, damage to the PSII reaction centre was the first target of inhibition, followed by disturbed regulation of heat dissipation (NPQ). Only after that, electron transport through PSII (Φ_{PSII}) was inhibited, and finally chlorophylls decreased. Copper accumulation in the plants was stable until 10 nM Cu in solution, but strongly increased at higher concentrations. At toxic levels Cu was sequestered from the vein to the epidermis and mesophyll, until export from the vein became inhibited. This re-distribution of Cu was accompanied by inhibition of Zn uptake.

Copper deficiency leading to a complete stop of growth was accompanied by high starch accumulation, although electron flow through PSII (Φ_{PSII}) decreased from 2 weeks. This was followed by a decrease in pigments and increase of non photochemical quenching (NPQ). Release of Cu from the plants below 10 nM Cu supply in the nutrient solution indicated lack of high-affinity Cu transporters. On the tissue level, copper deficiency led to a re-distribution of zinc.

Acknowledgments

We thank DESY for providing beamtime at the DORIS beamline L, and Karen Appel and Manuela Borchert for their support during our µXRF measurements. We would like to thank Prof. Chris Chang (UC Berkeley) for advice with the peroxide measurements. We are grateful for financial support by the DFG to HK (grant KU 1495/8), for an initial fellowship of the DAAD to GT, and basic funding of Universität Konstanz to HK.

Figures

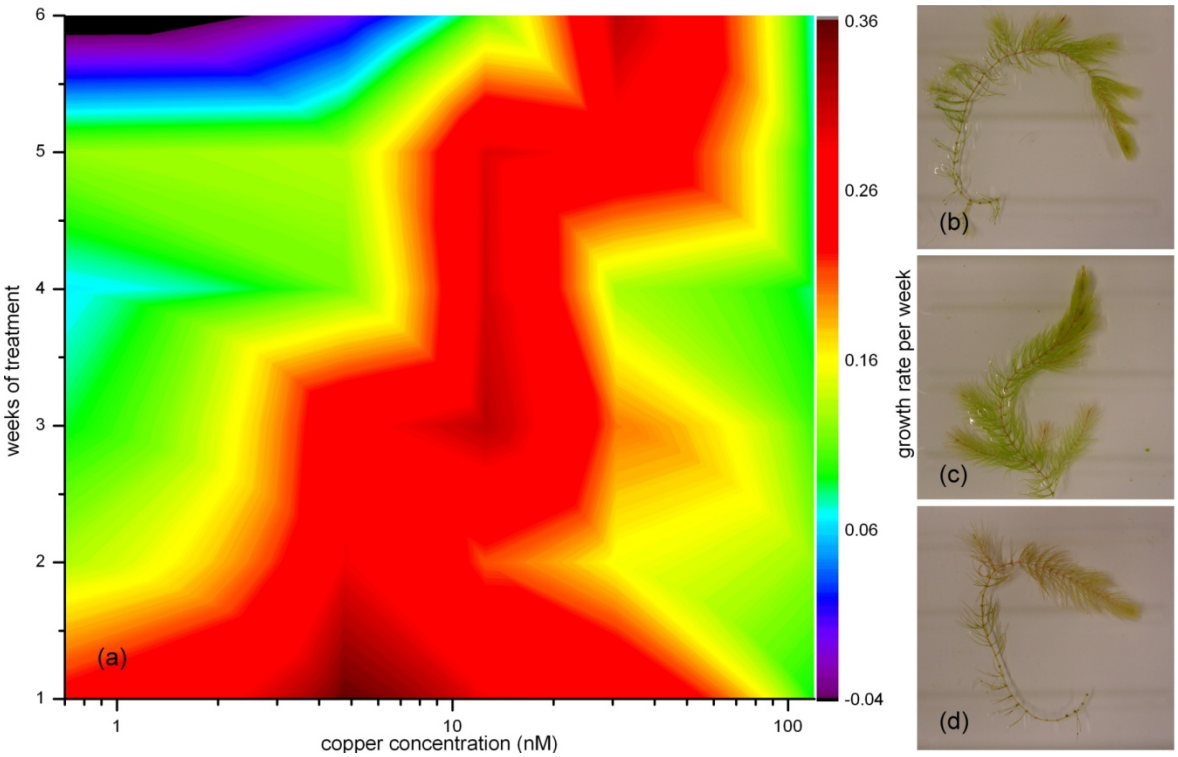

Figure 1. Effect of the different treatments of Cu on the growth of the plants. **(**a) Growth rate of the plants per week calculated on the basis of fresh weight. Values are given as means of five different experiments, (b-d) visual symptoms after six weeks of treatment at the respective copper concentration, (b) “0” nM Cu (c) 10 nM Cu, (d) 200 nM Cu.

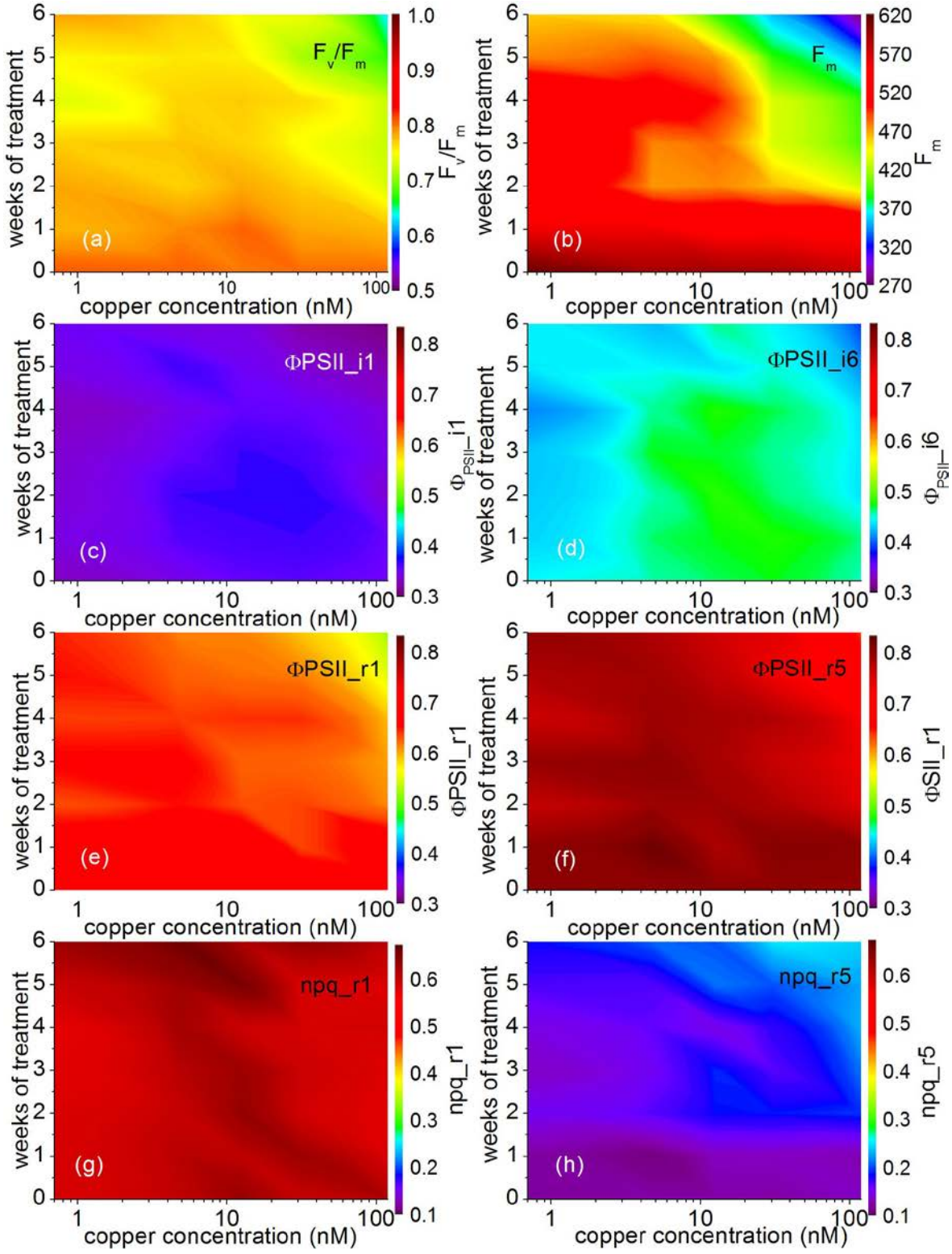

Figure 2. Effect of the different treatments of Cu on the photosynthesis biophysics measured by *in vivo* chlorophyll fluorescence kinetic measurements. Values are given as means of five different experiments with two replicates each. (a) Effect on the maximal dark-adapted photochemical quantum yield of the photosystem II reaction centre measured as

$F_v/F_m = (F_m-F_0)/F_m$, (b) effect on maximal fluorescence F_m in dark-adapted samples, (c, d) effect on light-acclimated electron flow through PSII measured as ($\Phi_{PSII} = (F_m'-F_t')/F_m'$) with Φ_{PSII}_i1 after 10 s of actinic light in (c) and Φ_{PSII}_i6 after 200 s of actinic light in (d), (e) Φ_{PSII}_r1 photochemical quantum yield of PSII after 10 s of relaxation in dark, (f) Φ_{PSII}_r5 = photochemical quantum yield of PSII after 200 s of relaxation in the dark, (g, h) effect of actinic light on the non-photochemical quenching of energy measured as $NPQ = (F_m-F_m')/F_m$) with NPQ_i6= after 200 s of actinic light in (g) and NPQ_r5= non-photochemical energy quenching after 200 s of dark phase in (h).

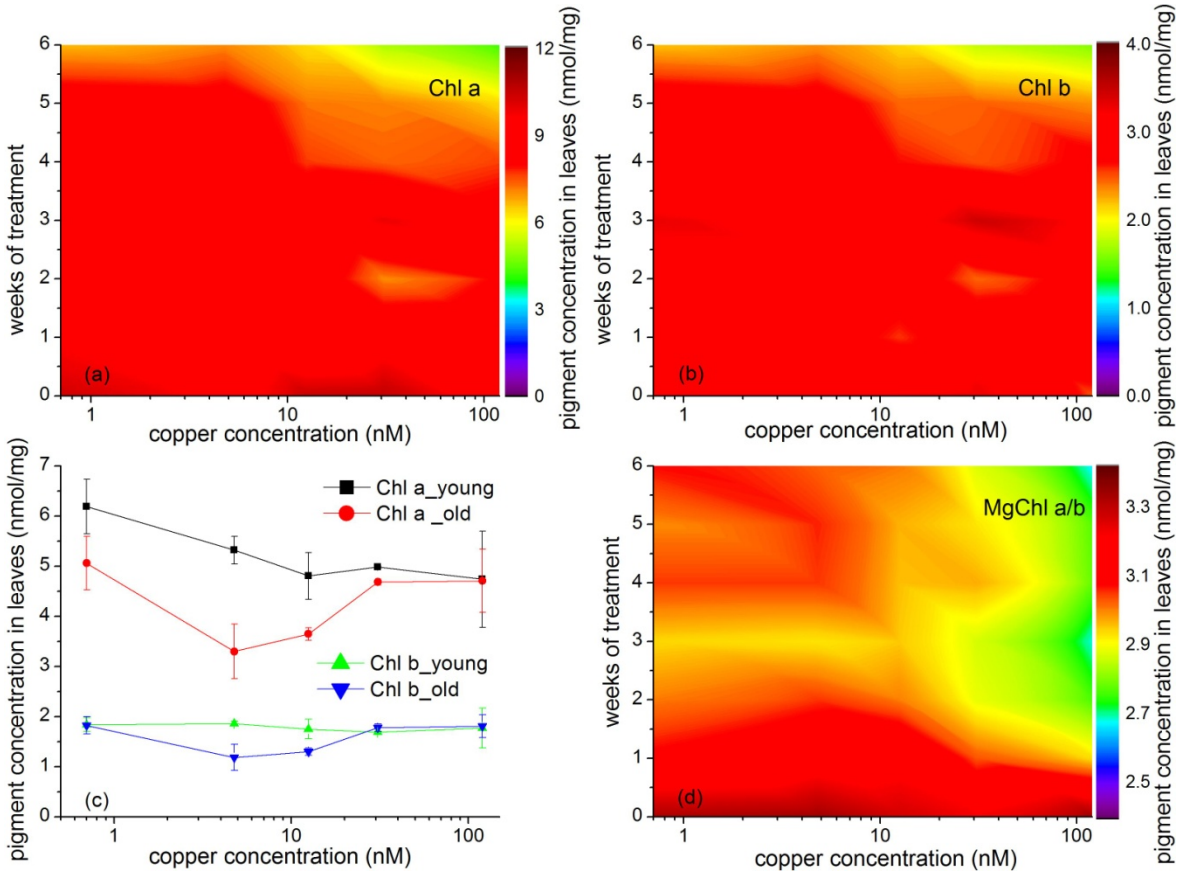

Figure 3. Effect of different treatments of Cu on photosynthetic pigments. Values are given as means of five different experiments, error bars represent standard error of the mean. (a) Chlorophyll a changes in young leaves during the six weeks of treatment, (b) chlorophyll b changes in young leaves during six weeks of treatment, (c) changes in chlorophylls measured in harvested young and old tissues after 6 weeks of Cu treatments, (d) changes in the ratio of the chlorophylls MgChl a and MgChl b in young leaves during the six weeks of treatment.

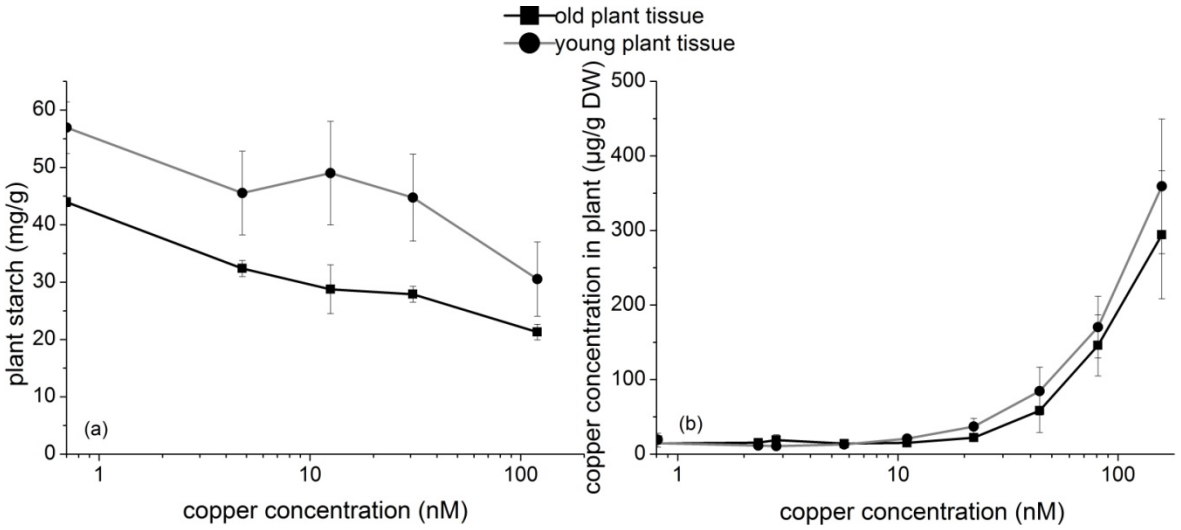

Figure 4. Effect of different treatments of Cu in the young and old tissues of the plant after six weeks of treatment (a) on the starch production or utilization. (b) on the metal accumulation. Values are given as means ± SE (n=4).

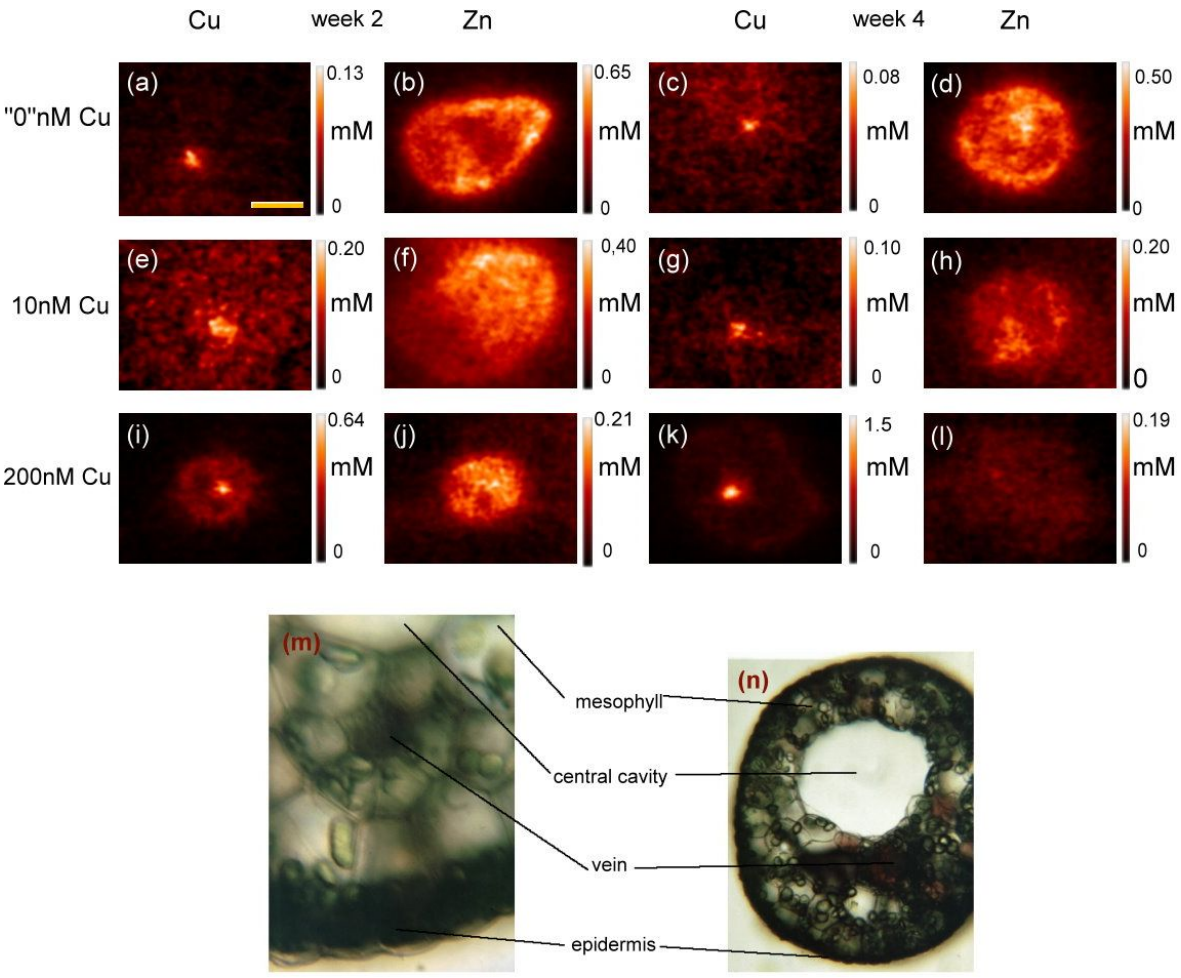

Figure 5. Metal distribution studies using µXRF in the Cu treated plants after 2 and 4 weeks of Cu treatment. Scale bar = 100 µm. Top row of images: “0”nM barrel Cu concentration, middle row: 10nM barrel Cu concentration, bottom row: 200 nM barrel Cu concentration. Left two columns of images: metal distribution after two weeks of treatment, right two column of images: metal distribution after four weeks of treatment. First and third column of images: Copper distribution; Second and fourth column of images: Zn distribution. (m, n) containing the light microscope picture of crossection through a *Ceratophyllum* leaf with tissue identification.

Appendix A. Supplementary data

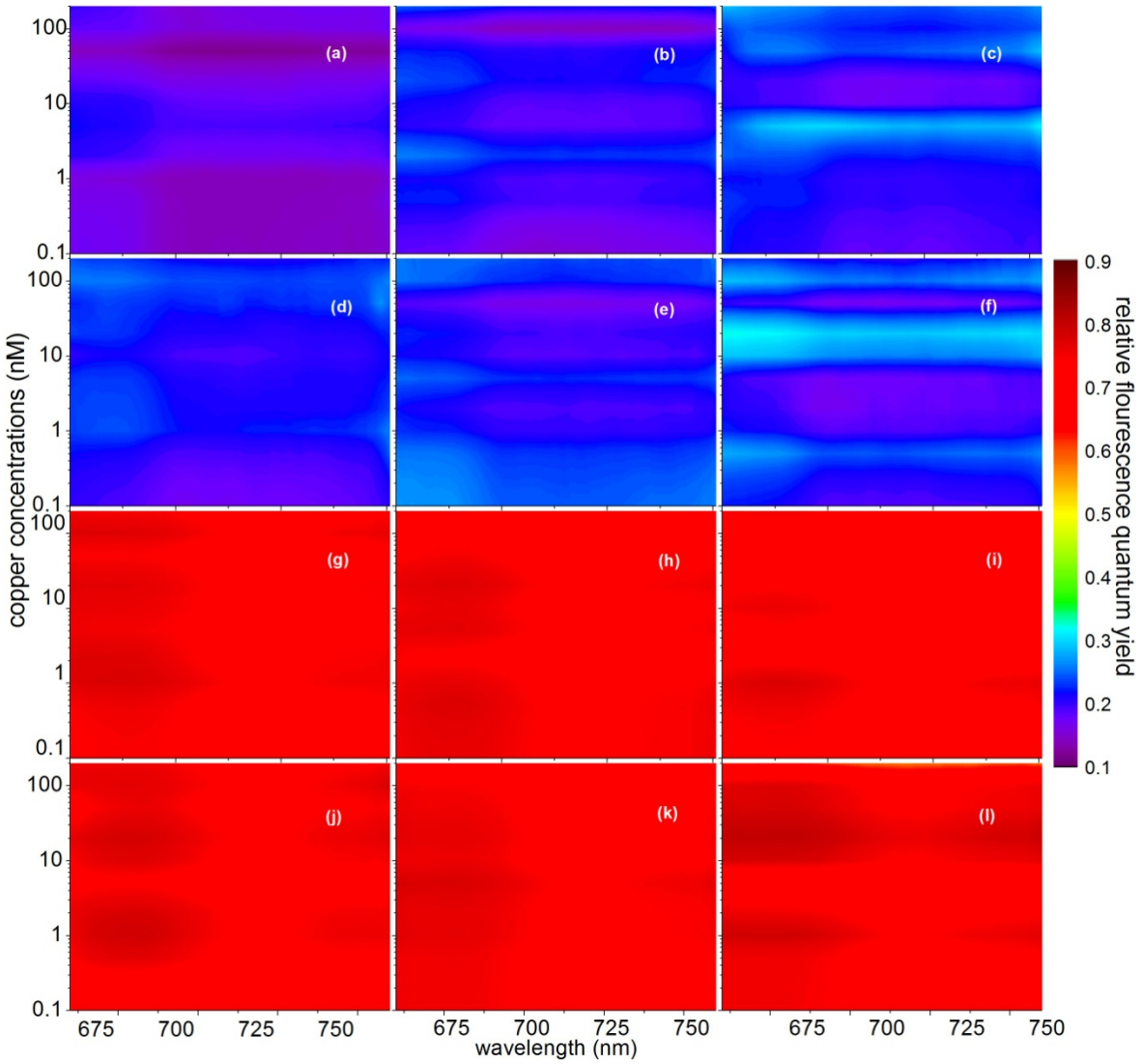

Supplementary Figure 1. Effect of different treatments of Cu under high light conditions on the non-photochemical quenching of energy measured by spectrally resolved *in vivo* chlorophyll fluorescence kinetics as NPQ = $(F_m-F_m')/F_m$.. Values are given as means of five different experiments. (a) NPQ_i6= non-photochemical energy quenching after 200 s s of actinic light after 1 week, (b) NPQ_i6 after 2 weeks, (c) NPQ_i6 after 3 weeks, (d) NPQ_i6 after 4 weeks, (e) NPQ_i6 after 5 weeks, (f) NPQ_i6 after 6 weeks, (g) NPQ_r5= non-photochemical energy quenching after 200 s of dark phase after 1 week, (h) NPQ_r5 after 2 weeks, (i) NPQ_r5 after 3 weeks, (j) NPQ_r5 after 4 weeks, (k) NPQ_r5 after 5 weeks, (l) NPQ_r5 after 6 weeks.

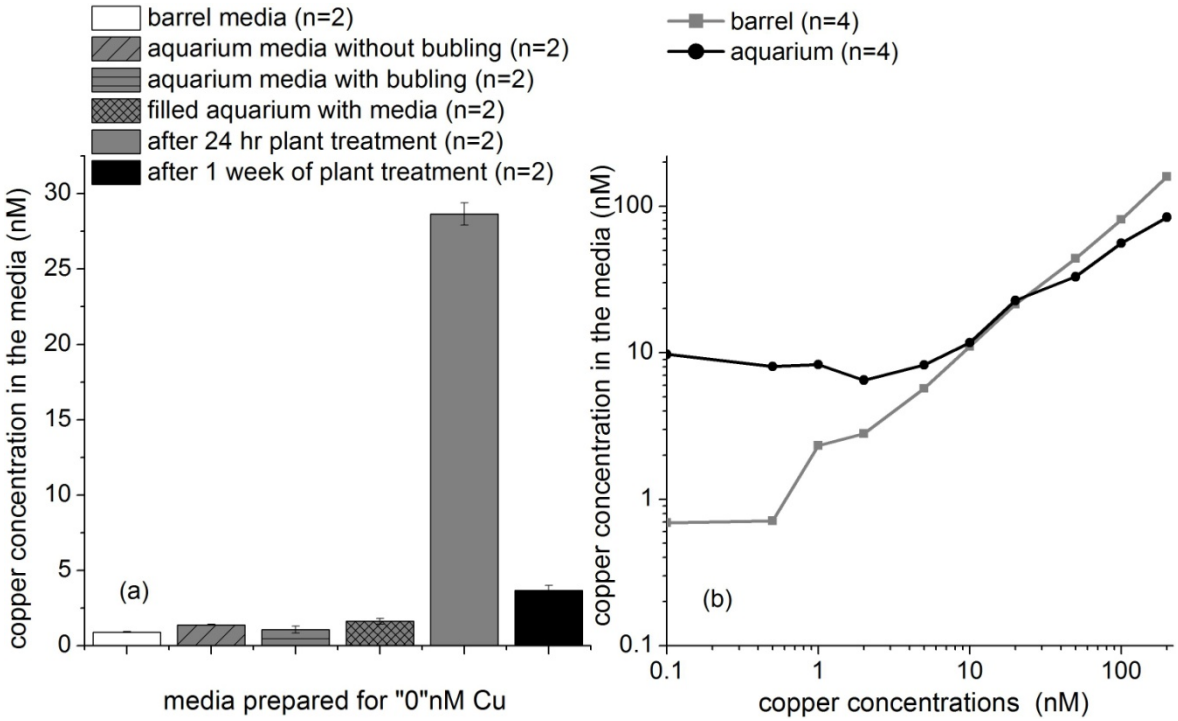

Supplementary Figure 2. Extra Cu entry in to the media prepared initially for "0" nM Cu concentration. Values are given as means ± SE. (n= number of replicates). (a) Comparison of the various possibilities of Cu entering into the media available to the plant, (b) media concentration in the aquaria and barrels after six weeks of plant treatment with deficient to toxic concentrations of Cu.

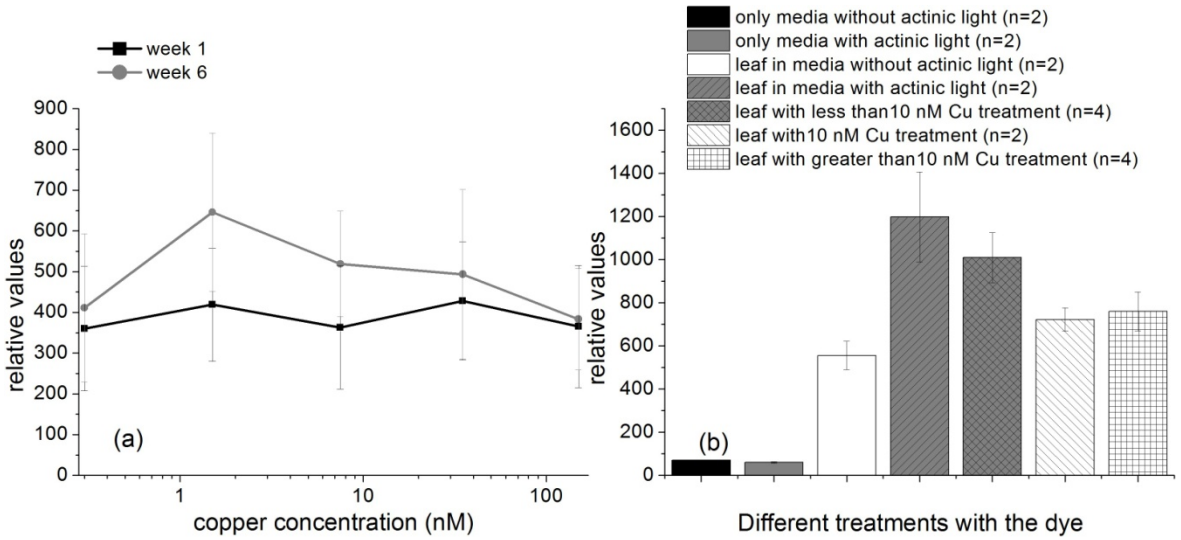

Supplementary Figure 3. H_2O_2 production in response to Cu treatments and actinic irradiation as determined by PF2 fluorescence. (a) H_2O_2 production from the leaf from the 1st and 6th week of treatment after actinic irradiation for 10 minutes. Values are given as means ± SE from three different experiments. (b) Comparison of the H_2O_2 production from the six week Cu treated plants after 10 minutes of actinic irradiation with the tests performed to study the hydrogen peroxide release in response to actinic irradiation. Values are given as means ± SE, n= number of replicates).

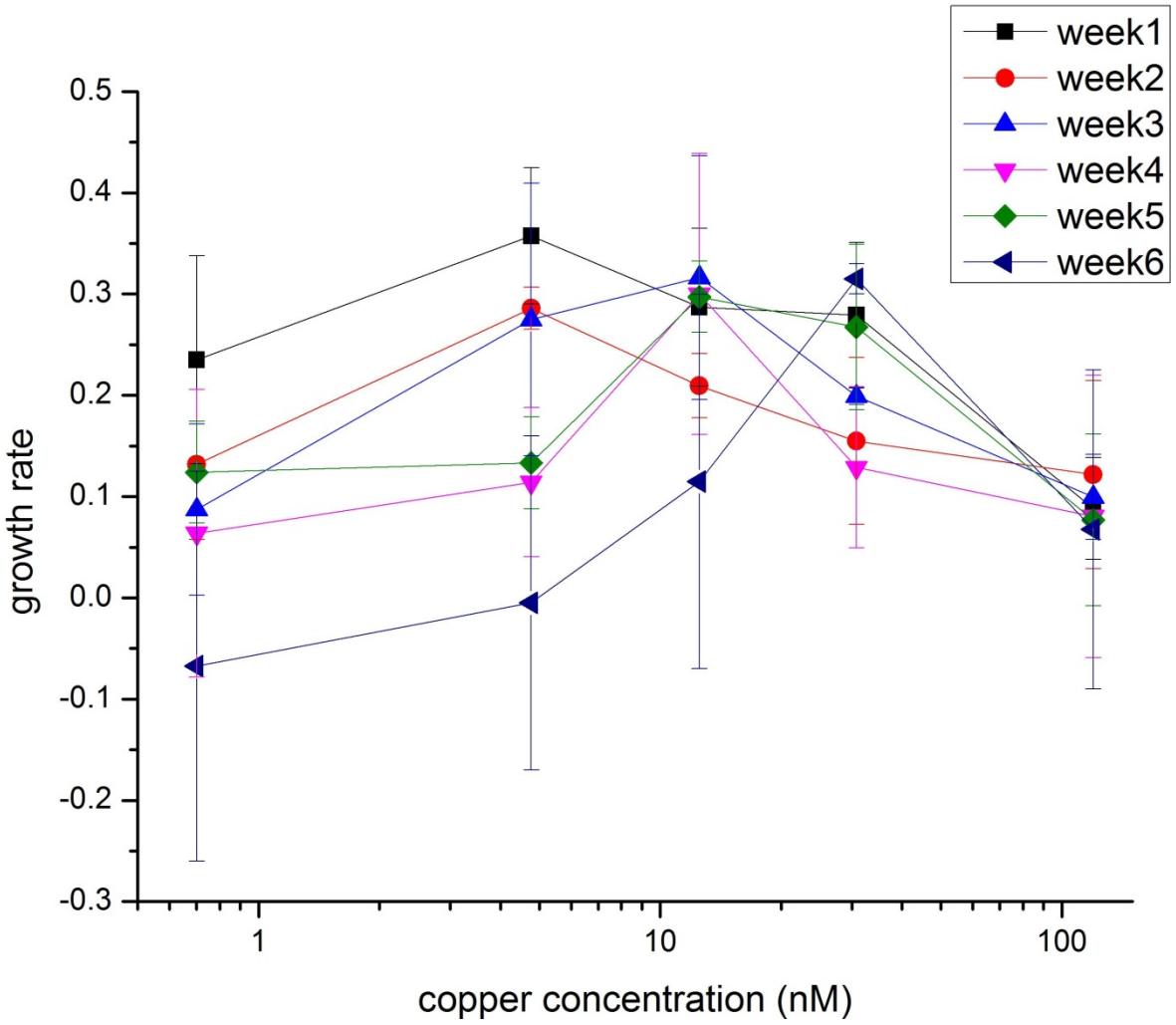

Supplementary Figure 4. Effect of the different treatments of Cu on the growth of the plants in high light. Growth rate of the plants per week calculated on the basis of fresh weight. Five experiments where performed. Values are given as means ± SE.

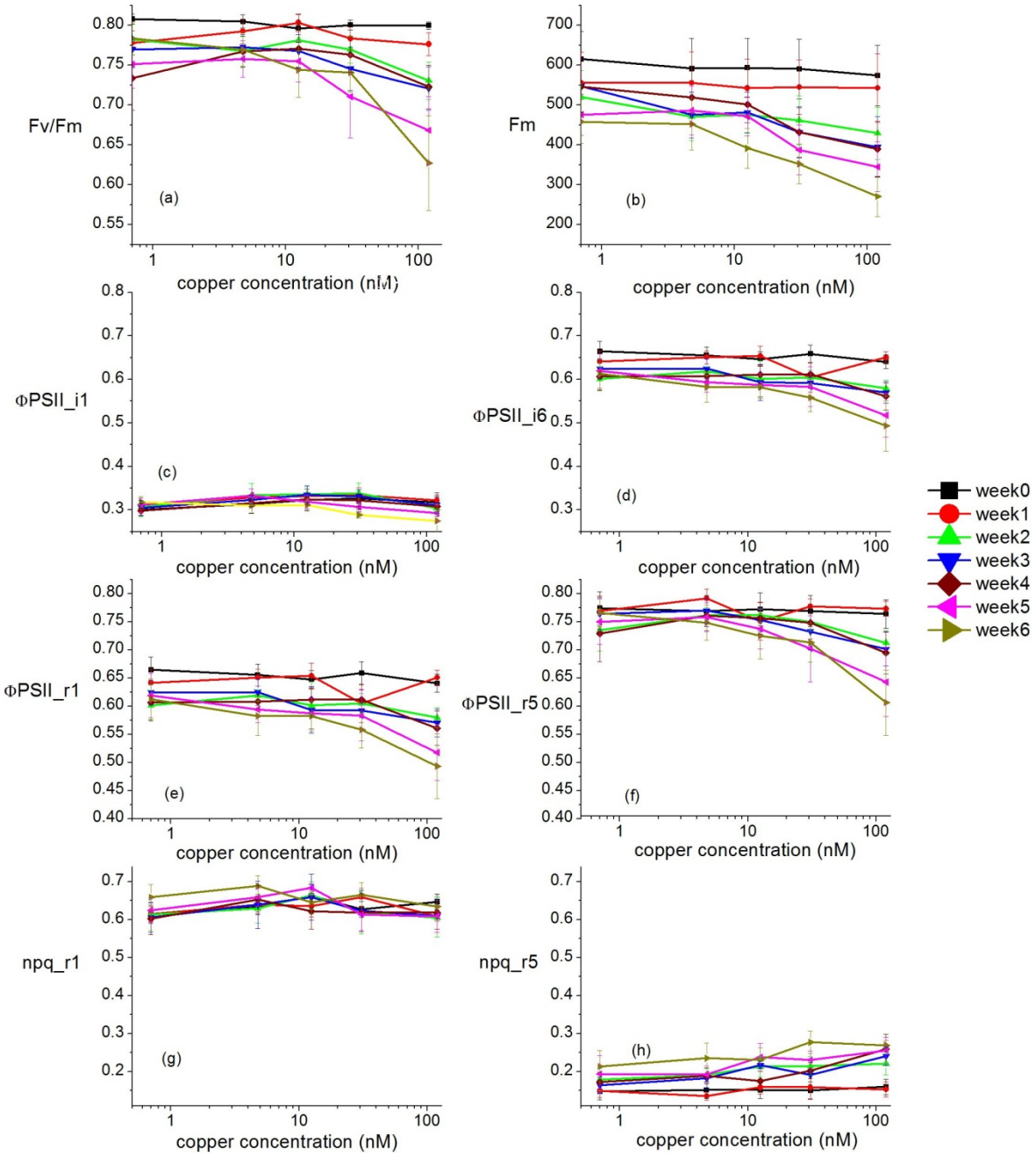

Supplementary Figure 5. Effect of the different treatments of Cu on the photosynthesis biophysics measured by *in vivo* chlorophyll fluorescence kinetic measurements under high light conditions with the different weeks of treatment. Five experiments where performed, with 2 replicated from each experiment. Values are given as means ± SE (a) Effect on the maximal dark-adapted photochemical quantum yield of the photosystem II reaction centre measured as $F_v/F_m = (F_m-F_0)/F_m$, (b) Effect on maximal fluorescence F_m in dark-adapted samples, (C, D) Effect on light-acclimated electron flow through PSII measured as

(Φ_{PSII} = (F_m'-F_t')/F_m') with Φ_{PSII}_i1 after 10 s of actinic light in (c) and Φ_{PSII}_i6 after 200 s of actinic light in (d), (e) Φ_{PSII}_r1 photochemical quantum yield of PSII after 10 s of relaxation in dark, (f) Φ_{PSII}_r5 = photochemical quantum yield of PSII after 200 s of relaxation in the dark, (g, h) Effect of actinic light on the non-photochemical quenching of energy measured as NPQ = (F_m-F_m')/F_m) with NPQ_i6= after 200 s of actinic light in (g) and NPQ_r5= non-photochemical energy quenching after 200 s of dark phase in (h).

Table S1: Composition of the nutrient solution optimised for growth of submerged macrophytes (SMNS, personal communication from HK, recipe of preparation and tests of performance will be published separately).

Substance	Concentration in the medium [µM]
Ca	40
Mg	150
K	119.4
Na	60.05
Cl	87.47
N	30
C	100
S	150.47
P	2
B	0.16
Co	0.01
Cr	0.02
Cu	0.01
Fe	0.4
Fe ligand: EDDHA	0.2
I	0.05
Mn	0.4
Mo	0.01
Ni	0.01
Zn	0.05
Hepes (as buffer)	500
pH (with KOH)	7.8

2.2. Effects of nanomolar copper on water plants in low irradiance – a metalloproteomic and physiological study

George Thomas[a], Jürgen Mattusch[b], and Hendrik Küpper[a,c] *

a) Universität Konstanz, Mathematisch-Naturwissenschaftliche Sektion, Fachbereich Biologie, D-78457 Konstanz, Germany . e-mail: george.thomas@uni.kn

b) UFZ – Helmholtz Centre for Environmental Research, Department of Analytical Chemistry, Permoserstr. 15, D-04318 Leipzig, Germany. e-mail: ha-jo.staerk@ufz.de.

c) University of South Bohemia, Faculty of Biological Sciences and Institute of Physical Biology, Branišovská 31, CZ-370 05 České Budejovice, Czech Republic

Drafted for Aquatic Toxicology

Abstract

Essential trace elements (Cu^{2+}, Zn^{2+}, etc) lead to toxic effects above a certain threshold, which is a major environmental problem in many areas of the world. Here, environmentally relevant sub-micromolar concentrations of Cu^{2+} and simulations of natural light- and temperature cycles were applied to the aquatic macrophyte *Ceratophyllum demersum*. In this low irradiance study resembling non summer conditions, growth was optimal in the range 10 - 20 nM Cu, while PSII activity (F_v/F_m) was maximal around 2 - 10 nM Cu. Damage to the light harvesting complex (LHC) was the first target of Cu toxicity (> 50 nM Cu) where Cu replaced Mg in the LHCII-trimer, leading to dissociation to monomers This was associated with decrease in the Chl content and a decrease in the the up-regulation of heat dissipation in respone to actinic light (NPQ). Growth rate decreased from the first week in copper deficiency at "0" nM Cu. The decrease in plastocyanin in the second week was associated with either removal of Cu from the active centre or decrease in its synthesis. This affected the electron flow through PSII (Φ_{PSII}). The pigment decrease added to the photosynthesis damage which resulted in decrease in starch and oxygen production.

Keywords: *Ceratophyllum*, biophysics of photosynthesis, chlorophyll fluorescence kinetics, copper deficiency, heavy metal stress, physiological stress, copper proteins, low light, LHCII proteomics.

1. Introduction

Copper is an essential plant micronutrient which belongs to the 3d transition elements along with Iron, Zinc, and others. In biological systems, the element usually shuttles between the two redox states: Cu(II) and Cu(I) (Solomon et al., 1992, 1996; Festa and Thiele, 2011). Most of the physiological processes of plants including photosynthesis, respiration, carbohydrate distribution, nitrogen reduction and fixation, protein metabolism, and cell wall metabolism (Sommer, 1931; Lipman and McKinney, 1931) are based on the participation of the enzymatically bound copper in the redox reactions (Marschner, 1995). Copper-binding proteins based on their spectroscopic properties and geometric structure of the active site are divided into three classes: type-1 or blue copper proteins, which are involved in electron-transfer (e.g., plastocyanin, halocyaninn and azurin); type-2 or non-blue copper proteins, which form part of the oxidoreductase family (e.g., galactose oxidase); and the type-3 or binuclear copper protein family, which comprises genes encoding tyrosinase, tyrosinase-related proteins, hemocyanin and catechol oxidase (Solomon et al., 1992, 1996; Mattar et al., 1994; Aguilera et al., 2013). During Cu deficiency or when there is removal of Cu from these enzymes, they become inactivated (Vallee and Wacker, 1970).

Copper has a particularly narrow beneficial range for the growth and development of the plant and becomes toxic after a particular concentration and causes deficiency effects on the plants when its concentration drops below the beneficial range. Thus the most important practical implications of the role of copper in plants are related to its deficiency and toxicity (Kabata- Pendias and Pendias, 1984).

The concentration of Cu in natural waters is less than 32 nM (Baccini, 1985), but these values reach up to 32 µM in polluted conditions mainly as a result of anthropogenic activities. These include industrial and domestic waste emissions, application of fertilizers, etc (Yamamoto et al., 1985; Zhang et al., 2003), resulting in the creation of copper toxicity for plants living in such environments (Moore and Ramamoorthy, 1984). Cu based pesticides and fungicides have been intensively used in European vineyards (Komárek et al., 2010), hop fields (Schramel et al., 2000; Komárek et al., 2009), coffee (Loland and Singh, 2004), apple orchards (Li et al., 2005) and also during cultivation of vegetables (Adriano,2001). This is currently a cause of public concern because of the resulting presence of these pesticide residues in water, fruits and wine products for human consumption (Jacobson et al., 2005).

The long term application and subsequent wash off from the fungicide treated plants have resulted in extensive Cu accumulation in these soils (Komárek et al., 2010).

The damage to photosynthesis is the main target of Cu excess in photosynthetic organisms (Küpper and Kroneck, 2005). Here the substitution of Mg^{2+} in the chlorophyll (Chl) molecule by heavy metal ions leading to the formation of heavy metal substituted chlorophylls ([Hms]-Chls) (Küpper et al., 1996, 2002). Unlike [Mg]-Chls, [Hms]-Chls are unsuitable for photosynthesis because of their less stable singlet excited state and lower tendency to bind axial ligands (Küpper et al., 2006). The excited energy from these altered chlorophylls may be accidentally transferred to oxygen resulting in the production of singlet oxygen, one of the reactive oxygen species (ROS) that causes oxidative damage (Pinto et al., 2003).

Symptoms of Cu deficiency including decreased growth rate, chlorosis of young leaves, curling of leaf margins and decrease in fruit formation were observed in plants when Cu decreased below 5 µg g^{-1}DW in the vegetative tissue (from review: Marschner, 1995). Cu deficiency leads to decrease in pigments (chlorophyll and carotenoids), damage to thylakoid membranes (Droppa et al., 1987), reduced plastoquinone synthesis, depressed CO_2 fixation (Bussler 1981) and decreased PSII activity (Thomas et al., 2013). The damage to the photosynthetic apparatus will divert absorbed light energy towards different processes, finally resulting in oxidative stress. Due to the decrease in Cu availability there is no proper functioning of Cu/Zn SOD, causing further rise of oxidative stress (Marschner, 1995; Küpper and Kroneck, 2005). Alteration of the functioning of electron transport chains in both the mitochondria and chloroplasts through the malfunctioning of the Cu proteins such as cytochrome c oxidase and plastocyanin where reported as a response of Cu deficiency (Andrés-Colás et al., 2013).

Earlier experiments used Cu concentrations much higher than environmentally relevant (e.g. from 1 µM to 240 µM; Palms et al., 1990) to show immediate response on physiology and protein biosynthesis with the time duration of the growth study between 10 h (Delhaize et al., 1985) to 13 d (Delhaize et al., 1986).

We used the model plant *Ceratophyllum demersum* L., which is an aquatic submerged macrophyte (without roots, all nutrients are taken up over a large surface area of the entire shoot) sensitive to heavy metal stress (from earlier studies Küpper et al., 1996; Mishra et al., 2008, 2009; Andresen et al., 2013; Thomas et al., 2013). They are dormant during winter season, forming buds that sink to the bottom of the lake or river, and have maximal growth

rate while swimming at the surface in summer conditions (Best, 1977). Thus, both in the transition periods in spring and autumn, as well as in shaded habitats and during cloudy/rainy days, *Ceratophyllum* grows in low light. At the same time, effects of metals strongly differ depending on the irradiance (see above). Therefore, plant responses to Cu stress should ideally be studied both in low light as in the current study, and in high light conditions (Thomas et al., 2013). The proteomics and the physiological response of the plant to environmentally relevant Cu concentrations from deficiency through optimal to toxic Cu concentrations were studied with the kinetic pattern and the concentration thresholds of the occurrence of different damage mechanisms.

2. Material and Methods

2.1 Plant material and cultivation

Ceratophyllum demersum L. plants were cultivated in an optimized nutrient solution for submerged macrophytes and water plants (SMNS, as used in Thomas et al., 2013). The strain was continuously cultivated since 2005 in hydroponic cultures under 12 h day/12 h night light conditions with two Osram FLUORA® fluorescent and two warm white fluorescent tubes and a temperature cycle from 18°C at 6 a.m., over 20°C at 9 a.m., to a maximum of 22°C at 3 p.m., back over 20°C at 9 p.m. to 18°C again at 6 a.m.. During the low light experiment, a slightly different set up was used, with "daylight" fluorescent tubes set to 12 h sinusoidal light cycle with maximal irradiance at 38- 40 µE inside the media and 12 h night. The temperature cycle was 19°C at 6 a.m., 21.5 at 9 a.m., 24 at 3 p.m., 23 at 9 p.m., 19 at 6 a.m.

For each copper treatment (“0”, 0.5, 1, 2, 5, 10, 20, 50, 100, 200, 500 prepared by $CuSO_4$), around 2 g of plants were placed into an aquarium. This contained 2 l of continuously aerated medium to secure a low biomass to water volume ratio for each treatment. In order to ensure that the metal uptake into the plants was limited only by the concentration, but not by the amount of nutrient solution available, a continuous exchange of nutrient solution (flow rate 0.5 $l.day^{-1}$) was set up. After each week, the plants were cleaned and the change in growth was measured after shaking off the remaining SMNS. Each experiment was carried out for 6 weeks, at the end of which the plants were harvested (removing the SMNS by shaking) and separated into young tissues, being 4 cm from the apex

and 2 cm from the apex of each side branch, and old tissues, being 8 cm from the stem end and the rest of the side branches. Samples were immediately frozen in liquid nitrogen and stored at -80°C until further analyses.

2.2 Photosynthesis Biophysics

The two-dimensional (imaging) microscopic measurements using the Chl fluorescence kinetic microscope (Küpper et al., 2007a) were performed to study changes in photosynthesis in response to copper. One leaf from the 5^{th} nodium, counted from the apex of the plant, from each week of treatment, was fixed in the measuring chamber with the help of cellophane. There was a continuous flow of the culture medium in the chamber (Küpper et al., 2008) that was used for the kinetics measurement. An area (approximate size of 1.1x1.1 µm) just before the last leaf branching point was measured. A detailed description of the microscope, the used protocols and analysed parameters of the Kautsky induction can be found in Küpper et al., 2007a.

2.3 Oxygen Exchange.

The whole content of one aquarium (1-3 plants) before the Cu treatments and after six weeks of Cu treatments was placed into a 200 ml measuring chamber (lab-made), maintained at 25°C and oxygen exchange was measured by a WTW CellOx 325 oxygen electrode connected to an inoLab Oxi 740 terminal (Wissenschaftlich-Technische Werkstatten GmbH, Weilheim, Germany). Oxygen uptake by dark respiration was measured by applying darkness for 20 min. Subsequently, net photosynthetic oxygen release was measured by exposing the plant to increasing irradiance. At the end, respiratory oxygen uptake in darkness was measured again. Data were recorded using the OxyCorder device with the software Oxywin 2.71 (Photon Systems Instruments, Brno, Czech Republic) and further data analysis was done in Origin Professional 8.1 (Originlab, Northampton, USA). The data are the mean of two different experiments.

2.4 Determination of pigment content

Pigments were extracted from the harvested plant material. Samples were lyophilized and ground with sand and a few grains of Bis-Tris (Sigma-Aldrich, St Louis, MO, USA) and

extraction of pigments was performed in 1 ml 100% acetone at 4°C overnight. The pigment extraction and determination were performed using established protocols by Küpper et al. (2007b, 2000b) as described in Thomas et al. (2013). Values are given as means of three different experiments.

2.5 Starch quantification

The amount of accumulated starch in the harvested plant samples after 6 weeks of treatment were analysed using the Total starch assay kit (AOAC Method 996.11 and AACC Method 76.13; Megazyme, Wicklow, Ireland) with an established protocol that was optimised for our demands (Thomas et al., 2013). Values are given as means of two different experiments.

2.6 Elemental analyses of digested plant samples

Following the protocol of Zhao, McGrath & Crosland (1994), 5-10 mg of lyophylized plant samples were digested in 250 µl (85:15%) nitric-perchloric acid for 30 min at room temperature and then gradually heated up to a maximum of 195°C until all liquid was vaporized. The remaining salts were re-dissolved in 0.5 ml 5% HCl, gradually heated to 80°C. The samples were allowed to cool and then the volume was filed to 1.5 ml with ddH_2O and used for analyzing the components by graphit furnace atomic absorption spectrometry (GBC 932 AA). The data are the mean of three different experiments.

2.7 Isolation of proteins

For isolation of protein, 400 mg of frozen harvested plants were ground to fine powder in a mortar cooled with liquid nitrogen. Isolation buffer (IB: 750 mM aminocaproic acid, 50 mM Bis-Tris, pH 7.6, 2% PVP 360 kDa, 1.2 mg/ml Protease Inhibitor Cocktail tablets "complete" EDTA-free from Roche Diagnostics, Mannheim, Germany) was also frozen by dropping into liquid nitrogen and ground with plant material in 1:1 (w/v) ratio. The powdered mixture was placed on ice for thawing. After thawing, the suspension was mixed with another 400 µl of IB and pipetted into a 1.7 mL ultracentrifuge tube (Beckmann, Palo Alto, CA, USA) and centrifuged for 1 h at 134,000x*g* at 4°C in a Beckman LE 80K preparative ultracentrifuge (Beckmann, Palo Alto, CA, USA). The supernatant was centrifuged immediately again for 10-60 min at 16,000x*g*, 1°C in a microcentrifuge (Centrifuge 5415 R, Eppendorf AG,

Hamburg, Germany) to remove the inadvertedly re-suspended pieces of pellets and was used for the soluble protein analysis. The pellet from the ultracentrifugation was washed twice by resuspendig it with IB and repeating the ultracentrifugation step, discarding the supernatant. The pellet was mixed with solubilisation buffer (750 mM aminocaproic acid, 50 mM Bis-Tris, pH 7.0 with HCl at 1-2°C - neutral to avoid allomerisation and saponification of Chl, 2% DDM, 1.2 mg/mL complete® protease inhibitor) and stirred overnight at 4°C. The supernatant, after centrifugation twice as mentioned above, was used for the analysis of the membrance proteins. The protein samples were stored on ice in the dark.

2.8 Metalloproteomics

The soluble and membrane protein fractions were each separated further through size exclusion chromatography. For separation, either one or two Superose 12 10/300 GL columns (GE Healthcare) were coupled in series in an Agilent 1100 series HPLC system (Agilent, Santa Clara, California, USA) equipped with two detectors: A UV/VIS absorption diode array detector (G1315B) and an inductively coupled plasma mass spectrometer (Agilent 7500ce ICP-MS) was used**.** Calibration of the molecular weights was performed with the standard 151-1901 from BioRad (Hercules, California, USA). In order to have identical conditions for the standard and the samples, the standards were dissolved in isolation buffer for the soluble protein analyses and in solubilisation buffer for the membrane protein analyses. The concentration of the standard injected into the chromatography column contained 0.5 $mg.ml^{-1}$ each of bovine thyroglobulin (670 kDa), bovine γ-globulin (158 kDa), chicken ovalbumin (44 kDa), and 0.25 $mg.ml^{-1}$ horse myoglobin (17 kDa) and 0.05 $mg.ml^{-1}$ vitamin B12 (1.35 kDa). Vitamin B12 (cobalamin) was added to all samples as an internal standard for calibration of the column. The samples were cleaned through a 0.2µm filter and 40 µL of sample (equiv. to 20 mg fresh biomass) containing 0.01 $mg.ml^{-1}$ vitamin B12 was injected into the column. All the samples were eluted with 150 mM ammonium hydrogen carbonate (LC-MS grade, Sigma-Aldrich, USA), pH 7.8 with 25% aqueous ammonia.

3. Results

From the whole range of parameters analysed on the response of the plants to copper from deficient via optimal to toxic concentrations, it was possible to establish the threshold concentrations and time sequence of events leading to optimal or suboptimal growth in low light conditions.

3.1 Visible symptoms

The plants looked healthy with green leaves and strong meristems with maximum growth rate in the range between 10 nM to 20 nM Cu especially towards the sixth week of treatment (Fig. 1). The plants did not show any visible symptoms of tox icity at the higher concentrations, but the growth rate did not reach the maximum when compared to the control (10 nM Cu as used in stock cultures) at any point of time. But the toxicity symptoms were severe above 200 nM Cu where negative growth rate, decrease in chlorophyll pigments, shrinking of the plant and loss of leaves from the stem had been reported. These plants died after the fourth week. Deficiency was registered with a reduction in growth rate from the first week mainly at "0" nM Cu. The deficiency of Cu from 1 nM Cu was registered in the fourth week with a decrease in growth rate. The deficiency symptoms such as decreased leaf size, fragile stem, loss of leaves from the bottom of the stem were registered only in the “0” nM Cu after six weeks of treatment.

3.2 Photosynthetic parameters by FKM

Changes in photosynthetic light reactions were identified using the fluorescence kinetic analysis. F_v/F_m, which measures the photosynthetic quantum efficiency of PSII RC in dark adapted state, was maximal between 2 nM and 10 nM Cu for most of the experiments (Fig. 2b). There was a decrease towards the higher Cu concentrations from the fourth week.

The photochemical activity of PSII in actinic light, which is related to electron flow through PSII (Φ_{PSII}i1 and Φ_{PSII}i6, also called "photochemical quenching", Genty et al., 1989), generally was optimal around 10 nM Cu. It decreased from the first week mainly in the deficient Cu concentrations compared to optimal Cu, when measured at the start of illumination (Φ_{PSII} i1). It also decreased in the most toxic Cu concentrations from the third week with the lowest values in the sixth week (Fig. 2c). Similar trends were observed also after longer time of illumination mainly at the deficient Cu treatments (Φ_{PSII} i6: Fig. d). The

recovery of PSII to the dark relaxed state was measured both at the start (Φ_{PSII} r1: Fig. e) and end (Φ_{PSII} r5: Fig. f) of the recovery time, after the actinic light was switched off.

There was a slight decrease in the non-photochemical quenching (NPQ = up-regulation of exciton dissipation as heat in response to actinic irradiance, measured as $(F_m-F_m')/F_m$) both in the light phase (NPQ i1 and NPQ i6, data not shown) and its relaxation in the dark phase (NPQ r1 and NPQ r5; Fig. 2g, h) from the fifth week of treatment at the toxic concentration while no changes were observed in other concentrations.

3.3 Pigment composition

The pigments were extracted from the harvested young and old plant tissue after the sixth week. The Chlorophyll a content decreased towards deficient and toxic Cu concentrations with the highest Cu concentration showing the maximum decrease compared to the optimal Cu plant in the old plant tissue (Fig. 3). There wasn't a remarkable change in the carotenoids

3.4 Oxygen production

To assess overall impact of hampered photosynthetic parameters on gas exchange, the oxygen production was measured before the Cu treatments and after six weeks of treatment. Plants at deficient Cu concentrations had a strong decrease in oxygen release per fresh weight at higher irradiances when compared to the control plants. A slight decrease of photosynthetic oxygen release was noticed in plants that suffered from toxic Cu concentrations (Fig. 4).

3.5 Starch accumulation

The starch content of the plant was measured after six weeks of treatment. At deficient Cu concentrations, plants had lower starch than those at optimal Cu. In contrast, starch accumulation increased towards toxic Cu, mainly in the old tissues. Generally, there was higher starch content in the younger parts of the plant compared to the old (Fig. 5)

3.6 Metal accumulation

Metal accumulation was measured on the harvested young and old plants. There was a strong accumulation of Cu after 10 nM Cu (while it remained stable until this concentration) in the

nutrient solution. It reached a maximum of 400 ppm at 200 nM Cu concentration. The young tissues had slightly more metal accumulation compared to the old tissues (Fig. 6).

3.7 Proteomics

The Cu containing proteins in soluble and membrane protein fractions were separated and identified using the size exclusion liquid chromatography coupled to ICP-MS and UV/VIS spectroscopy. In the soluble fraction, the ICP-MS showed three major peaks of Cu at 30, 56 and 68 min corresponding to peak no. 1, 2 and 3 respectively (Fig. 7, 8, 9). These peaks were present in all soluble fractions isolated from different Cu treatments, however, in varying ratios with varying Cu treatment concentrations. The peak 1 had the highest protein content as observed from the UV-Vis signal at all concentrations. The intensity of the Cu peaks (1, 2 and 3) increased from 20 nM towards 200 nM treatments (Fig. 9f, h, j, l). This was associated with a decrease in Zn signal in ICP-MS. Cu deficiency, when compared to the control, was associated with a decrease in Cu peaks (1, 2 and 3) accompanied with an increase in the Zn peaks as observed by ICP-MS (Fig, 7, 8). The molecular mass of major Cu peaks 1, 2 and 3 were around 550, 45 and 6 kDa, respectively, as derived from the molecular weight standards calibration curve (Fig 1b). Zn peaks were also found at these same molecular mass but slightly shifted in the ICP-MS chromatogram.

In the membrane fractions, the ICP-MS showed five peaks of Cu at 29, 48, 55, 69 and 78 min corresponding to peak no. 1, 2, 3, 4 and 5 respectively (Fig. 10, 11). These peaks were present in all membrane fractions isolated from different Cu treatments, except peak 3 at “0” nM Cu treatment. They occurred, however, in varying ratios with varying Cu treatment concentrations. Increase in the intensity of all the Cu peaks was observed from 20 nM towards 200 nM Cu treatments (Fig. 11h, j, m, o). This was associated with a decrease in Zn peaks. The molecular masses of major Cu peaks 1, 2, 3, 4 and 5 were around 530, 48, 21, 3 and 1.5 kDa, respectively, as derived from the molecular weight standards calibration curve (Fig 1b). The Mg peak with the elution time of 43 min (which corresponded to 85 kDa) decreased with increase in Cu concentration. This was accompanied with a simultaneous increase in the peaks associated with Mg and Cu (peak 3) at the same elution time of 48 min (which corresponded to 30 kDa), especially in the 100 nM (Fig 11m) and 200 nM (Fig 11o) Cu treatments.

4. Discussion

The whole range of responses of the aquatic model plant *C. demersum* to Cu from deficient, via optimal to toxic copper concentrations under low light conditions was studied by biophysical and biochemical methods. These results where compared to the earlier study under high light conditions (Thomas et al., 2013) and thus yielded better understanding of the time and concentration thresholds of different previously proposed damage mechanisms. In the current study, further new insights were yielded by complementing the array of methods with metalloproteomics - an analysis of changes in copper binding to proteins, including replacement of native metal centres in proteins.

The Cu concentrations in the range between 10 nM and 20 nM, was noted as the optimal Cu concentration for the proper growth and functioning of the plant as observed from the various responses ranging from physiological to proteomics, in these plants when compared to other Cu concentrations. The major Cu proteins in the soluble fractions (Fig. 7, 8, 9) from our metalloproteomic analysis could be identified with the molecular weights associated with the Cu peaks 1, 2 and 3 corresponding to Rubisco (540 kDa), SOD (35 kDa) and Plastocyanin (10.5 kDa). Increase in the level of the Cu signal in ICP-MS could be related to either an increase in the level of Cu proteins, increased physiological copper loading of these proteins (less empty binding sites) or incorporation of Cu at unphysiological sites of proteins. The former two cases might lead to enhanced metabolic performance, while the latter would lead to toxicity. In a similar way, a decrease in the Cu-peaks at decreasing Cu concentration could be related to a decrease in the amount of Cu protein or removal of Cu from their active centres. In the membrane fractions, only one major Cu containing protein could be identified by its size and Mg content; this was the monomeric version of LHCII, where the insertion of Cu could be by replacement of Mg (peak 2). The other peaks could not be identified yet. It is possible that Cu gets bound to other proteins as well. This will be discussed further in the following sections.

4.1 Copper deficiency

Copper deficiency was associated with a decrease in growth rate. The deficiency was attained for “0” nM Cu in the nutrient solution already from the first week of treatment, when Cu

limitation became significant in the growth, which further decreased towards the sixth week. This pattern was similar to the high light conditions, when the plants utilized an internal reserve of Cu for their normal functions during the initial weeks, after which deficiency symptoms occurred, affecting growth (Thomas et al., 2013). This became more clear from our metalloproteomics analysis, where the Cu binding to proteins (including SOD, plastocyanin, etc) decreased below optimal Cu concentration (Fig. 7, 8). There could also be a release of copper from the plant tissues into the nutrient solution if the Cu^{2+} concentration in the nutrient solution is below 10 nM as shown in the high light experiment (Thomas et al., 2013), which indicated that *C. demersum* does not have copper transporters suitable to achieve an active uptake below this threshold concentration. Comparison of the low light and high light studies also indicates that increase in light intensity added to the Cu deficiency stress within the plant. Studies state that light stress along with the Cu deficiency would exacerbate oxidative stress (Yu and Rengel, 1999). The Cu deficiency in these conditions leads to a disruption of the carbon assimilation and /or impairment of the photosynthate transport, which further increases the production of reactive oxygen species (ROS) (Bowler et al., 1992). These may have been responsible for the negative growth rate in high light conditions (Thomas et al., 2013).

In Cu-deficient conditions, electron flow between the photosystems became limiting. $\Phi_{PSII}i1$ and $\Phi_{PSII}i6$ decreased at deficient copper, while no inhibition of the photochemical yield of PSII by copper deficiency was found before (F_v/F_m) (Fig. 2). The Cu peak 3 in the soluble fraction (with molecular weight and specific UV-Vis signals at 597 nM both corresponding to plastocyanin) was reduced at deficient Cu concentrations (Fig. 7, 8). Since the corresponding protein-specific absorption peak (OD278 nm) did not decrease, this indicates a removal of Cu from the active centre of the protein. This and also earlier studies (Baszynski et al., 1978) suggests that Cu deficiency hampers the plastocyanin formation and functioning which in turn reduces the electron transport from PSII to PSI both in high light (Thomas et al., 2013) and low light conditions.

The plant tried to rescue plastocyanin by various means, including downregulation of SOD and making the Cu available to plastocyanin as it was observed in *Arabidopsis* (Abdel-Ghany and Pilon, 2008), where furthermore the Fe-SOD gene was strongly induced when the Cu-SOD gene was downregulated (Abdel-Ghany et al., 2005). There could also be an induction of Zn-SOD in our experiment as there was an increased concentration of Zn in deficient conditions as shown by the metalloproteomics (Fig. 7, 10), and a recent µXRF study

(Thomas et al., 2013). This agrees with the reports on the compensatory absorption of micronutrients under deficiency stress (Del Rio et al., 1978).

4.2 Copper toxicity

From earlier studies, even though toxicity thresholds vary between plant species, the inhibitory effects were visible when the plant Cu concentrations were higher than 20 ppm (Gupta, 1979; Stevenson, 1986, Marschner, 1995). Here as well, plants were able to tolerate up to a threshold level (internal Cu concentration of around 20 ppm), which was at the 10 nM Cu treatment in the nutrient solution (Fig. 6). At higher copper concentrations, i.e. already directly above the optimum Cu concentration, accumulation of Cu in the plant increased, which indicated the loss of control over the intracellular copper. The Cu peaks associated with the proteins increased from this threshold in both the soluble and membrane fractions (Fig. 8, 9, 11).

It was clear from the comparison of high and low light experiments that the irradiance also plays an important role in the toxicity. In high light, toxicity was observed with visible toxicity symptoms and growth reduction at Cu concentrations greater than 50 nM after six weeks (Thomas et al., 2013). These symptoms were not observed in low light conditions, though the optimum growth rate was not attained. However, the plants could not tolerate a Cu concentration above 200 nM even in low irradiance as in the current experiment. The growth rate decreased from the first week of treatment above this concentration, which was associated with a decrease in chlorophyll and loss of leaves from the stem (data not shown). At 500 nM Cu the plants were dead after four weeks of treatment

The decrease of Zn with increased Cu concentration indicates a displacement of Zn by excess Cu concentration from the plant (Frausto da Silva and Williams 2001; Dudev and Lim, 2013). This agreed to the Zn peaks in the metalloproteomic analysis (Fig. 9) and the µXRF study (Thomas et al., 2013). Here the young tissues where more active in Zn displacement compared to old tissues. This would also indicate a Zn deficiency adding to the stress caused by Cu toxicity in the plant.

Copper accumulated more in the younger than in the older parts of the plant (Fig. 6). This stronger uptake in metabolically more active parts of the plant (as shown by the generally higher starch contents in young compared to old tissues) indicates that copper was actively taken up both in the deficient and toxic Cu treatments.

The low light conditions used in the experiment partially depicted the "shade reaction" type of damage to the photosynthesis process, meaning damage mostly to the LHCII antenna (Küpper et al., 1996). This is a very indication of damage of the LHC complex, which is a clear pattern of shade reaction (Küpper et al., 1996, 2002) where Chl a of the antenna of the LHC is more accessible to Cu substitution resulting in formation of Cu-Chl resulting in decrease of the minimal and maximal quantum yield of in vivo Chl fluorescence (F_0 and F_m,) at the toxic concentrations. Further, there was a decrease in the fluorescent parameters towards toxic copper concentrations including F_v/F_m and Φ_{PSII} along with a decrease of Chl a, indicating that in contrast to earlier reports of "shade reaction" (e.g. Küpper et al., 1998, 2002) non-functional photosynthetic units with >0 fluorescence emission existed.

LHCII is isolated as a trimer of polypeptides with molecular weight of the monomers between 25- 28 kDa (Kühlbrandt et al., 1994). By the size exclusion chromatography at the optimal Cu conditions we could clearly separate out the Mg peak corresponding to the trimer with an elution time at 43 min (which corresponds to 85 kDa from the MW. standard calibration curve) followed by a smaller Mg peak with an elution time at 47 min (corresponding to around 30 kDa), resembling the LHCII monomer peak (Fig. 10h and 11h). In the current study, the trimer peak decreased at toxic Cu. This is in agreement with studies which suggest that during light stress (Garab et al., 2002) or heavy metal stress (Janik et al., 2010), the release of Mg ion from the trimer would result in the formation of monomers. This would affect the light harvesting and quenching mechanisms in the plant (Horton et al., 1996), resulting in damage to the photosynthesis. This is consistent with the decrease in NPQ and Chl a at the toxic Cu concentrations from the fifth week of treatment at 100 nM and 200 nM (Fig. 2g, i). Studies in *Secale cereal* state that heavy metal stress had different responses on the LHCII based on the type of metal ions. Cd toxicity (50 µM) enhanced the trimerization and Cu toxicity (50 µM) increased the complex aggregation as was observed from the Chl a fluorescence emission (Janik et al., 2010). Speculations have been made based on the findings by Fagioni et al. (2009) that Cd response on the Lhcb proteins are by post-translational or gene expression modification (Janik et al., 2010) while Cu doesn't affect the expression of the Lhcb gene (Atienza et al., 2004). The decrease of the trimer peak together with the increase of Cu and decrease of Mg in the monomer peak (Fig. 11m, o) and the decrease of F_0 strongly supports the interpretation that a Cu replacement of Mg in the Chls of the LHCII took place as a result of the shade reaction type of damage (Küpper et al., 1996, 2002). This Cu replacement in the LHCII would induce conformational changes in the pigment-protein

complex because Cu-Chl does not have axial ligands (Boucher and Katz, 1967) that are required for Chl binding to the protein (Rebeiz and Belanger, 1984). Since Chl binding is required for correct LHCII folding (Paulsen et al., 1993), the formation of Cu-Chl will ultimately lead not only to dissociation of the trimeric LHCII but finally result in denatured monomers.

Acknowledgments

We are grateful for the financial support by the DFG (grant KU 1495/8) and basic funding of Universität Konstanz to HK. Initial work by GT in the lab of HK was supported by the DAAD (IAESTE programme). We also thank Elisa Andresen for the support in the protein isolation and Stefan Strungaru for the support in data analysis.

Figures

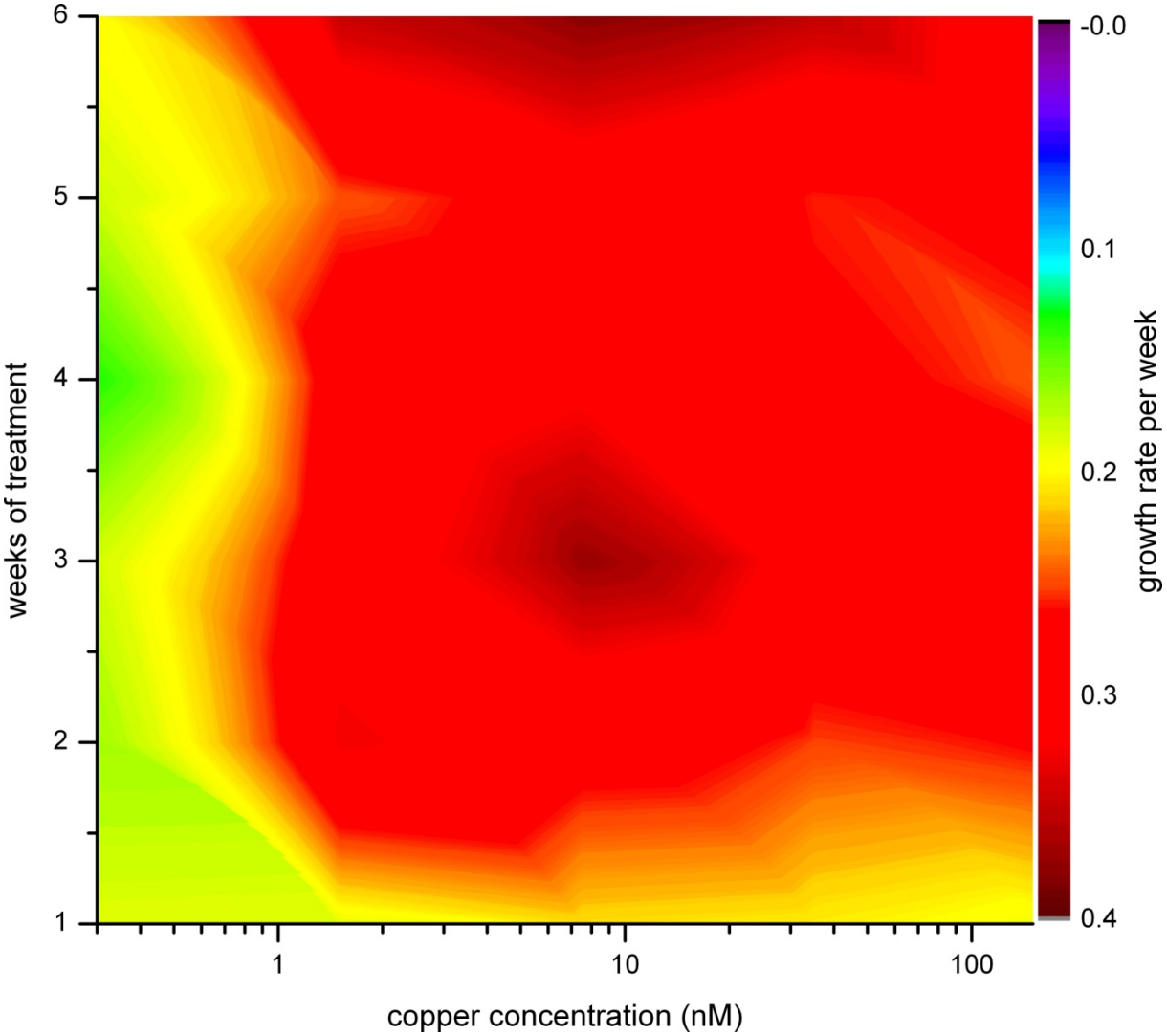

Figure 1. Effect of the different treatments of Cu on the growth of the plants in low light**.** Growth rate of the plants per week calculated on the basis of fresh weight. Values are given as means of three different experiments.

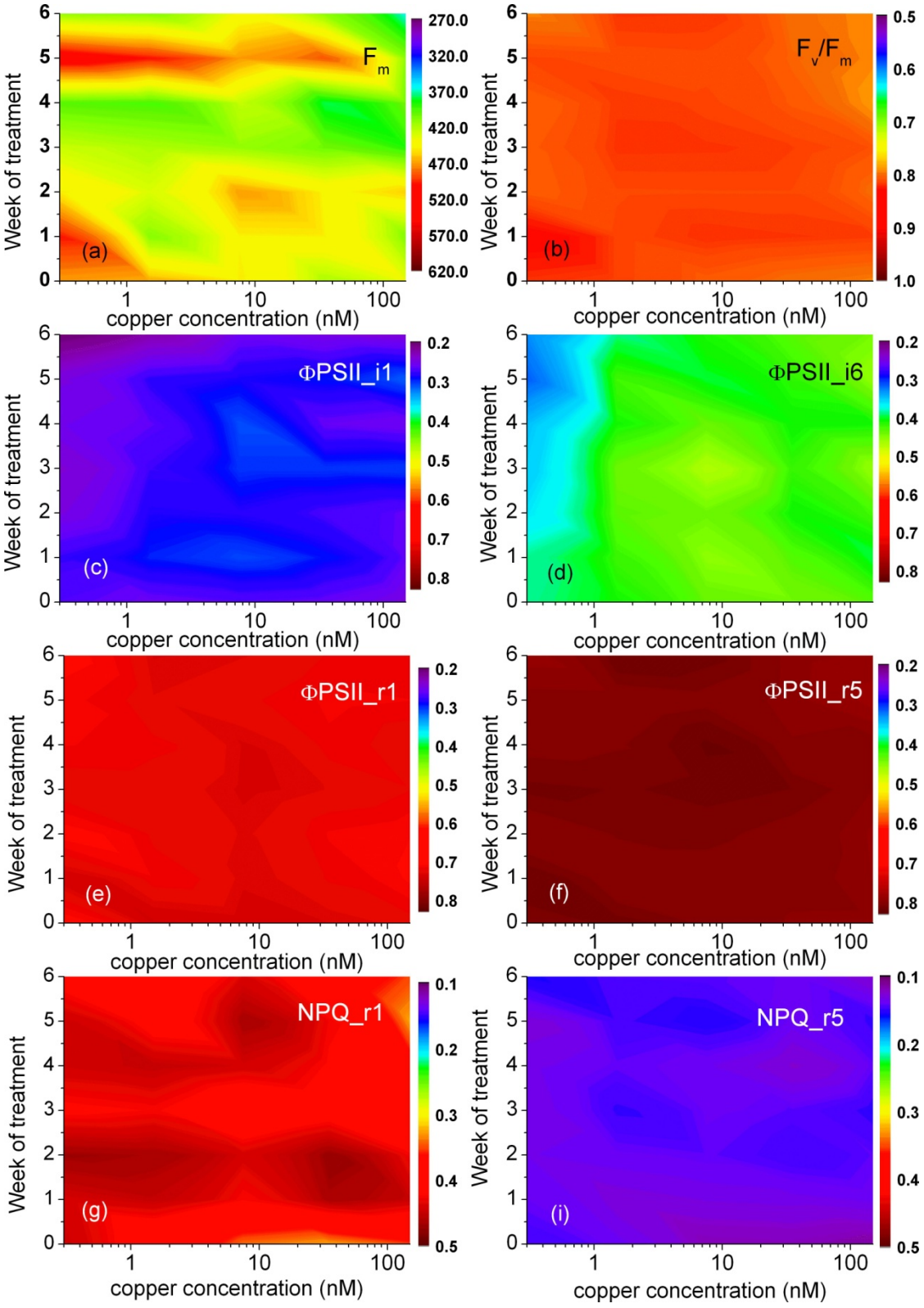

Figure 2. Effect of the different treatments of Cu on the photosynthesis biophysics measured by *in vivo* chlorophyll fluorescence kinetic measurements under low light conditions. Values are given as means of three different experiments with two replicates each. (a) Effect on maximal fluorescence F_m in dark-adapted samples, (b) Effect on the maximal dark-adapted

photochemical quantum yield of the photosystem II reaction centre measured as $F_v/F_m = (F_m-F_0)/F_m$, (c, d) Effect on light-acclimated electron flow through PSII measured as ($\Phi_{PSII} = (F_m'-F_t')/F_m'$) with Φ_{PSII}_i1 after 10 s of actinic light in (c) and Φ_{PSII}_i6 after 200 s of actinic light in (d), (e) Φ_{PSII}_r1 photochemical quantum yield of PSII after 10 s of relaxation in dark, (f) Φ_{PSII}_r5 = photochemical quantum yield of PSII after 200 s of relaxation in the dark, (g, h) Effect of actinic light on the non-photochemical quenching of energy measured as $NPQ = (F_m-F_m')/F_m$) with NPQ_r1= non-photochemical energy quenching after 10 s of dark phase (g) and NPQ_r5= non-photochemical energy quenching after 200 s of dark phase in (h).

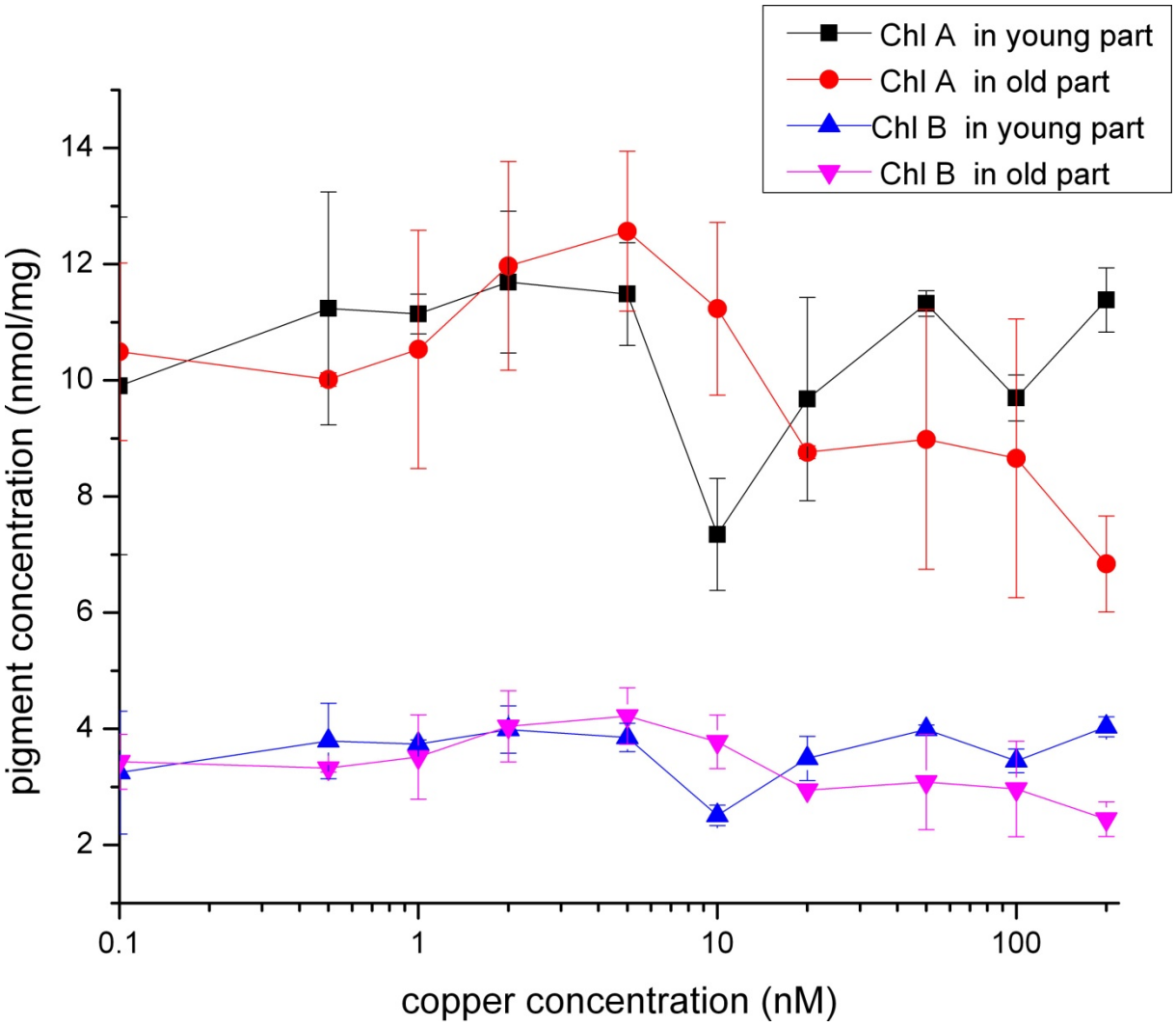

Figure 3. Effect of different treatments of Cu on chlorophylls MgChl a and MgChl b pigments under low light conditions after six weeks of treatment in the young and old tissues of the plant. Values are given as means ± SE (n=3).

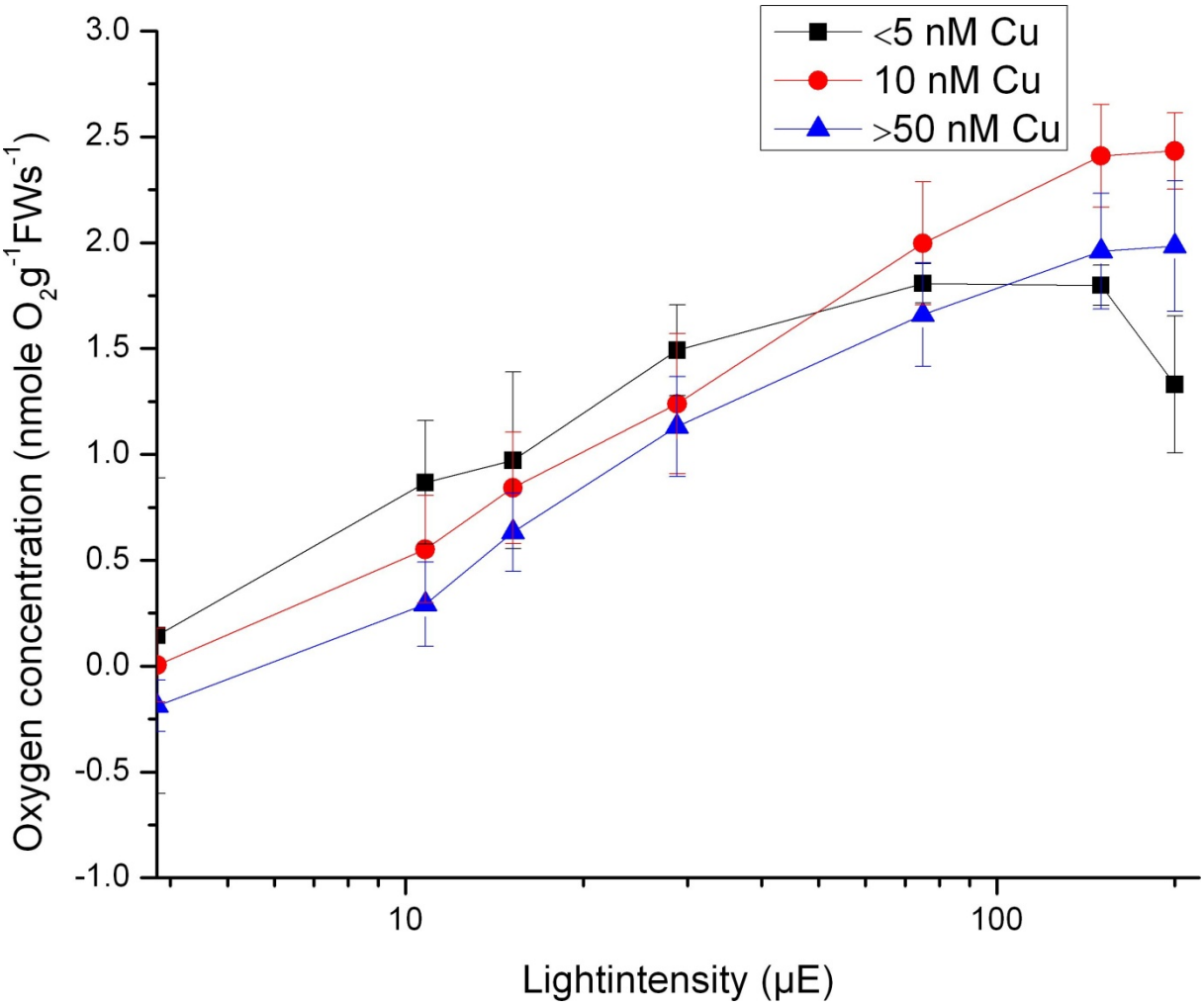

Figure 4. Effect of different treatments of Cu on the net photosynthetic oxygen release by the plant at different irradiances after six weeks of treatment in low light conditions. Values are given as means± SE (n=2).

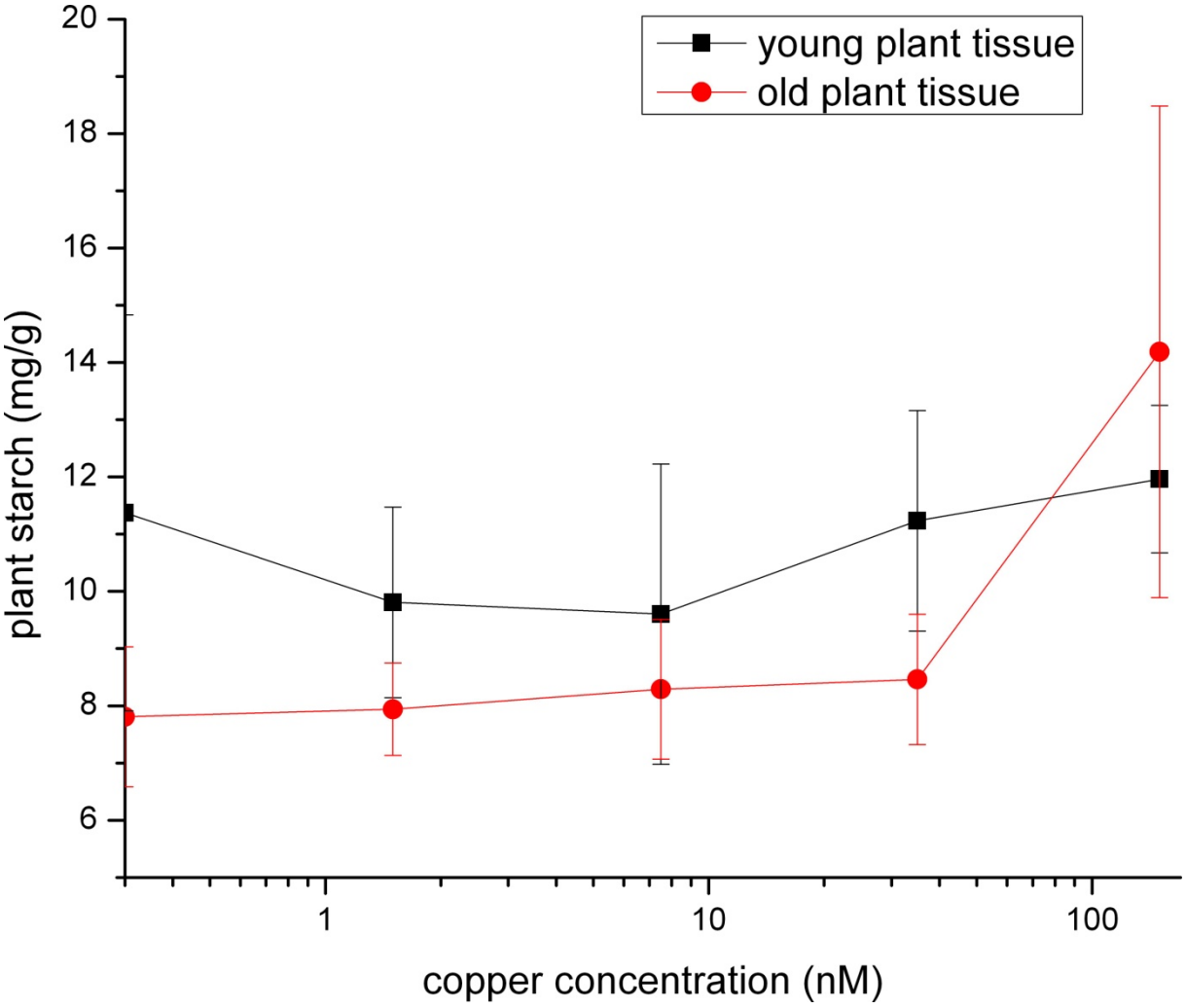

Figure 5. Effect of different treatments of Cu on the starch production or utilization of the young and old tissues of the plant after six weeks of treatment in low light. Values are given as means ± SE (n=3).

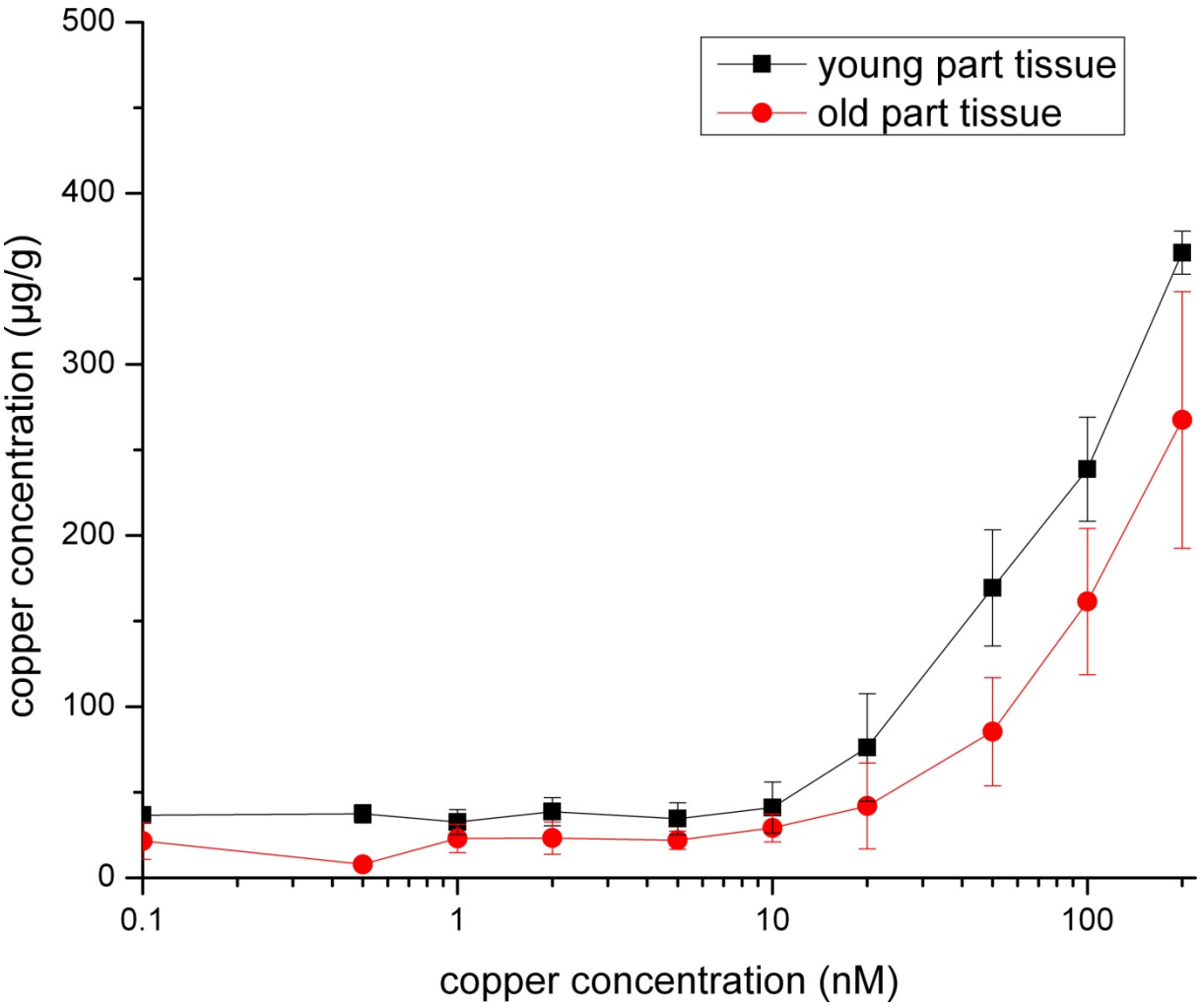

Figure 6. Effect of different treatments of Cu on the metal accumulation in the young and old tissues of the plant after six weeks of treatment in low light. Values are given as means ± SE (n=3).

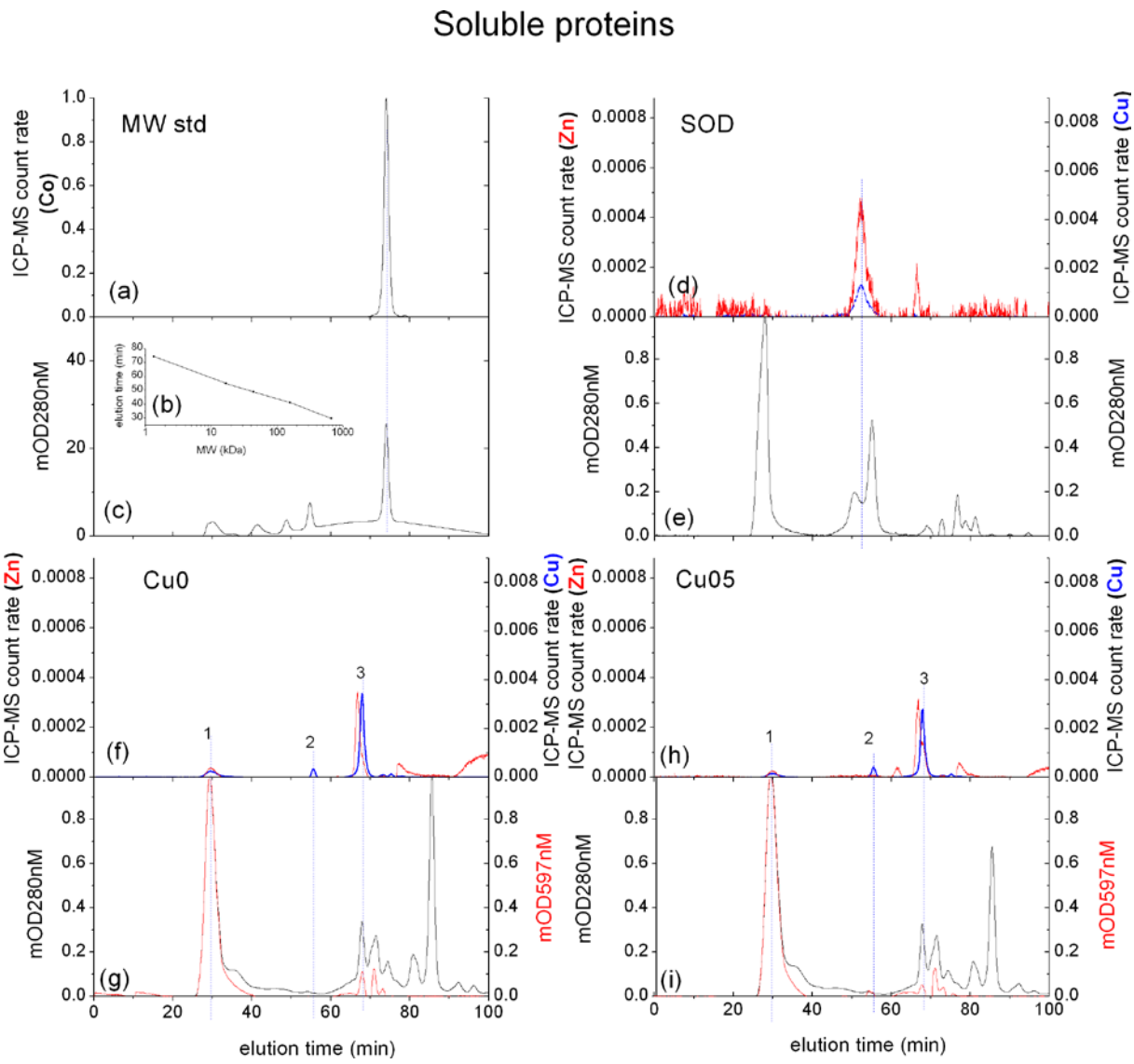

Figure 7: Analysis of the Cu containing proteins. The soluble fraction of proteins isolated from *C. demersum* after six weeks of treatment with different concentrations of Cu were separated through two serial size exclusion chromatography coupled to ICPMS and UV/Vis in parallel. (a, d, f, h) ICPMS signal intensities (cps) of the molecular weight standard, SOD standard, soluble fractions from Cu treatments 0 nM, 0.5 nM, (b) molecular weight standard containing bovine thyroglobulin (670 kDa), bovine γ-globulin (158 kDa), chicken ovalbumin (44 kDa), horse myoglobin (17 kDa), vitamin B12 (1.35 kDa) in soluble protein isolation buffer, (c, e) UV/Vis signal intensities (mOD) at 280 nm, of the molecular weight standard, SOD standard, (g, i) UV/Vis signal intensities (mOD) at 280 nm and 597 nm, of the soluble fractions from Cu treatments 0 nM, 0.5 nM, with respect to the elution time. UV/VIS and ICP-MS signal intensities were normalised to their highest peak. The data are from a single analysis.

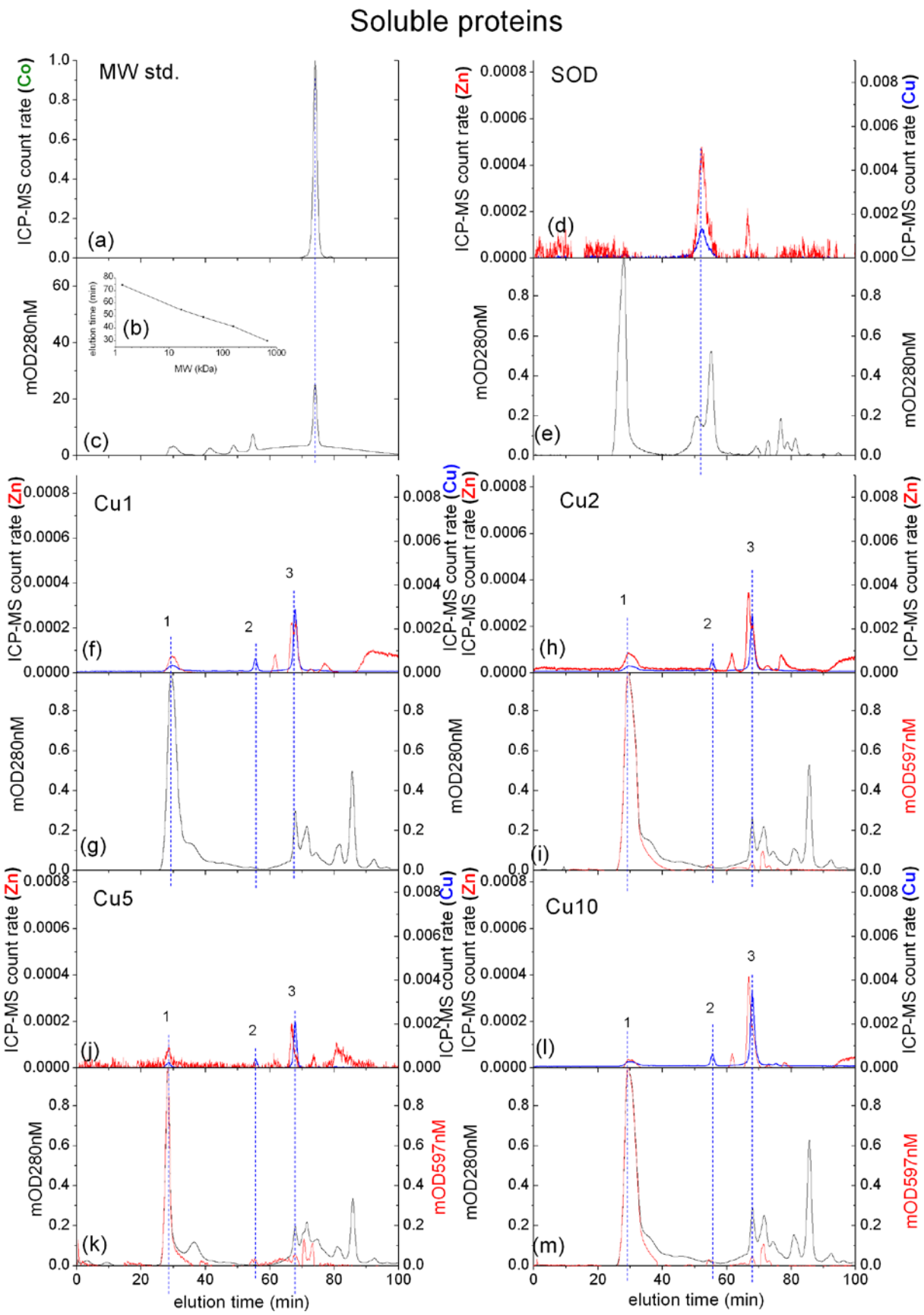
Soluble proteins
MW std.
SOD
Cu1
Cu2
Cu5
Cu10
(a)
(b)
(c)
(d)
(e)
(f)
(g)
(h)
(i)
(j)
(k)
(l)
(m)
ICP-MS count rate (Co)
ICP-MS count rate (Zn)
ICP-MS count rate (Cu)
mOD280nM
mOD597nM
elution time (min)
MW (kDa)
1
2
3

Figure 8: Analysis of the Cu containing proteins. The soluble fraction of protein isolated from *C. demersum* after six weeks of treatment with different concentrations of Cu were separated through two serial size exclusion chromatography coupled to ICPMS and UV/Vis in parallel. (a, d, f, h, j, l) ICPMS signal intensities (cps) of the molecular weight standard, SOD standard, soluble fractions from Cu treatments 1 nM, 2 nM, `5 nM and 10 nM, (b) molecular weight standard in soluble protein isolation buffer (as explained in Fig. 7), (c, e, g) UV/Vis signal intensities (mOD) at 280 nm, of the molecular weight standard, SOD standard, soluble fractions from Cu treatments 1 nM, (i, k, m) UV/Vis signal intensities (mOD) at 280 nm and 597 nm, of the soluble fractions from Cu treatments 2 nM, 5 nM and 10 nM, with respect to the elution time. UV/VIS and ICP-MS signal intensities were normalised to their highest peak. The data are from a single analysis.

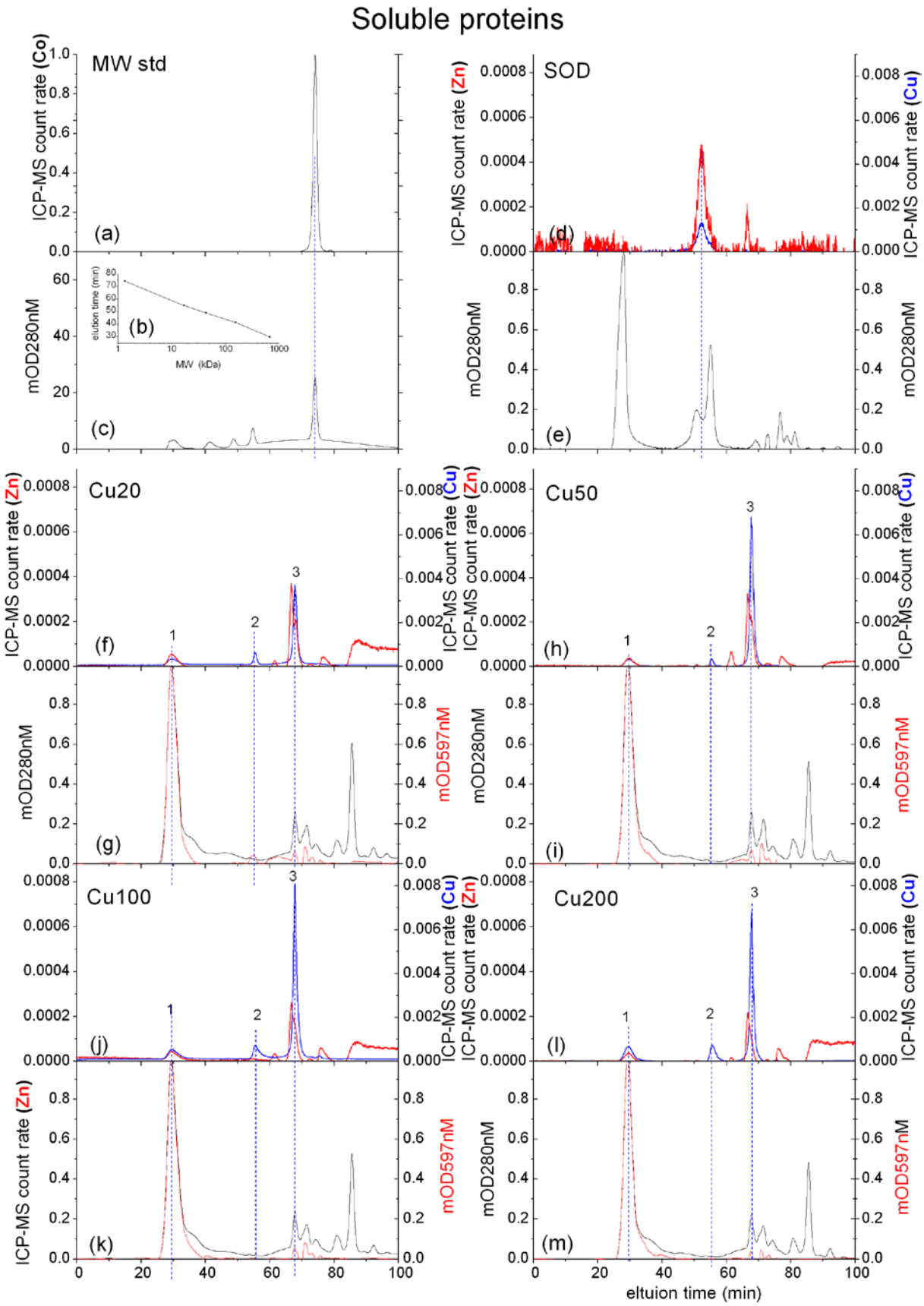
Soluble proteins
MW std
(a)
ICP-MS count rate (Co)
mOD280nM
(b)
elution time (min)
MW (kDa)
(c)
SOD
(d)
ICP-MS count rate (Zn)
ICP-MS count rate (Cu)
(e)
Cu20
(f)
(g)
mOD597nM
Cu50
(h)
(i)
Cu100
(j)
(k)
Cu200
(l)
(m)
eltuion time (min)

Figure 9: Analysis of the Cu containing proteins. The soluble fraction of protein isolated from *C. demersum* after six weeks of treatment with different concentrations of Cu were separated through two serial size exclusion chromatography coupled to ICPMS and UV/Vis in parallel. (a, d, f, h, j, l) ICPMS signal intensities (cps) of the molecular weight standard, SOD standard, soluble fractions from Cu treatments 20 nM, 50 nM, 100 nM and 200 nM, (b) molecular weight standard in soluble protein isolation buffer (as explained in Fig. 7), (c, e) UV/Vis signal intensities (mOD) at 280 nm, of the molecular weight standard, SOD standard, (g, i, k, m) UV/Vis signal intensities (mOD) at 280 nm and 597 nm, of the soluble fractions from Cu treatments 20 nM, 50 nM, 100 nM and 200 nM, with respect to the elution time. UV/VIS and ICP-MS signal intensities were normalised to their highest peak. The data are from a single analysis.

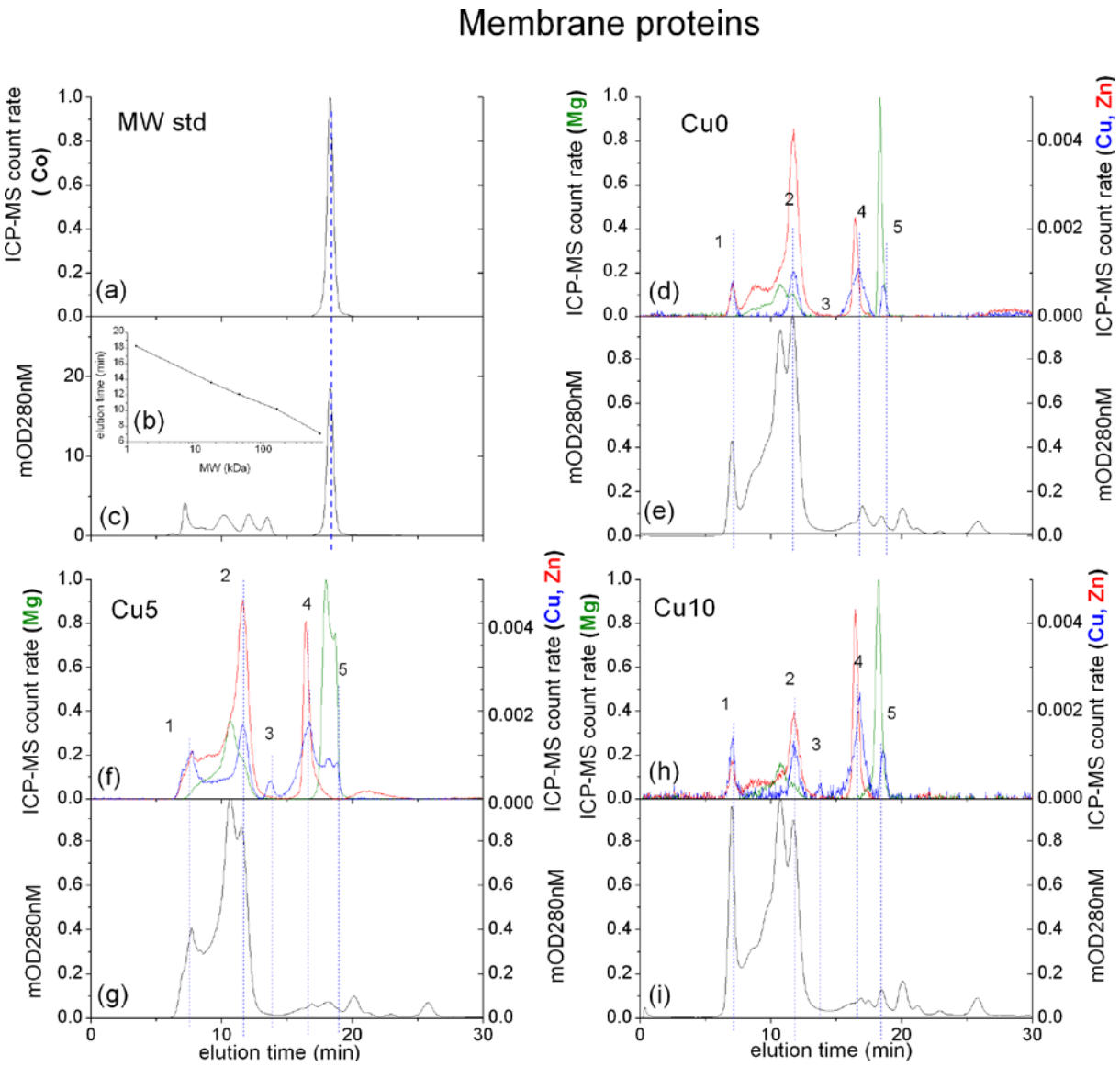

Figure 10: Analysis of the Cu containing proteins. The membrane fraction of protein isolated from *C. demersum* after six weeks of treatment with different concentrations of Cu were separated through size exclusion chromatography coupled to ICPMS and UV/Vis in parallel.. (a, d, f, h) ICPMS signal intensities (cps) of the molecular weight standard, SOD standard, membrane fractions from Cu treatments 0 nM, 5 nM, 10 nM, (b) molecular weight standard in membrane protein solubilization buffer (as explained in Fig. 7), (c, e, g, i) UV/Vis signal intensities (mOD) at 280 nm, of the molecular weight standard, membrane fractions from Cu treatments 0 nM, 5 nM, 10 nM, with respect to the elution time. UV/VIS and ICP-MS signal intensities were normalised to their highest peak. The data are from a single analysis.

Membrane proteins

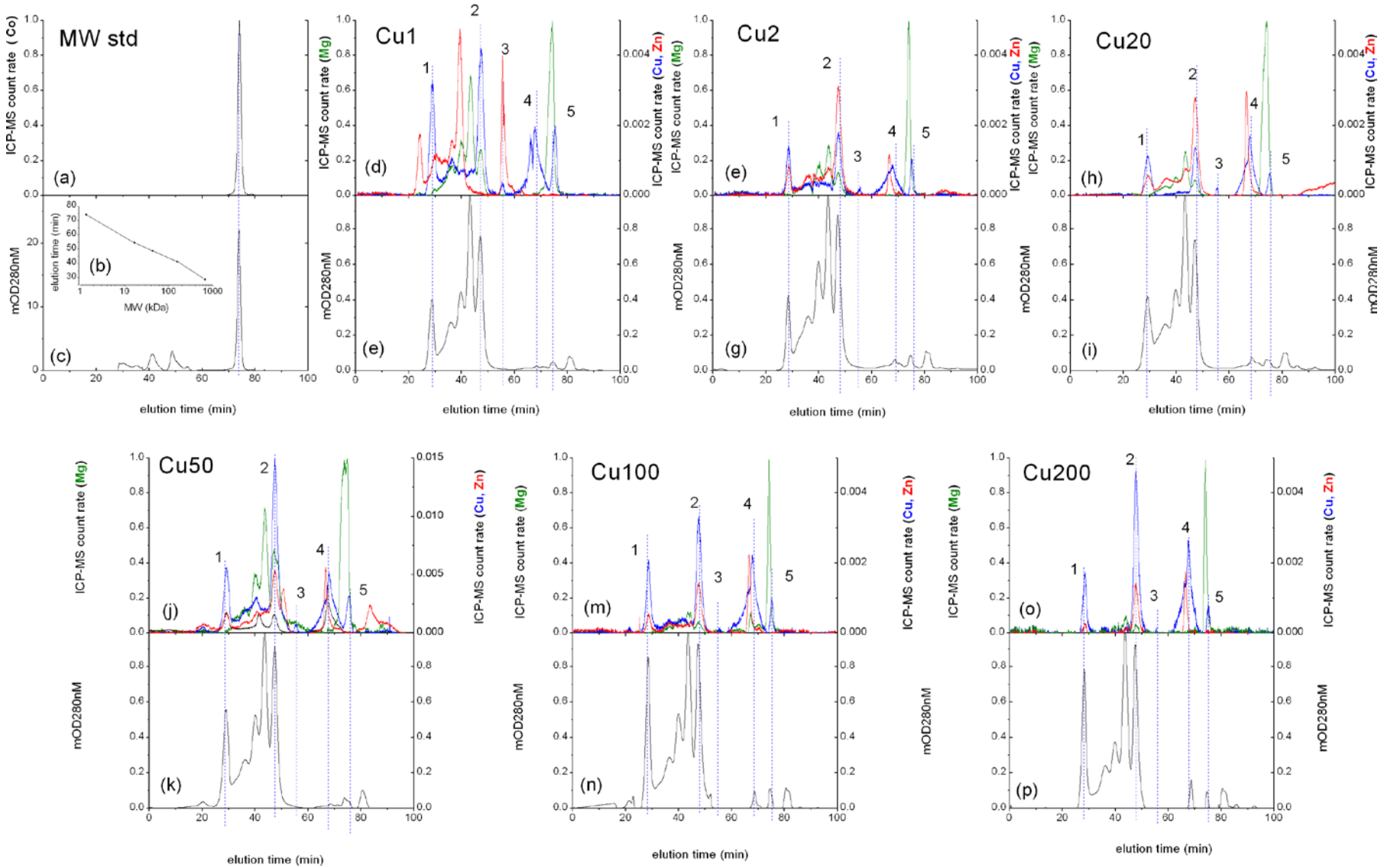

Figure 11: Analysis of the Cu containing proteins. The membrane fraction of protein isolated from *C. demersum* after six weeks of treatment with different concentrations of Cu were separated through two serial exclusion chromatography coupled to ICPMS and UV/Vis in parallel. (a, d, f, h, j, m, o) ICPMS signal intensities (cps) of the molecular weight standard, membrane fractions from Cu treatments 1 nM, 2 nM, 20 nM, 50 nM, 100 nM, 200 nM, (b) molecular weight standard in membrane protein solublization buffer (as explained in Fig. 7), (c, e, g, i, k, n, p) UV/Vis signal intensities (mOD) at 280 nm, of the molecular weight standard, membrane fractions from Cu treatments 1 nM, 2 nM, 20 nM, 50 nM, 100 nM, 200 nM, with respect to the elution time. UV/VIS and ICP-MS signal intensities were normalised to their highest peak. The data are from a single analysis.

2.3 Different strategies of cadmium detoxification in the submerged macrophyte *Ceratophyllum demersum* L.

Elisa Andresen [a], Jürgen Mattusch[b], Gerd Wellenreuther[c], George Thomas[a], Uriel Arroyo Abad[b] and Hendrik Küpper[*a,d]

a) Universität Konstanz, Mathematisch-Naturwissenschaftliche Sektion, Fachbereich Biologie, D-78457 Konstanz, Germany .

b) UFZ – Helmholtz Centre for Environmental Research, Department of Analytical Chemistry, Permoserstr. 15, D-04318 Leipzig, Germany.

c) HASYLAB at DESY, Notkestr. 85, 22603 Hamburg, Germany.

d) University of South Bohemia, Faculty of Biological Sciences and Institute of Physical Biology, Branišovská 31, CZ-370 05 České Budejovice, Czech Republic

Published in Metallomics (2013) 5(10): 1377-1386.

Abstract

The heavy metal cadmium (Cd) is highly toxic to plants. To understand the mechanisms of tolerance and resistance to Cd, we treated the rootless, submerged macrophyte *Ceratophyllum demersum* L. with sub-micromolar concentrations of Cd under environmentally relevant conditions. X-ray fluorescence measurements revealed changing distribution patterns of Cd and Zn at non-toxic (0.2 nM, 2 nM), moderately toxic (20 nM) and highly toxic (200 nM) levels of Cd. Increasing Cd concentrations led to enhanced sequestration of Cd into non-photosynthetic tissues like epidermis and vein. At toxic Cd concentrations, Zn was redistributed and mainly found in the vein. Cd treatment induced the synthesis of phytochelatins (PCs) in the plants, with a threshold of induction already at 20 nM Cd for PC_3. In comparison, in plants treated with Cu, elevated PC levels were detected only at the highest concentrations (100-200 nM Cu). Our results show that also non-accumulators like *C. demersum* store toxic metals in tissues where the heavy metal interferes least with metabolic pathways, but remaining toxicity interferes with micronutrient distribution. Furthermore, we found that the induction of phytochelatins is not proportional to metal concentration, but has a distinct threshold, specific for each PC species. Finally we could show that 20 nM Cd, which was previously regarded as non-toxic to most plants, already induces detoxifying mechanisms.

1. Introduction

Cadmium is an important environmental pollutant and toxic to most organisms. It is highly water soluble, rather immobile in soils but nevertheless can easily accumulate in plants, thus entering the human food chain (McLaughlin et al., 1999). Cd concentrations in the environment range from 0.2 -0.4 nM in unpolluted areas (e.g. Lake Constance: Petri, 2006; www.zvbwv.de) to 5 nM in different slightly contaminated rivers in Germany (Bachor et al., 2012). Cd release from car tires increased Cd concentration to ~ 17 nM in New Zealand (Fergusson et al., 1980). And in a heavily contaminated stream in North Central Nigeria, Cd concentrations of 17 nM, 195 nM and 1334 nM were measured (Ahmed et al., 2011). Although there are some indications that Cd may have a positive effect at very low concentrations (e.g. in Zn-limited diatoms: Lane and Morel, 2000), there is overwhelming evidence for Cd-induced toxicity in plants (Andresen and Küpper, 2013; Hasan et al., 2009). Due to chemical similarity of Cd with Zn, many toxic effects of Cd are correlated with Zn limitation or replacement, starting with uptake into the plants by transporters with similar affinities for Cd and Zn (Clemens, 2001, 2006). However, both synergistic and antagonistic effects of Cd on Zn accumulation have been found in roots and shoots, depending on cultivar and genotype of wheat (Zhang et al., 2002) and tomato seedlings (Dong et al., 2006).

As plants cannot avoid unfavorable conditions like soils with high heavy metal concentrations, they developed several detoxification methods, including immobilization, exclusion, chelation and compartmentalization (Benavides et al., 2005; Hasan et al., 2009). One group of detoxifying substances are the enzymatically synthesized phytochelatins (PCs), which after their discovery (Grill et al., 1985) have been found in higher plants, algae, yeast, some fungi (see review by Clemens, 2006 and citations within) and also in the nematode *C. elegans* (Vatamaniuk et al., 2001). Phytochelatins have the general structure (γGlu-Cys)n-Gly (with n=2-11) and are generated by the constitutive enzyme phytochelatin synthase (PCS), which is post-translationally activated only after blockage of thiols by a broad range of heavy metal(loid)s (Rea, 2012), most efficiently by Cd and As, but also by Ag, Pb, Cu, Hg, Zn, Sn, and Au (Clemens, 2006; Grill et al., 1987). Metal-PC-complexes are most likely transported into and stored in the vacuole where the heavy metal(loid)s cannot interfere with photosynthetic actions.

The storage of heavy metal(loid)s in compartments or tissues where they cannot damage metabolic pathways is a general tolerance mechanism for reducing the amount of heavy

metal(loid)s in the cytosol. Furthermore, the few enzymes found in the vacuole (Wink, 1993) have never been found to be sensitive to heavy metal stress. This protective mechanism is best studied in hyperaccumulator plants. These plants actively accumulate >100 ppm Cd, >1,000 ppm Cu or Ni, or >10,000 ppm Zn in their above ground tissues (Baker et al., 2000). It should be noted that it was suggested to change the definition of "hyperaccumulator" to >500 ppm Cd in shoots under environmentally relevant conditions with less than 20% growth reduction until the stage of maturity and a bioaccumulation coefficient >5 at a Cd concentration leading to >500 ppm in shoots (Küpper and Leitenmaier, 2013). By tolerating heavy metals, these plants gain advantage over related non-accumulator species as they can colonize soils with elevated heavy metal concentrations. Due to the specialization, many metallophytes become endemic to metalliferous soils (Milner and Kochian, 2008). Compared to equally metal-tolerant non-accumulators, hyperaccumulators have the additional benefit of being protected against herbivores. This was originally shown in 1994 (Boyd and Martens, 1994; Martens and Boyd, 1994) and since then has been shown for many further metals and plant species including the Cd/Zn hyperaccumulator (formaly *Thlaspi) Noccaea caerulescens*: the Cd-accumulation deterred thrips (*Frankliniella occidentalis*) from feeding on *N. caerulescens* leaves (Jiang et al., 2005). It was shown that especially the vacuole of large epidermal cells is used for the storage of the heavy metals (Frey et al., 2000; Küpper et al., 1999, 2001). Küpper et al. found that in *N. caerulescens* the relative Zn concentration in epidermal cells was positively correlated with cell length in young as well as in mature leaves (Küpper et al., 1999). In the related species *N. praecox* collected from a heavy-metal polluted area in Slovenia, Cd was localized in the epidermis, the vascular bundle, but also the mesophyll while Zn was preferentially accumulated in the epidermis cells (Vogel-Mikus et al., 2008). Also in the non-accumulator *Anthyllis vulneraria*, cadmium depositions were found in the central vein, in epidermis cells and the (epidermal) trichomes (Huguet et al., 2013).

There are different techniques to investigate metal accumulation in plants. If one is interested in the cellular or sub-cellular distribution, however, it is important to analyze intact tissues as fragmentation will disrupt the different organelles: metals that were bound to weak ligands in the vacuole may bind stronger ligands present in the cytosol (Küpper et al., 2004). For the same reason any fixation techniques besides rapid freezing should be avoided. In this study, we used µ-X-ray fluorescence to determine the localization of Cd, Zn and Cu in frozen hydrated leaves of the rootless, submerged macrophyte *Ceratophyllum demersum*. It is

sensitive to heavy metal stress and as it does not possess roots, no root-specific inhibition or detoxification mechanisms are possible.

2. Material and Methods

2.1 Plant material and culture conditions

The submerged, rootless macrophyte *Ceratophyllum demersum* was used for the stress experiments. The strain was obtained from an aquaria shop and continuously cultivated since 2005 in hydroponic solution with 12 h day/12 h night light conditions provided by two Osram FLUORA® fluorescent and two warm white fluorescent tubes (Osram, München, Germany) and a temperature cycle from 18°C at 6 a.m., over 20°C at 9 a.m., to a maximum of 22°C at 3 p.m., back over 20°C at 9 p.m. to 18°C again at 6 a.m. The nutrient solution (Tab. 1) was optimized for growth of submerged macrophytes (personal communication from H.K., unpublished) and resembles the situation of typical oligotrophic waters, in particular soft waters. The pH was adjusted to 7.8 with KOH. All experiments were carried out under simulations of natural light and temperature conditions: 12 h sinusoidal light cycle with maximal irradiances at 750 µmol photons m^{-2} s^{-1} (supplied by Dulux L 55 W / 12-954, OSRAM München, Germany) and 12 h night; 19°C at 6 a.m., 21.5°C at 9 a.m., 24°C at 3 p.m., 23 C at 9 p.m., 19 C at 6 a.m. For each treatment around 1.5g (fresh weight) of plants were used. For the two experiments of PC-induction each aquarium contained 2 or 3 plants. The experiments used for metal accumulation and µ-XRF were carried out with 2 or 4 plants. The number of individual plants was consistent for each concentration within the same experiment. Differences occurred due to weight and size of the plants at treatment start. Each aquarium contained 2 L of continuously aerated medium to secure a low biomass to water volume ratio. The nutrient solution was continuously exchanged (flow rate 0.5 L day^{-1}) to ensure that the metal uptake into the plants was limited only by the concentration, but not by the amount of nutrient solution available. After 1 week of acclimation to the high light conditions, cadmium was applied as $CdSO_4$, copper as $CuSO_4$ to the medium. The concentrations were “0” (background Cd/Cu~ 0.2 nM), 0.5, 1, 2, 5, 10, 20, 50, 100, and 200 nM. Epiphytic algae and cyanobacteria were weekly removed from the macrophytes by gentle brushing and the aquaria cleaned. During the treatment duration, stress symptoms were

determined weekly by measuring chlorophyll fluorescence of individual leaves as described previously (Küpper et al., 2007).

For phytochelatin analyses, plants were harvested after 2 weeks of treatment, separated into young (4 cm from apex, 2 cm from branch) and old (remaining) parts, the respective weight was determined and the plants frozen in liquid nitrogen until further analyses. Plants from one Cu treatment were harvested after 4 weeks to ensure Cu limitation inside the plants. For µ-XRF analyses, leaves from Cd treated plants after 3 and 6 weeks of treatment were prepared as described below.

2.2 Phytochelatin extraction and determination

The harvested plant material was ground in a pre-cooled mortar in liquid nitrogen. The ground material was halved and transferred into two 2 ml cups and covered with 1% formic acid in a concentration of 2 mL g^{-1} fresh weight. The material was thawed, and phytochelatins were extracted for 1.5 hours at 4°C. The cups were vortexed three times in between. The material was than centrifuged for 15 min at 2500xg at 5°C using a swinging bucket rotor. The purple supernatant was transferred into new cups, rapidly frozen in liquid nitrogen and kept at -80°C until analysis.

The used synthetic PCs with a purity of >95% were purchased from MoBiTec (Göttingen, Germany). A mix of PCs with a concentration of 0.05 mM each (PC_2-PC_6) was prepared in 1% formic acid solution as external standard stock solution. Standard mixtures of PC_2 to PC_6 were used as calibrants. On the basis of the peak areas of the "Extracted Ion Chromatogram" (EIC) of the reduced and oxidized forms of the PCs the PC-specific calibrations were performed and the concentrations of the PCs in the extracts calculated. The limit of detection of PC_3 was calculated to be 0.4 µM. The reproducibility (relative standard deviation) differs for the PC under investigations in the following order: PC_2 and PC_3 <5%, PC_4 <7.5%, PC_5 <9% and PC_6 <15%. In all cases the peak areas for the oxPCs and redPCs were added and used for calculation of the concentration. After each 10 measurements a control standard was injected to check the performance of the instrument. The instrument was tuned daily to maintain the accurate mass analysis.

Phytochelatins were analyzed using an HPLC-ICP-MS/ESI-Q-TOF-MS system consisting of a UHPLC Series Infinity 1290 (Degasser, binary pump, thermostated autosampler) coupled with an ICP-MS 7500ce and Accurate Mass Q-TOF LC/MS 6530 in parallel (all Agilent

Technologies, Santa Clara, USA) by splitting the mobile phase 1:1 by adjustable flow splitter (Analytical Scientific Instruments, CA, USA). The injection volume used was 20 µL. The samples were cooled to 278 K in the autosampler. The conditions for the separation and detection are listed in Table 2. To reduce carbon deposits on the sampler cone of the ICP-MS originating from acetonitrile in the mobile phase, a gas mix of O_2/Ar (20% / 80%) was added to the carrier gas flow and the spray chamber was cooled. For data acquisition and qualitative analysis the MassHunter (MH) software and therein occurring tools (Agilent Technologies, Santa Clara, USA) were used. The free phytochelatins were identified on their retention time and accurate mass. Cadmium-PC-complexes are not stable under the acid extraction and analysis conditions, that only the concentrations of the free Cd^{2+} were detected with element-selective ICP-MS detection at *m/z* 111 and an integration time of 0.5 s.

2.3 µ-XRF

For sample preparation, capillaries (1 mm diameter, 0.1 mm wall; Hilgenberg GmbH, Malsfeld, Germany) were cut to adequate size and filled with water. One leaf from the 7th nodium counted from apex was inserted into the water filled capillary and fixed on a custom made sample holder. For calibration, we prepared an aqueous multielement standard containing 1 mM each of Na_3AsO_4, $CdCl_2$, $CrCl_3$, $CuCl_2$, NaFe(III)-EDTA, $NiCl_2$, $ZnCl_2$ in 20% glycerol and 5% HCl, adjusted to final volume with water and filled into the same capillaries as used for the leaves. A zero standard containing only 20% glycerol and 5% HCl served as a negative control. An aqueous standard can be used as an approximation as frozen leaves consist to over 90% of water. The glycerol hereby serves as C-matrix. The capillaries containing standards or leaves were shock frozen in supercooled isopentane (-140°C). After freezing, the samples were stored in liquid nitrogen until the analysis. To limit beam damage, throughout the measurement the sample was cooled in a cryostream to about 100 K (Cryocool LN3; Cryoindustries of America, Manchester, New Hampshire, USA). All µ-XRF measurements were done at beamline L of the synchrotron DORIS at the Deutsches Elektronen-Synchrotron (DESY, Hamburg, Germany). X-rays created in a bending magnet were monochromatized using a multilayer monochromator at 30.8 keV with a bandpass of approximately 2.3%. Focussing was achieved using a single-bounce capillary to approximately 10 µm spotsize in both horizontal and vertical dimension. µ-XRF tomography was done approx. 3 mm above the branching point of the leaf with step size of 5 µm and a

dwell time of 0.8 s per step. Ninetyone linescans were measured, with the sample being rotated by 2°, yielding a 180° tomogram. Two fluorescence detectors (Vortex-60 EX / Vortex-90 EX; SII Nanotechnology USA Inc., Northridge, California, USA) were used under 90° and 270° with respect to the incident beam to maximize detected fluorescence counts from the sample while minimizing background caused e.g. by elastic scattering due to the polarized nature of the synchrotron radiation. The detected µ-XRF spectra were fitted using PyMca (Solé et al., 2007). The fluorescence line areas were then normalized to 100 mA DORIS current, the resulting sonograms were tomographically reconstructed with XRDUA (De Nolf and Janssens, 2010) using the maximum likelihood expectation maximization ("MLEM") algorithm. Absolute concentrations were obtained using the tomographic reconstruction of the multielement-standard measured in the identical geometry.

2.4 Determination of accumulated elements

After 6 weeks of Cd-treatment, plants were harvested, separated into young and old parts and lyophilized for 48 hours. 5-10 mg of the material was put into acid-washed (5% HNO_3) glass tubes and digested in 500 µL (85:15%) nitric-perchloric acid for 30 min at room temperature and then gradually heated up to a maximum of 195°C until all liquid was vaporized (Zhao et al., 1994). The remaining ashes were re-dissolved in 0.5 mL 5% HCl, gradually heated to 80°C. After cooling, the volume was filled to 1.5 mL with ddH2O and used for analyzing the components using a graphite furnace atomic absorption spectrometer (GBC 932 AA with GF 3000, Braeside, VIC, Australia). Standard solutions for Cd, Zn and Cu were diluted from AAS Standards (TraceCERT, Sigma-Aldrich, St. Louis, MO, USA). Digested plant samples were appropriately diluted to optimal detection range with ultrapure 1.66% HCl (ROTIPURAN ultra, Roth, Karlsruhe, Germany).

3. Results

3.1 Toxicity determination

Cadmium treatment led to a reduction in the maximum quantum efficiency of PSII photochemistry, measured as $F_v/F_m = (F_m - F_0)/F_m$ (Fig. 1). While the values were constant over the treatment duration for the control (0.2 nM) and the low Cd concentration (2 nM), a

slight decrease occurred for the plants treated with 20 nM Cd towards the end of the treatment (P=0.051). The plants treated with the highest Cd concentration showed a clear reduction of F_v/F_m from the 2nd week onwards. The Cd-induced inhibition of the photosynthetic apparatus is a great threat to photosynthetic organisms as it was shown to be an important inhibition site (Andresen and Küpper, 2013). And although the decrease in F_v/F_m is often part of a very complicated phenotype, it was established as a stress monitor (Baker, 2008).

3.2 Phytochelatin determination – Method evaluation

After extraction of phytochelatins with a cooled aqueous solution of 1% formic acid, their high-resolution separation by UHPLC and their detection using ICP-MS and ESI-Q-TOF-MS in parallel was successfully applied within 10 min for PC_2 to PC_6. The ESI-Q-TOF-MS allows the detection of accurate masses with an *m/z* error less than 3 ppm. With these accurate masses, proposals for ion formulas were created and used for the identification of reduced and oxidized PCs in the plant extracts. In the present case the parallel occurring ICP-MS detection was applied to quantify the uncomplexed Cd ions in the extracts, because the acidic mode of extraction and separation do not allow the analysis of initial Cd-PC-complexes. Despite of the dissociation of the Cd-PC-complexes, an excellent chromatographic separation of the free reduced and oxidized PCs can be performed using 0.1% formic acid combined with an acetonitrile gradient as eluent. The dissociation of the complexes is not a drawback for the aim of our work, because grinding tissues anyhow leads to mixing of all soluble constituents of all cells and cellular compartments, so that originally weakly bound metals from the vacuole would be mixed with strong ligands, e.g. PCs, in the cytoplasm. Thus immediate binding of previously weakly bound Cd to the PCs would occur once the ground plant material melts. Therefore, we concentrated on identifying and quantifying the different phytochelatin species. Figure 2 and Table 3 concludes qualitative values for the identified reduced and oxidized PCs under investigation. In Figure 2 the ESI-Q-TOF-MS signals (total ion current (TIC) and extracted ion current (EIC)) are presented and used for identification and quantification of PCs in the plant extracts. Additionally to the reduced PCs, also the oxidized PC isomers were considered for quantification. The y-axis scales for each EIC were adjusted for optimal view of the peaks. In Figure 2 the shoulder on the PC_3 peak could be identified as $(PC_2)_2$. In this case two PC_2 are linked together via an inter disulphide bridge. In

Figure 3 the peak at 3.08 min has an accurate mass of *m/z* 595.1433 that did not correspond to known canonic and iso PCs. The peak at 5.485 min could be identified as an isomer of oxPC_3.

3.3 Phytochelatin induction

Cadmium treatment induced phytochelatin synthesis in the plants (Fig. 4; $P<0.001$, 2-way ANOVA). The induction of phytochelatins was not proportional to metal concentration, but had a distinct threshold, specific for each PC species: While PC_2 was the only PC-species detected in both tissue ages of all extracts PC_6 was present mainly in extracts from the higher Cd treatments. In the control treatment (no Cd added; 0.2 nM, background concentration), only traces of PC_2 and PC_3 were detected. PC_2 levels in the young tissue significantly differed only between the lowest (control and 1 nM Cd) and the highest Cd concentration ($P=0.001$). In the old tissue, Cd concentrations from 0.2 nM up to 10 nM led to different PC_2 inductions than both 100 nM and 200 nM Cd. Altogether, this means that induction of PC_2 by Cd stress was rather weak. PC_3, in contrast, had the most prominent induction in response to the metal treatments and yielded the highest amounts. The PC_3 content was not different within the group of low Cd (0.2 nM – 10 nM) or the group of high Cd (20 nM - 200 nM) in young tissue, but between these two groups ($P\leq0.002$), emphasizing the switch-like response of PC_3 synthesis. Regarding the old tissue, only the two highest Cd concentrations induced PC_3 in amounts different from the other Cd concentrations. PC_4 was present in most extracts, but not detected in the control plants, in young tissue of the plants treated with 1 nM and 2 nM, and in old tissue of the plants at 0.5 nM Cd. Up to 5 nM Cd for the young and 10 nM for the old tissues, the amounts of PC_4 were very low. Moderately elevated (maximum like PC_2) levels of PC_4 occurred for the young tissue in the three highest Cd treatments, for the old tissue only in the 100 nM treatment. Compared to the shorter PCs, PC_5 was detected only in trace amounts, mostly from 10 nM (young tissue) or 20 nM Cd (old tissue), onwards. PC_6 was detected only in the plants treated with the highest Cd concentrations (50, 100, 200 nM Cd for PC_6-induction in young tissue; 100, 200 nM Cd for PC_6-induction in old tissue), with the exception of a trace amount being detected in the old tissue of the plant treated with 1 nM Cd. Generally, the respective amounts of PC_6 were much higher in the young than the old tissues ($P<0.008$); in young tissues PC_6 reached double the maximum concentration compared to PC_5. Phytochelatins were also extracted from Cu-treated plants, in order to compare the induction threshold because Cu is an essential metal and not a main inducer of PCs (Fig. 4).

Here, only PC_2 and PC_3 were detected in all samples. The respective contents were only significant in the old tissue of plants treated with 200 nM Cu. PC_4 was present, and only in trace amounts, solely in the young tissue of some plants (0.2, 1, 2, 20, 100, 200 nM Cu) and in the old tissue in plants treated with 50 nM or more Cu. In all copper-treated plants, the amounts of the respective PCs were much lower than in the plants treated with cadmium.

3.4 Elemental accumulation and distribution

The higher the applied Cd concentration, the higher was the Cd accumulation in the leaf as revealed by µ-XRF (Fig. 5, left panel). Also when looking at the whole-plant level as analyzed by GF-AAS in acid-digests of tissues, the Cd accumulation within the young and old tissue after 6 weeks of treatment was increasing with the applied concentration (Tab. 4). The treatments with more than 2 nM Cd led to significant increase ($P \leq 0.013$) up to more than 2500 ppm. Solely the plants treated with 20 nM Cd showed differences in Cd accumulation depending on the age of the tissue. No Cd was detected by µ-XRF in the leaves of the control treatment. More importantly, Cd distribution changed depending on the Cd treatment concentration and time. With 2 nM of Cd, the distribution was homogenous over the whole area of the leaf after 3 weeks of treatment, the maximal accumulation being 10.5 µM. After 6 weeks, a stronger accumulation of Cd within the mesophyll and the epidermis was observed and the maximal Cd concentration nearly tripled (28 µM). There was no enhanced accumulation within the vein. A more defined distribution occurred after 3 and 6 weeks of 20 nM Cd treatment and the Cd concentration in the leaves was more than 20-fold increased (640 µM). Cd accumulation was detected mainly in the epidermis and the vein, but also in the mesophyll. After 6 weeks, Cd-accumulation in the epidermis was less pronounced compared to 3 weeks of 20 nM. An enhanced accumulation was also observed in the thorn (epidermal structure) of the plant treated with 20 nM Cd for 6 weeks. When 200 nM were applied, Cd was mainly observed in the vein. The maximum Cd accumulation in the second replicate was even twice as high as in the shown one.

On the whole-plant level, Cu was in the range of 17-30 ppm and decreased at higher Cd concentrations (Tab. 2). µ-XRF revealed that Cu was always accumulated solely in the vein, no change in its distribution or concentration was observed in response to Cd toxicity (not shown).

On the whole-plant level, zinc accumulation ranged between 400 and 600 ppm and was only slightly decreased at 20 nM of Cd treatment. However, the decreases were not significant (Tab. 4). In contrast, the tissue-level distribution pattern of Zn strongly depended on what Cd concentration was applied (Fig. 5). While in the lower Cd concentrations (0.2 and 2 nM) Zn was mainly found in the epidermis of the leaf, at higher Cd concentrations (20 nM) Zn was more homogenously distributed. Zn concentration was highest after 3 weeks of treatment with 20 nM Cd (4.5, 4.5 and 3.2 mM). At the highest applied Cd concentration, Zn accumulation was reduced and mainly detected in the vein and the mesophyll, but hardly in the epidermis anymore, which is particularly surprising in view of the almost unchanged Zn concentration on the whole-plant level.

4. Discussion

The synthesis of phytochelatins is one major strategy of heavy metal(loid) detoxification (Cobbett and Goldsbrough, 2002; Hall, 2002). In many previous studies Cd-PC-complexes were isolated from plants, e.g. transgenic and wild type *Arabidopsis thaliana* plants treated with 10 µM of Cd (Sadi et al., 2008). To break the cell walls and to isolate the substances, plants were lyophilized and ground to a homogenous mixture. During these processes all cell components get mixed and it cannot be assured that Cd was indeed bound to the PCs before disrupting the cells. Therefore we examined the different PC species rather than Cd-PC-complexes. In the present study we showed that not only the concentration of the single PCs but also the occurrence of different PC species (PC_2 to PC_6) in *Ceratophyllum demersum* is dependent on the applied Cd concentration, and that this occurs at several orders of magnitude lower Cd concentrations than previously known. A previous study on *C. demersum* treated with 5000 and 10,000 nM of Cd for a short period (2 or 4 days) revealed the induction of PC_2 and PC_3. After 4 days of treatment with 10,000 nM Cd, the amount of PCs decreased while the accumulation of Cd within the tissue continued to increase (Mishra et al., 2009). The overall content of NP-SHs (non-protein thiols; including PCs) was significantly increased in the plants treated with 5,000 nM Cd, and highest in those plants treated for 4 days. In the present study, induction of phytochelatins started already in the low nanomolar range, and the strongest rise in their induction occurred at 20 nM Cd, i.e. 250 times lower than the lowest Cd in the previous study. In the present study, also PC_4-PC_6 were detected in plants treated with

the highest Cd concentration (200 nM), which was still 25 times less than the lowest Cd concentration in the study of Mishra and colleagues.[36] However, they used the Hoagland solution (Hoagland and Arnon, 1950), which contains Fe-EDTA and may have led to chelation of Cd ions. In different macrophytes (*Pistia stratiotes*; water lettuce) treated for 21 days with environmentally relevant concentrations of Cd (10 nM to 1 µM applied Cd, but these authors also used EDTA), enhanced phytochelatin concentrations were detected from 20 nM on, both in leaves and roots (Wang et al., 2010). The respective concentration was always higher in the shoots, while GSH was higher in roots. The involvement of PCs in Cd detoxification especially in non-hyperaccumulator plants is well documented and non-controversial. In the present study, however, we could show the dose-dependency for the different PC species under naturally occurring Cd concentrations and culture conditions. This revealed a switch-like induction, with different Cd concentration thresholds for different PC species. Thus an increase in Cd toxicity stress does not just lead to a further overall increase in PC synthesis, but to a change in PC composition. This may suggest that different PCs have different tasks (e.g. homeostasis vs. detoxification) or that plants only invest the synthesis effort into producing long-chain PCs once it becomes critical for survival, while for alleviating moderate toxicity only PC_3 is formed.

Unlike Cd, Cu is essential for plant growth (Lipman and McKinney, 1931; Sommer, 1931). It is mainly required in at least six locations in a plant cell including the cytosol, the endoplasmic reticulum (ER), the inner membrane of the mitochondria, the stroma of the chloroplast, the thylakoid lumen and the apoplast (Marschner, 1995). Cu can be found in the active center of various enzymes, e.g. of plastocyanin, a small protein involved in the electron transfer from cytochrome b_6f to the PSI reaction centre; the Cu/Zn superoxide-dismutase (Cu/Zn SOD) and also in the cytochrome c oxidase (Yamasaki et al., 2008). 10 nM Cu were used for the stock cultures and within the Cd treatment as this had been found to be the optimal concentration for *C. demersum* (personal communication, G.T. & H.K.). At Cu concentrations over the optimum, the plants nevertheless cannot detoxify all Cu but need to retain the essential Cu for plastocyanin and other Cu containing enzymes (Thomas et al., 2013). Metallothioneins (MTs; gene encoded and expressed metal-binding proteins) and PCs as well as high molecular weight ligands seem to be involved in the detoxification process (Kholodova et al., 2011). In this context, the non-induction of PCs by low Cu (Fig. 4) was expected, even though there have been studies indicating an increase in MTs activating the Cu-chelate-reductase in pea plants at Cu deficiency (Fordham-Skelton et al., 1997; Welch et

al., 1993). Apparently, only the highest of the applied Cu concentrations in this study induced enhanced PC production (Fig. 3). Around 400 ppm of Cu was accumulated by the plant at this concentration while the lower concentrations were below 100 ppm which clearly indicates the PC enhancement at the higher concentrations (Thomas et al., 2013).

The technique of µ-XRF of frozen hydrated samples allows to determine the distribution of heavy metal(loid)s in plants without chemical fixation and potential alteration and should be favored over techniques that require dehydration, resin embedding or fractionation (Punshon et al., 2009). In combination with silencing or deleting genes that encode for metal transporters, µ-XRF can also reveal information about metal homeostasis (Kim et al., 2006). Studies in which µ-XRF was applied to detect Cd were mainly done with hyperaccumulator plants and the results may be very different in non-hyperaccumulators, especially because Cd will be bound to different ligands (Cobbett and Goldsbrough, 2002; Küpper et al., 2004). Cd distribution patterns were examined by µ-XRF in two ecotypes of *Sedum alfredii*, one of which is a Cd-hyperaccumulator and one not. In the hyperaccumulator ecotype (HE), Cd was distributed very homogenously across the stem cross section within the parenchym tissue, with the exception of the vascular bundle where Zn was located. In the non-hyperaccumulator ecotype (NHE) Cd and Zn were distributed mainly in the cells surrounding the vascular bundle (Tian et al., 2011). Laser-ablation ICP-MS of whole unprepared leaf samples within the same study revealed an even distribution of Cd over the whole area (except the leaf tips) and the vein, and in the palisade mesophyll and the vascular bundle regarding the leaf cross section. In contrast, Zn accumulation was mainly found in the epidermal layers of the HE, but also in the vascular bundle. In this study, only leaf samples of *Ceratophyllum demersum* were subjected to µ-XRF analyses. The distribution of Cd and Zn was mostly similar, but changing at higher Cd concentrations: In the plants subjected to control conditions or low non-toxic Cd concentrations, Zn was localized mainly in the epidermis cells (Fig. 5), whereas Cd was either not detected (control treatment), or found mostly all over the leaf (2 nM). With increasing Cd concentrations, a strong and increasing sequestration of Cd and also Zn into the vascular bundle and the thorn was observed. Metal sequestration into the epidermis is a phenomenon well-known for hyperaccumulator plants; it protects the more sensitive mesophyll from metal toxicity (e.g. Zn (Küpper et al., 1999), Ni (Küpper et al., 2001)). In *Arabidopsis halleri*, a Cd-hyperaccumulator, Cd and Zn accumulation was found to behave only somewhat similar, as sequestration was stronger in the mesophyll, while in the epidermis it was found specifically within the trichomes,

unicellular leaf hairs on the surface of the leaves (Küpper et al., 2000), which were located around the main vein (Fukuda et al., 2008). A changing distribution over time was observed in *A. halleri* by Huguet et al. (2012): After 3 weeks of treatment, Cd accumulation occurred in the vein and petiole. After 9 weeks, more Cd was found within the leaves, towards the edges. Furthermore, the distribution of Zn was different from that of Cd at the leaf scale (Huguet et al., 2012). The non-hyperaccumulator *Arabidopsis thaliana* also showed enhanced Cd accumulation in the trichomes (Isaure et al., 2006). The sequestration into the leaf hairs and epidermis seems to be part not only of a detoxification mechanism, but also a defense strategy. Herbivores like snails will indispensably ingest the leaf hairs and other epidermal cells by moving over them and will be deterred from further feeding (Küpper et al., 2000). A similar situation is also possible for the thorns in *C. demersum*.

Despite the induction of PCs at high Cd concentrations and their expected storage in vacuoles, highest amounts of Cd were observed in the vein at 200 nM Cd. This may suggest that the applied Cd concentration could not be exported out of the vein into the mesophyll. Already from 20 nM (3 weeks) onward, the distribution of Cd became less differentiated, suggesting limited export due to inhibited transporters. Cd shares chemical properties with Zn and Cd enters plants most likely via Ca channels or Zn transporters (Clemens, 2001; Perfus-Barbeoch et al., 2002; Tian et al., 2009). Due to chemical similarity, Cd can replace Zn in the active center of enzymes (Aravind and Prasad, 2004) and inhibit its uptake by competing for transporters or by interfering with the transporter's gene expression (Küpper and Kochian, 2010). Cd can inhibit transporters and limit the uptake of other nutrients, and in the same way transporters localized in the vein can be inhibited. This could explain why high Cd had an effect on the distribution of Zn (Fig. 5). The high amount of Cd therefore most likely inhibited Zn distribution at the highest Cd concentration (200 nM, 3 weeks), and after longer treatment duration with moderately toxic Cd (20 nM, 6 weeks). In both samples, Zn was relocated from the epidermis to the vein (and the thorn). The export of Zn from the vein into the mesophyll will also be inhibited by Cd, when the same transporters are used due to chemical similarity. This Cd-induced inhibition of Zn distribution, which will lead to Zn starvation of tissues outside the vein and possibly added Zn toxicity inside the vein, could be an important factor in overall Cd toxicity in the plants. Interestingly, this inhibited Zn export from the vein was not linked to inhibition of Zn uptake into the plant as measured on the whole-plant level. There was an increased Zn accumulation in the plant treated with 20 nM for 3 weeks, probably showing a defense mechanism against moderately toxic Cd. An increased uptake of

Zn could ensure sufficient Zn within the tissue and has been observed in previous studies (McKenna et al., 1993). However, Zn content in the young and old tissue of *C. demersum* did not alter due to Cd treatment (Tab. 4).

5. Conclusion

C. demersum can tolerate low or moderately toxic Cd concentrations due to upregulation of phytochelatin synthesis and sequestration into non-photosynthetic tissues. Toxicity of Cd inhibited export of Zn from the vein, and various phytochelatins were switch-like induced at individual Cd threshold concentrations. These aspects of toxicity and detoxification were induced already at very low and environmentally relevant Cd concentrations. The switch-like response of PC synthesis could be used as a toxicity marker in natural habitats.

Acknowledgments

We thank DESY for providing beamtime at the DORIS beamline L, and Karen Appel and Manuela Borchert for their support during our µ-XRF measurements. We are grateful for the financial support by the DFG (grant KU 1495/8) and basic funding of Universität Konstanz to H.K.

Figures

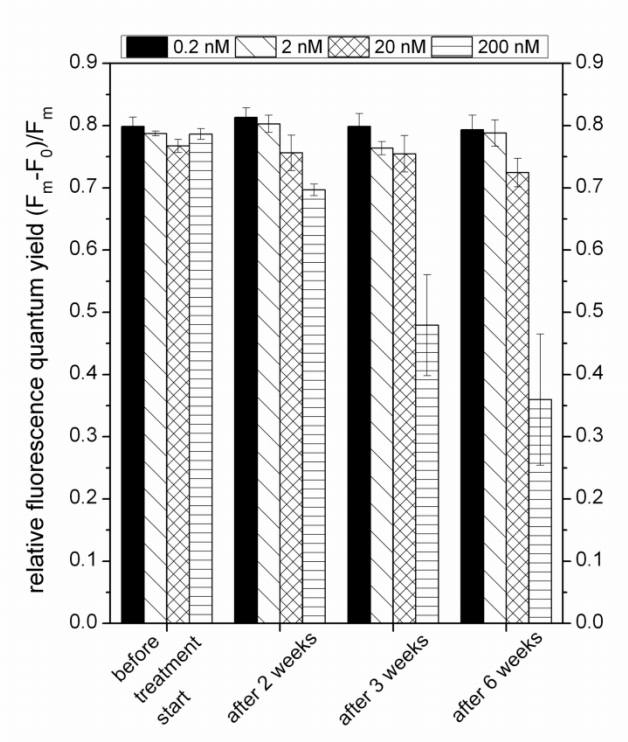

Figure 1. Fluorescence quantum yield of PSII measured as $F_v/F_m = (F_m-F_0)/F_m$ before treatment start and at different times during the treatment duration for 0.2, 2, 20 and 200 nM of Cd. F_0 = minimal fluorescence quantum yield in dark-adapted tissue; all PSII reaction centers open, F_m = maximal fluorescence quantum yield in dark adapted tissues; all PSII reaction centers closed. F_v = variable fluorescence. Values are from 2 experiments and 2 different leaves each. Error bars show error of the mean.

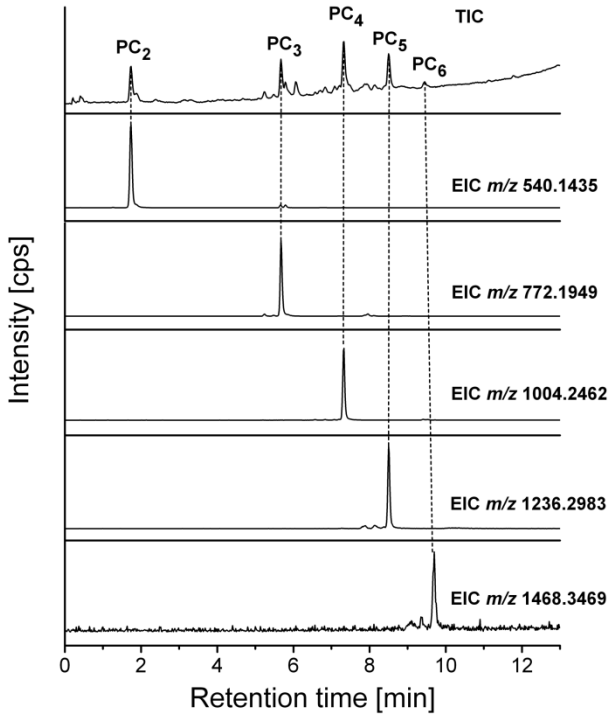

Figure 2. UHPLC-ESI-Q-TOF-MS Chromatograms (Total Ion Counting (TIC); Extracted Ion Counting (EIC)) of a PC standard solution containing PC_2, PC_3, PC_4, PC_5, and PC_6 each with a concentration of 30 µM.

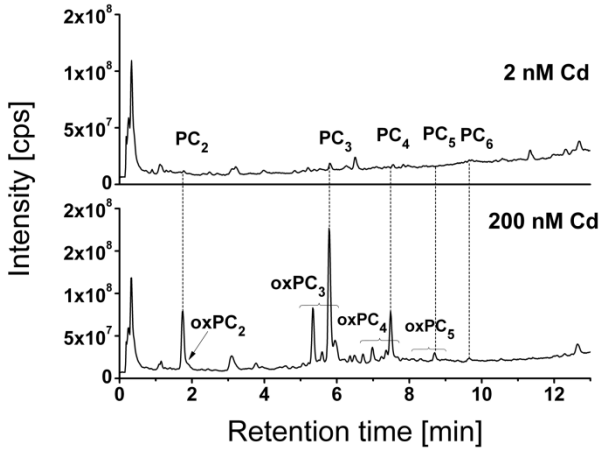

Figure 3. UHPLC-ESI-Q-TOF-MS Chromatograms of extracts originating of young plants under different Cd stress conditions.

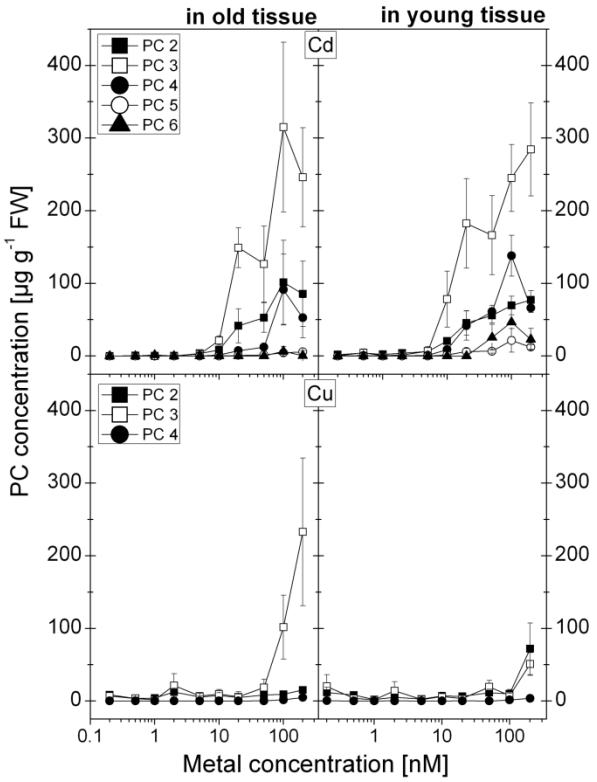

Figure 4. Induction of different phytochelatin species after 2 (Cd) or 2 & 4 (Cu) weeks of metal treatment in young and old tissue Values are averages of 2 experiments and 2 technical replicates Error bars show error of the mean.

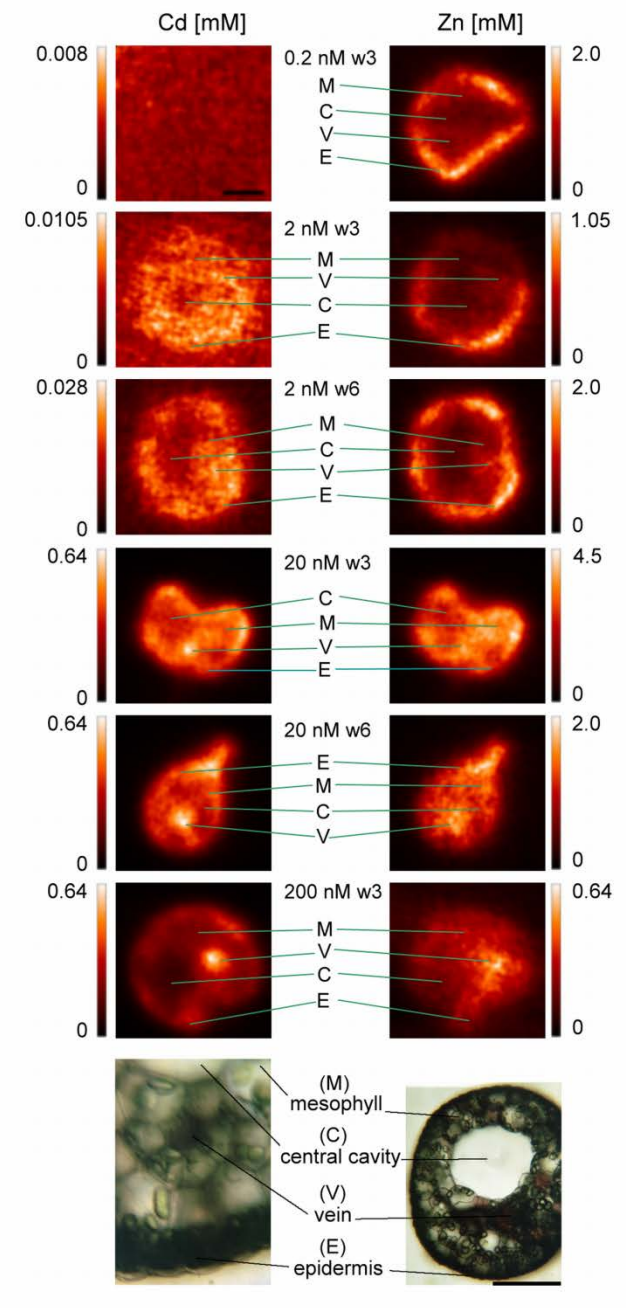

Figure 5. µ-XRF imaging of *C. demersum* leaves treated for 3 or 6 weeks with different Cd concentrations shown for Cd and Zn of the same leaf containing the light microscope picture of a cross section through a *C. demersum* leaf with tissue identification. The position of the different structures was verified by comparing the shown µ-XRF images with the ones for other elements (e.g. Cu). For each concentration, 2 (0.2 nM, 2 nM w 6, 20 nM w 6) or 3 (2 nM w 3, 20 nM w 3, 200 nM) different leaves from different plants of the same experiment were measured. Scale bar = 100 µm. Note that individual scales were used.

Tables

Cations		Anions	
Ca^{2+}	80	BO_3^{3-}	0.16
Co^{2+}	0.01	Cl^-	88.02
Cu^{2+}	0.01	CO_3^{2}/HCO_3^{--}	100
Fe^{3+}(aq.)	0.2	CrO_4^{2-}	0.002
K^+	650	$H_2PO_4^-$ /HPO_4^{2-}	2
Mg^{2+}	150	I	0.05
Mn^{2+}	0.4	MoO_4^{2-}	0.01
Na^+	60.1	NO_3^{2-}	40
NH_4^+	10	SO_4^{2-}	150.5
Ni^{2+}	0.01		
Zn^{2+}	0.05		
Others			
Fe-EDDHA	0.2	Hepes	500

Table 1: Concentrations of the ions in the nutrient solution in µM.

LC-ICP-MS/ESI-Q-TOF-MS	Conditions
LC	
Column	ZORBAX Eclipse Plus C_{18} 2.1 x 50 mm, 1.8 µm
Mobile phase	Eluent A: 0.1 % HCOOH in Eluent B: 0.1 % HCOOH in
Gradient	0-3 min 0 % B; 3-20 min 0-100% B (linear)
ESI-Q-TOF-MS	
Polarity	Positive
Fragmentor voltage	175 V
Capillary voltage	3500 V
Mass range	500-3200 mu
Gas temperature	325 °C
Drying gas	10 L min^{-1}
Nebulizer pressure	20 psi
Sheath gas temperature	400 °C
Sheath gas flow	12 L min^{-1}
Nozzle voltage	2000 V
ICP-MS	
RF power	1600 W
Plasma gas flow rate	Ar 15 L min^{-1}
Carrier gas flow	0.6 - 0.7 L min^{-1}
Sample depth	6 mm
Element monitored	*m/z* 114 (Cd^{+})

Table 2: Parameters for LC-ICP-MS/ESI-MS.

PCs	Retention time (min)	*m/z* theor.	*m/z* exper.	Δ *m/z* (ppm)
PC_2	1.774	540.1429	540.1435	1.1
$oxPC_2$	1.936	538.1272	538.1267	0.9
PC_3	5.705	772.1946	772.1949	0.4
$oxPC_3$ isomers	5.241 5.485 5.875	770.1790	770.1800	1.3
PC_4	7.363	1004.2464	1004.2462	0.2
$oxPC_4$ isomers	6.590 6.850 7.094 7.207 7.500	1002.2308	1002.2298	1.0
PC_5	8.532	1236.2982	1236.2983	0.1
$oxPC_5$ isomers	7.662 7.906 8.150 8.393 8.588	1234.2825	1234.2834	0.7
PC_6	9.475	1468.3500	1468.3469	2.1

Table 3: Retention time, theoretical and experimental *m/z* and mass error Δ of selected PCs.

	Cd [ppm]		Cu [ppm]		Zn [ppm]	
Cd treatment	Young tissue	Old tissue	Young tissue	Old tissue	Young tissue	Old tissue
0.2 nM	9.1 ± 4.3 a	1.29 ± 0.65 a	27.9 ± 2.2	28.6 ± 2.7	476 ± 193	499 ± 154
2 nM	41.3 ± 15.8 a	24.3 ± 8.3 a	30.9 ± 0.99	26.4 ± 1.5	544 ± 219	593 ± 91
20 nM	791 ± 17.4 b	453 ± 48.4 c	22.2 ± 4.8	29.6 ± 2.6	398 ± 10.5	408 ± 74
200 nM	2461 ± 702 d	3676 ± 157 d	18.2 ± 3.6	22.7 ± 0.48	648 ± 8.3	628 ± 8.5

Table 4: Cd, Zn and Cu accumulation in young and old tissue after 6 weeks of treatment with 0.2, 2, 20 or 200 nM Cd. Values are averages from 2 experiments and technical triplicates within AAS measurement. Error = standard error of the mean. Different letters in the Cd column indicate significant differences ($P < 0.05$) according to the Holm-Sidak method (2-way-ANOVA with comparison of age and applied Cd concentration). Accumulation of Cu and Zn did not differ depending on the Cd treatment ($P>0.4$).

2.4 Effects of Cd & Ni toxicity to *Ceratophyllum demersum* under environmentally relevant conditions in soft & hard water including a German lake

Elisa Andresen[1], Judith Opitz[1], George Thomas[1], Hans-Joachim Stärk[2], Holger Dienemann[3], Kerstin Jenemann[4], Bryan C. Dickinson[5] and Hendrik Küpper[1,6]*

1) *University of Konstanz, Department of Biology, D-78457 Konstanz, Germany.*

2) UFZ – Helmholtz Centre for Environmental Research, Department of Analytical Chemistry, Permoserstr. 15, D-04318 Leipzig, Germany.

3) Saxon State Company for Environment and Agriculture; Business Domain 5 (laboratory), Department 53, Bitterfelder Str. 25, D-04849 Bad Düben, Germany.

4) Sächsisches Landesamt für Umwelt, Landwirtschaft und Geologie, Abteilung Wasser, Boden, Wertstoffe, Zur Wetterwarte 11, D-01109 Dresden, Germany.

5) Harvard University, Department of Chemistry and Chemical Biology, 12 Oxford Street, Massachusetts, USA.

6) University of South Bohemia, Faculty of Biological Sciences and Institute of Physical Biology, Branišovská 31, CZ-370 05 České Budejovice, Czech Republic

Published in Aquatic Toxicology (2013) 142-143: 387-402.

Abstract

Even essential trace elements are phytotoxic over a certain threshold. In this study, we investigated whether heavy metal concentrations were responsible for the nearly complete lack of submerged macrophytes in an oligotrophic lake in Germany. We cultivated the rootless aquatic model plant *Ceratophyllum demersum* under environmentally relevant conditions like sinusoidal light and temperature cycles and a low plant biomass to water volume ratio. Experiments lasted for six weeks and were analysed by detailed measurements of photosynthetic biophysics, pigment content and hydrogen peroxide production. We established that individually non-toxic cadmium (3 nM) and slightly toxic nickel (300 nM) concentrations became highly toxic when applied together in soft water, severely inhibiting photosynthetic light reactions. Toxicity was further enhanced by phosphate limitation (75 nM) in soft water as present in many freshwater habitats. In the investigated lake, however, high water hardness limited the toxicity of these metal concentrations, thus the inhibition of macrophytic growth in the lake must have additional reasons. The results showed that synergistic heavy metal toxicity may change ecosystems in many more cases than estimated so far.

Keywords: heavy metals; Freshwater ecosystem; Environmentally relevant conditions; Submerged macrophytes; Photosynthesis biophysics; Chlorophyll fluorescence kinetics

1. Introduction

Many heavy metals like copper (Cu), nickel (Ni), manganese (Mn), molybdenum (Mo) and zinc (Zn) are essential trace elements needed in nutrition of plants, and even cadmium (Cd) has been found to have a metabolic significance in Zn-depleted diatoms (Lane and Morel, 2000). When heavy metals are limited, normal plant growth is often not possible. Over a certain threshold, however, they can lead to growth inhibition and other toxic effects (e.g. reviewed by Chen et al., 2009; Küpper and Kroneck, 2005). This happens either by directly affecting proteins and other cell components, or by interfering with uptake of other essential metals, which leads to their limitation in the plant.

Heavy metals can accumulate in the environment due to industrial activities, pollution and mining. Pesticides and fertilizers containing or contaminated with heavy metals (Frank et al., 1976; Gimeno-Garcia et al., 1996; Mantovi et al., 2003) can lead to heavy metal accumulation in crop plants and threaten human health by entering the food chain (McLaughlin et al., 1999; Senesi et al., 1999). Levels of heavy metals in water and soil can increase rather easily in many areas of the world, reaching µM concentrations that are lethal to many water plants (reviews e.g. by Andresen and Küpper, 2013; Küpper and Kroneck, 2005). The outcome of a large scale meta-study about lakes in Scandinavia and north-western Russia showed that heavy metal pollution is a minor issue on the broad scale, but still can cause ecological problems on the local scale (Skjelkvåle et al., 2001). Nickel concentration in Finnish streams and lakes were in a normal range (low nM), but one peak could be directly traced back to a nickel refinery in north Russia (Skjelkvåle et al., 2001; Tarvainen et al., 1997). This shows how industrial point sources can influence the aquatic environments. Many previously contaminated areas still show elevated levels of heavy metals exceeding limits set by environmental authorities (Bachor et al., 2012).

In photosynthetic organisms, heavy metal induced damage is diverse. Among various possible targets, the inhibition of the photosynthetic apparatus is especially deleterious, for example by non-functional replacement of Mg^{2+} by other metal ions in chlorophyll (reviewed e.g. by Küpper and Kroneck, 2005). In many plants Cd exposure led to reduced chlorophyll content (Lagriffoul et al., 1998). Another proposed mechanism of Cd-induced stress is the formation of reactive oxygen species (ROS), although for Cd this can only be indirectly via malfunction of photosynthesis as Cd is biologically redox-inert. ROS can lead to lipid peroxidation (Mediouni et al., 2008), causing membrane damage followed by ion leakage

(Kumar and Prasad, 2004). Long-term effects of Cd toxicity, and plant acclimation to it, have been studies in detail in the Cd/Zn hyperaccumulator *Noccaea* (formerly *Thlaspi*) *caerulescens*. However, in some studies, Cd seemed to have a positive effect (Ornes and Sajwan, 1993) when present only in low concentrations.

Ni is an essential element in plants being the central ion in the active centre of urease. Most plants need only minute amounts of Ni and limitation is rarely achieved, most easily occurring in Ni-hyperaccumulators that are adapted to high soil Ni (Küpper et al., 2001). At higher concentrations, Ni can inhibit cell proliferation (Rao and Sresty, 2000) and disrupt photosynthesis (Chen et al., 2009; Küpper and Kroneck, 2005). The symptom of chlorosis results from Fe and/or Mg deficit, which are imported less when concentrations of Ni in the environment are above optimum (Piccini and Malavolta, 1992).

However, most studies about Cd and Ni toxicity in plants dealt with acute toxicity, i.e. rather short incubation times of hours to days, and µM or even higher concentrations were used. Further, EDTA, which was often used for iron chelation, also binds to other heavy metals, reducing their bioavailability. For aquatic environments, the maximal allowable concentrations for Cd and its compounds are 4 - 13 nM (depending on water hardness), for Ni and its (bioavailable) compounds 579 nM (European Commission, 2012). The annual averages are even lower (0.7 - 2.22 nM Cd; 68 nM Ni). Biotic ligand models (BLMs) can predict concentrations that will have an effect on aquatic organisms (Deleebeeck et al., 2009b; Schlekat et al., 2010).

The present study dealt with an actual environmental problem. Lake Ammelshain (51.296 N; 12.615 E) is a groundwater lake without any influxes. It is located near Leipzig, Germany. Its size is around 50.6 ha and its maximal depth is 27 m. The lake was formed in the 1930s due to gravel stripping. After the stripping was stopped from 1981 on, the lake turned to an oligotrophic level. Concentrations of chlorophyll and phytoplankton are noticeably low (1 µg L^{-1} Chl; Bernhard, 2010). However, different species of phyto- and zooplankton and even fish can be found in the lake, but besides some *Myriophyllum* plants, no macrophytes (Bernhard, 2010; Nixdorf et al., 2008). To elaborate the reasons for the absence of the macrophyte flora, in particular a possible involvement of Cd and Ni toxicity, relevant parameters of the lake water were measured in August and October 2010, and March and May 2011. Furthermore, lake water samples were taken from the epilimnion and the hypolimnion in summer, autumn 2010 and spring 2011. The model plant *Ceratophyllum demersum* L. was cultivated in these lake water samples and systematic simulations of the lake water for 6

weeks using environmentally relevant conditions of nutrient levels, light and temperature conditions. *C. demersum* is a submerged macrophyte sensitive to heavy metal stress and has no roots, which means that all nutrients are taken up over the whole shoot.

2. Materials and methods

2.1 Determination of physical parameters of the lake

In August and October 2010, as well as March and May 2011, lake parameters were measured. The sampling periods were chosen to be consistent with the year's seasons. In winter the lake was covered with a thick ice layer and sampling was not possible. The winter sample was therefore taken in March, when the ice was gone.

The depth profile was recorded in 50 cm steps with DS5 (Hydrolab, Hach Hydromet, Loveland, CO, USA) and the parameters depth, pH, temperature, electric conductivity, oxygen amounts and saturation (LDO sensor, Hach) and air pressure (ADC Summit Silva, Sollentuna, Sweden) were measured. Light intensity was measured between water surface and 9 m depth in summer, and 27 m depth in winter with a light meter Li-Cor 250 equipped with the spherical underwater sensor Li-193 (Li-Cor Lincoln, NE, USA) and a CTM sensor (Sea&Sun, Trappenkam, Germany). Water samples for cultivation of plants (30 l in PE barrels) and ICP-MS analyses (50 ml in PFA tubes; AHF, Tübingen, Germany) were taken with a IWS II (Hydro-Bios, Kiel, Germany) in 5 l steps from the epi- and hypolimnion (Wetzel, 2001) when the lake was separated into distinct layers. During the circulation period, epilimnion water was taken as a mixed sample between 0-7 m depth and hypolimnion water as a single sample 1 m above the ground for which the IWS II was controlled by a cable (Sea&Sun, Treppenkam, Germany). The maximal deviation of the sampling position was less than 0.25 m. The water was very clear, without visible particles and therefore not filtered.

2.2 Plant material and cultivation

We used the submerged, rootless macrophyte *Ceratophyllum demersum* L. for the experiments. The strain was continuously cultivated since 2005 in hydroponic solution with 12 h day/12 h night light conditions provided by two Osram FLUORA® fluorescent and two warm white fluorescent tubes (Osram, München, Germany) and a temperature cycle from

18°C at 6 a.m, over 20°C at 9 a.m., to a maximum of 22°C at 3 p.m., back over 20°C at 9 p.m. to 18°C again at 6 a.m.

Plants of stock cultures were cultivated long term in a nutrient solution that was previously optimised (personal communication from HK) for submerged macrophytes and water plants (SMNS) and consists of 0.1 µM B, 100 µM C, 40 µM Ca, 87.5 µM Cl, 0.01 µM Co, 0.02 µM Cr, 0.01 µM Cu, 0.2 µM Fe, 0.2 µM Fe-EDDHA, 500 µM Hepes, 0.05 µM I, 120 µM K, 150 µM Mg, 0.4 µM Mn, 0.01 µM Mo, 30 µM N, 60 µM Na, 0.01 µM Ni, 2 µM P, 151 µM S, 0.05 µM Zn. The pH was adjusted to 7.8 with KOH. This nutrient solution is, in principle, a simulation of conditions in oligotrophic freshwater habitats with low water hardness, where submerged macrophytes thrive. Experimental treatments were, therefore, performed in SMNS as control, in water from the epi- and hypolimnion of Lake Ammelshain and in different simulations of lake water investigating which of the differences between SMNS and the lake water caused inhibition of plant growth in the lake water. The different simulations are displayed in table 1. Further, for investigating the effect of water hardness, the experiments using SMNS with Cd, Ni and reduced phosphate which caused the greatest inhibitory effects were repeated with increased water hardness (CdNi-P (hard water)). Finally, a lake simulation as accurately as possible (Lakesimulation) and the same simulation without extra Cd, Ni and P-stress (Lakesimulation – CdNi-P) were performed. The respective concentrations can be found in table 2. Elevated Na and Cl levels were also tested, but the samples did not show any effect (not shown).

Lake water from the March 2011 sampling was carried out at 4°C and led to shrinking of all plants. Therefore only the metal accumulation was used for analyses. All experiments were carried out under simulations of natural light and temperature conditions: 12 h sinusoidal light cycle with maximal irradiances at 750 µmol photons m^{-2} s^{-1} (supplied by Dulux L 55 W / 12-954, OSRAM München, Germany) and 12 h night; 19°C at 6 a.m., 21.5 at 9 a.m., 24 at 3 p.m., 23 at 9 p.m., 19 at 6 a.m.. For each treatment around 1.5 g of plants (fw; 1-2 plants) were placed into an aquarium containing 2 l of continuously aerated medium to secure a low biomass to water volume ratio. The number of individual plants was consistent for each treatment within the same experiment. Differences occurred due to weight and size of the plants at treatment start. There was a continuous exchange of nutrient solution (flow rate 0.5 l day^{-1}). In this way, the total amount of nutrient solution supplied per plant in the 6 weeks ensured environmentally relevant, i.e. low, biomass to metal ratios in contrast to most earlier studies where rather high biomass to volume ratios were applied. Thus we ensured that the

metal uptake into the plants was limited only by the concentration, but not by the amount of nutrient solution available, while the latter was likely a problem in most earlier studies. In lake Ammelshain, the biomass per volume ratio is even lower than in our experiments. Each experiment lasted for 6 weeks. Measurements were carried out weekly, or only at the end of the treatment.

2.3 Fluorescence kinetic microscope (FKM)

Physiological changes in the plants induced by heavy metals were determined by two-dimensional (imaging) microscopic measurements using the Chl fluorescence kinetic microscope (Küpper et al., 2007a, 2000a). One leaf from the 5th nodium counted from the apex of the plant was fixed in the measuring chamber by gas-permeable cellophane (Küpper et al., 2000a). The chamber had a continuous flow of the culture medium (without micronutrients (Rochetta and Küpper, 2009). The area just before the branching (approximate size of 1.1 mm x 1.1 mm) was used for the kinetics measurement. A detailed description of the microscope and the used protocols of the Kautsky induction can be found in Küpper et al. (2007a) and Andresen et al. (2010). These measurements were done weekly, but values from the beginning (week 1+2), the middle (3+4), or end (5+6) of the treatment, respectively, were averaged to reduced the noise level.

2.4 Oxygen exchange

After 6 weeks of treatment net photosynthetic oxygen release and respiratory oxygen uptake were measured with a Clark-type electrode (CellOx® 325, OxiCal-SL, WTW, Weilheim, Germany) in a custom-made 200 ml measuring chamber at 25°C. Oxygen uptake was measured in the dark, oxygen release under increasing light intensities (from 8.1 to 600 µmol photons m^{-2} s^{-1}). Data were recorded and analysed using the OxyCorder measuring device with the software Oxywin 3.1 (Photon Systems Instruments, Brno, Czech Republic).

2.5 Determination of H_2O_2 production with PF2

Intracellular hydrogen peroxide (H_2O_2) production was determined with a H_2O_2-specific fluorescent indicator based off of a boronate deprotection mechanism (Chang et al., 2004; Lippert et al., 2011), Peroxyfluor-2 (PF2, Dickinson et al., 2010). One leaf from the 5th

nodium counted from the apex of the plant was incubated in 100 µM PF2 in 0.5 ml of SMNS (without micronutrients) for 30 min in the dark. After 30 min of destaining in 15 ml SMNS in the dark, the leaf was fixed to the measuring chamber of the FKM. The medium was exchanged after every measurement and all tubes washed with ddH_2O. The H_2O_2-specific fluorescence was measured in the FKM using filter set from AHF (Tübingen, Germany) with an excitation filter 420-500 nm (AHF F42-468), dichroic mirror 505 nm (AHF F71-302) and 520-550 nm emission filter (AHF F47-535). Flashes of blue supersaturating light were given at increasing signal integration times (20 µs up to 20 ms). For each sample, the integration time that led to the highest signal intensity without saturating the camera was chosen for quantitative analysis to avoid noise at too short exposure times and oversaturation of the camera at too long exposure times. For each exposure time, hundreds of single pictures were taken and averaged. Background signal for each exposure time was subtracted automatically via a measurement without light.

Images of the measurement were analysed with the FKM software and the fluorescent signal was re-calculated to one integration time according to an empirical calibration of exposure times vs. signal intensity. The values from the beginning (week 1+2), the middle (3+4) and the end (5+6) of the treatment were averaged to minimize noise levels.

2.6 Harvest

After 6 weeks of treatment, plant samples were harvested. Plants were washed in SMNS without micronutrients and young and old tissues were separated from each other. Young tissues being 4 cm from the apex and 2 cm from the apex of each branch, old tissues 8 cm from the stem end and the rest of the branches. While the young tissues contained biomass which was only generated during the treatment duration, the old tissue also contained remainders from the pre-treatment phase of the stock cultures. Remaining SMNS was removed by shaking, and the plants were frozen in liquid nitrogen. Samples were stored at -80°C until further analyses.

2.7 Determination of pigment content

Pigments of the harvested material were extracted and determined following established protocols by Küpper et al. (2007b, 2000b).

2.8 Elemental analyses of water, nutrient solutions and digested plant samples with ICP-MS

Following Zhao et al. (1994), 5-10 mg of lyophilized plant samples were digested in 250 µl (85:15%) nitric-perchloric acid for 30 min at room temperature and then gradually heated up to a maximum of 195°C until all liquid was vaporized. The remaining ashes were re-dissolved in 0.5 ml 5% HCl, gradually heated to 80°C. After cooling the volume was filed to 1.5 ml with ddH_2O and used for analyzing the components.

Element concentrations were analysed using an inductively coupled plasma sector field mass spectrometer ICP-sfMS (Element XR, Thermo Fisher Scientific, Waltham, MA, USA). Prior to analysis ICP-sfMS parameters were optimised every day and samples were diluted 1:20 prior to analysis. The calibration with up to 5 standards was verified using the following reference materials: SLRS-5 (River Water Reference Material for Trace Metals, NRCC), SPS-SW1 (Surface Water Level 1, Spectra Pure Standards) and SRM 1643e (Trace Elements in Water, NIST). The instrumental parameters for determination of the investigated elements are reported in table 3.

3. Results

3.1 Micro- and macronutrient distribution and limnological parameters of lake Ammelshain

The measured parameters depth, light intensity, temperature, pH, conductivity, amount of oxygen, and saturation are shown in Fig. 1. Lake Ammelshain shows typical characteristics of a dimictic lake. After an ice cover in winter, there was a complete intermixture of the water (visible in the March data in Fig. 1), as well as in November/December (Bernhard, 2010). After spring circulation the epilimnion was formed as a stable layer (sampling May 15th 2011, data not shown). The thermocline, which separates epi- from hypolimnion, was most pronounced in summer, showing summer stagnation (see August data in Fig. 1). These changes were best visible in the oxygen content and oxygen saturation (Fig. 1). Except for the winter sample, pH was higher in the epilimnion compared to meta- and hypolimnion due to primary production combined with the very limited buffering capacity of the water. The pH range of 6.8-7.2 corresponds with the pH of the groundwater influx. The decrease in conductivity in the epilimnion in August and October may be due to the incorporation of the

ions into biomass in the higher water levels and the following effects on temperature and carbon dioxide solubility.

The distribution of nutrients in the lake is depicted in table 2. For better judging the limitation or potential toxicity, values are compared with those from lake Constance and a nutrient solution. Lake Constance is an oligotrophic lake and accommodates many different species of algae, macrophytes (incl. *Ceratophyllum*), insects and fish. The amounts did not differ much between epi- and hypolimnion. Obvious differences between lake Ammelshain and lake Constance are generally higher amounts of macronutrients (Ca, Na, Mg, K, Cl, S) and some micronutrients (Ni and Cd) in lake Ammelshain. The high amounts of Mg and Ca ions define lake Ammelshain as a hard water lake, while lake Constance has medium water hardness. Iron was higher in the water of lake Ammelshain and although the same nominal concentration was applied in the lake simulation, the measured concentrations were much lower. Fe in the lake water is most likely not completely bioavailable and likely in part in colloidal form. The Fe in Fe-EDDHA used in our nutrient solution is known for its good bioavailability. In general, among all trace metals the bioavailability of iron is known to be by far the hardest to predict. Other micronutrients are present in lower (Mo) or equal (Cu) concentrations in lake Ammelshain compared to lake Constance. Compared to our nutrient solution, phosphate in lake Ammelshain is also lower. However, in lake Constance macrophytes grow although phosphate is only slightly higher than in lake Ammelshain, therefore it is unlikely that low P is limiting in lake Ammelshain. Zn is higher in lake Ammelshain than lake Constance, but still lower that in our control medium so that Zn toxicity can be excluded.

3.2 Visible symptoms

Plants cultivated in the lake water, especially from the April 2011 sample, lost leaves every week and were nearly decomposed after 6 weeks of treatment. Plants from the CdNi-P treatment behaved similarly. The Ni-only treatment led to noticeable bleaching of the leaves. The Cd-only treated plants, like the Control and Control-P, showed no visible symptoms of stress. The newly generated biomass (“young”) of those plants treated with the real (epi- and hypolimnion), the simulated lake water, or the Metals-P nutrient solution had a noticeably reddish / brownish colour.

3.3 Photosynthetic parameters by FKM

All inhibitory treatments led to a reduction in the maximal fluorescence quantum yield in dark-adapted samples (F_m) compared to the Control, both in soft and in hard water. (Fig. 2A). All hard water treatments led to slight reduction in F_m towards the end of the treatment. In soft water with Cd-treatment, the F_m values were stable throughout the 6 weeks. All other treatments showed a decrease from the first week on (Fig. 2A, right). Especially the plants cultivated in the nutrient solution containing additional nickel, cadmium and less phosphate (CdNi-P) showed strongly decreased F_m from week 3 on and may have reached even lower values after a longer time of treatment.

The same trend was observable in the light saturation parameter (measured as $(F_p-F_0)/(F_m-F_0)$; Küpper et al., 2007a). For the plants cultivated in the epi- and hypolimnion (Fig. 5A), saturation decreased from the 3rd week on after a slight increase in the first week. The effect was hardly observed in the other treatments in hard water. In soft water, decrease occurred most noticeably in the CdNi-P plants (soft water) (Fig. 5A).

The maximal photosynthetic quantum efficiency of photosystem II (PSII) in dark adapted state (measured as $F_v/F_m = (F_m-F_0)/F_m$) was highest for the Control plants, and interestingly also for the Cd-treated ones in soft water (Fig. 2B). Their F_v/F_m values were stable throughout all weeks of treatment. All other treatments led to a subsequent reduction of PSII activity from the first week on in soft, from the third in hard water. The decrease was far less pronounced in hard water (Fig. 2B, left). Highest inhibitory effect was observable for the CdNi-P plants (soft water) (2-way ANOVA showed significant $P<0.05$ effects for Cd, Ni and P and significant interactions between P and metals). For these plants, the same effect occurred under actinic light (Φ_{PSII} = light-acclimated electron flow through PSII = "photochemical quenching", measured as $(F_m'-F_t')/F_m'$). The electron flow through PSII after some time of illumination (Φ_{PSII} i6) decreased strongly for CdNi-P, CdNi (both soft water), and the two lake water samples (Fig. 3). The plants cultivated in medium containing Cd, Ni, Metals-P or solely phosphate limitation (all soft water) showed a high (slightly higher or equal Control) electron flux until the end of the experiment. The effect was even stronger pronounced in the recovery time after the actinic light was switched off again (Φ_{PSII} r5), most treatments led to a strong decrease in Φ_{PSII} at the end of treatment (week 5+6).

In contrast to the photochemical quenching, the non-photochemical quenching (NPQ = light-induced change of exciton dissipation as heat, measured as $(F_m-F_m')/F_m$) gave rather noisy results (Fig. 4). However, there was a decrease of NPQ at the end of the light phase

(NPQ i6) for the CdNi-P-plant (soft water) and the plants cultivated in the real lake water (Fig. 4). Right after start of the dark phase (NPQ r1), NPQ values were generally higher (data not shown) than at the end of the dark phase (NPQ r5), showing the recovery of the photosynthetic components.

To better elaborate the plants' ability to recover after the actinic light phase, we introduced the relaxation parameter, measured as (Φ_{PSII} r5-Φ_{PSII} i6) / (F_v/F_m-Φ_{PSII} i6). This parameter describes whether the PSII / PQ-system can recover completely to reach the dark adapted state of F_v/F_m. In that case, the relaxation value will be 1. Most treatments in soft water led to a reduced recovery from the first week on, while the hard water samples showed hardly any decrease in relaxation recovery besides the real lake water samples (Fig. 5B). The CdNi-P plant (soft water) showed the least recovery ability after 6 weeks of treatment (Fig. 5B).

For all described parameters, a homogenous distribution all over the measured area of the leaf was observed (Fig. 9).

3.4 Photosynthetic oxygen exchange

After 6 weeks of treatment, most plants cultivated in the lake water or the simulated lake water showed a decreased photosynthetic oxygen release (Fig. 6A). In case of the hard water nutrient solutions, the highest inhibitory effect was observable in the plants that were cultivated in the epi- and hypolimnion lake water. While in these treatments photosynthesis did not increase with higher irradiances but decreased, the Control (hard water) plant did not even reach saturation at the highest light intensity. Regarding the soft water treatments, plants that were grown with limited phosphate (Control-P, Metals-P and CdNi-P) also showed reduced oxygen release compared to the Control. The other treatments though did not inhibit the plants' oxygen production ability; plants cultivated in nutrient solution containing additional nickel (Ni), cadmium (Cd) or cadmium+nickel (CdNi) reached Control or even higher levels. In the case of CdNi, the values may not be different from the Control regarding the error bars. For the Cd-only treatment however, already from rather low irradiances onward, the plants released more oxygen. Respiration was highest in the latter two treatments (Cd, CdNi) and the Control (hard water), followed by the Control (soft water), and lowest in the plants cultivated in epilimnion or hypolimnion water (Fig. 6B).

3.5 Pigment composition

The metal treatments significantly affected the pigment composition (1-way ANOVA on treatment vs. pigment concentration for total Chl $P < 0.001$).

The amount of total Chl was highest in the plants that were cultivated in the control medium (hard water & soft water), in the nutrient solution with additional Cd and in the medium with CdNi-P (hard water) (Fig. 7, top row). Plants that were cultivated in the epi- and hypolimnion contained least amounts of total Chl. The age of the tissues did not modify the effects of the treatments on Chl concentration.

Betacarotene and zeaxanthin have the same absorption spectra and were, therefore, determined together as "betacarotene-like pigments" (Küpper et al., 2007b). The amount of betacarotene-like pigments increased in the young and old tissues of plants cultivated in simulated lake water with Cd or Ni (Fig. 7, middle row) compared to the control in soft water. In hard water, the Control plants contained highest amounts, followed by the CdNi-P (hard water) treatment. In contrast, the amount was lower in the plants cultivated in the real lake water. For both, the epi- and the hypolimnion, there were fewer amounts of pigments in young tissues than in old. The remaining soft water treatments (Control-P, CdNi, CdNi-P, Metals-P) did not alter the concentration of betacarotene-like pigments compared to the control. The remaining hard water treatments contained less betacarotene-like pigments. The ratio of total chlorophyll to total carotenoids was around 2:1 for most plants (Fig. 7, bottom row), highest in the plants of the Lakesimulation without CdNi-P stress (3.5:1) and lowest in the old tissue of the Ni-treated plants (1.8:1) and the CdNi-P-plants. For antheraxanthin and cis-/trans-lutein, treatment-specific trends did not exceed the noise level of the measurement (not shown).

3.6 Accumulation of heavy metal and other elements

Accumulation of heavy metals was higher in plants that were treated with these metals specifically (Tab. 4). Cadmium accumulation was higher in the plants treated with a mixture of metals (both the hard and soft water versions of the CdNi and CdNi-P treatments, Metals-P and the lake simulation) than in the Cd-only treatment. Cd accumulation was also higher in the plants from the hypolimnion than the epilimnion, although Cd concentration in the water was equal (Tab. 2). The age of the tissue did not affect Cd accumulation ($P<0.1$). For Ni the opposite trend was observable. Plants that were treated with Ni only accumulated most of it,

the CdNi, CdNi-P, Metals-P treatments led to slightly less Ni-accumulation. Plants from the epi- and hypolimnion had amounts of Ni not different from the control (hard water) samples ($P = 0.096$), while hardness did not diminish Ni uptake in the CdNi-P treatments. Also for Ni, there was no difference regarding the age of the tissues. The treatments did not have any clear effect on Cu or Zn accumulation in the plants. Mo was highest in the young tissue of the Cd treated plant though the amount of Mo in the nutrient solution was not different from the control solutions. (Within the "Cd" treatment, there was an effect of the age of the tissue.) Iron was highest in the plants cultivated in the real lake water, but this certainly includes iron adhesion to cell walls. Despite the low phosphate concentrations in the water of lake Ammelshain, plants cultivated in the lake water had comparable P amounts in their tissues as control plants. An overall difference of the age of the tissue was observed, but the effect of the treatment did not depend on what age was present. S was higher in the plants from the hard water than in the soft water treatments, which is consistent with higher S concentrations in the hard water.

3.7 H_2O_2 production

The relative H_2O_2 production increased mostly in the plants cultivated in the hypolimnion of the lake water from the first week on (Fig. 8). Towards the end of the treatment the production decreased again, but stayed higher than before treatment start. The Cd-treated plants showed the same trend, but after a peak at the beginning, relative H_2O_2 production decreased and fell under the level of the starting value. Plants treated with water from the epilimnion and CdNi-P showed a continuous increase of H_2O_2 production until end of treatment. Plants from the Control, Control--P, CdNi and Metals-P treatments balanced around a baseline and the Ni-plant showed increased H_2O_2 production only at the end of the treatment. None of the other plants from any hard water treatment showed increased H_2O_2 production, but rather a decrease (Fig. 8). There was a strong heterogeneity of H_2O_2 production in the leaves. Some cells had much brighter fluorescence than others (Fig. 9).

4. Discussion

Though the lake water and the simulated media contained heavy metals only in the nanomolar range, under certain circumstances they already became toxic to the plants. Before discussing this main result in more detail, it should also be noted that the Cd only treatment interestingly led to positive effects instead of inhibition. Ornes & Sawjan (1993) found that *Ceratophyllum* cultivated in rather low Cd concentrations (89 nM, but chelating agent also used, so most likely much less bioavailable) had longer lateral shoot lengths compared to the Control. This at first glance may look like the Zn-limited cultures of the diatom *Thalassiosira weissflogii*, where Cd was found to have a metabolic function; a specific Cd-carbonic anhydrase (Cd-CA) was expressed (Lane and Morel, 2000). As the water of lake Ammelshain had even more Zn than the Control medium (Tab. 2), however, this scenario seems rather unlikely to take place in *Ceratophyllum*. Furthermore, Zn-accumulation was not different in Cd-treated plants compared to the Control plants (Tab. 4). Cadmium exposure to *T. caerulescens* led to consistent increase of CA activity despite the Cd-initiated decrease of Zn in the shoots (Liu et al., 2008). Whether Cd enhanced CA activity or led to expression of a Cd-CA remains unclear.

Ceratophyllum was also tested for its Cd-accumulation capacities (Bunluesin et al., 2004; Gupta and Chandra, 1996) and found to be a hyperaccumulator at low concentrations and therefore suggested for phytoremediation purposes (Bunluesin et al., 2004). The current study sheds doubt on that suggestion, as already very low Cd concentrations, when combined with nickel, can become very inhibitory. And the high metal bioaccumulation factor at extremely low concentrations is a common feature of many aquatic organisms, not a special property of *Ceratophyllum* (McGeer et al., 2003).

The Ni-only treatment led to decreases in photosynthetical parameters (like F_m, F_v/F_m, Fig. 2) compared to the start of the treatment and to the Control. Electron flow through PSII decreased towards the end of the treatment. Non-photochemical quenching in the actinic light phase was seemingly not affected (Fig. 4). These findings indicate reduced photosynthetic activity (less photochemical quenching, less maximal fluorescence, less activity of PSII). The lower maximal fluorescence is consistent with a reduced Chl content (compared to the Control). Also that NPQ in the light phase did not increase could be a consequence of reduced Chl, as less excitation energy is directed to the reaction centres so there is less likelihood that excess energy has to be dissipated as heat. Interestingly, in the dark phase there was an increase (compared to the Control) of non-photochemical quenching towards the end of

treatment, indicating that relaxation of NPQ mechanisms was disturbed. The reduction of photochemical quantum yield of PSII (F_m-F_0)/F_m), however, cannot be caused just by reduced Chl as this parameter measures only the activity of the PSII core. In this way, it is clear that the nanomolar metal stress already directly inhibited photochemistry.

The concentration of Ni in the lake water and the different Ni-treatments was 30 times higher than in the Control medium (Tab. 2), and plants cultivated in the Ni supplied nutrient solution accumulated around 45 times more Ni than the Control plants. High Ni concentrations were discussed to have several toxic effects in plants. Unfortunately, as well as for Cd, most studies dealt with much higher Ni concentrations and only seldom with aquatic macrophytes or multicellular algae. Li and Xiong (2004) found that colonies of *Lemna paucicostata* collapsed when treated with 5 µM of Ni. Another species of duckweed, *Spirodela polyrhiza*, showed reduced multiplication rate with increasing concentrations of Ni (Singh et al., 2011). The authors found that concentrations above 9 mg l^{-1} (= 150 µM) were toxic to the duckweed, and above 1 mg l^{-1} (=17 µM) there was a gradual decrease in contents of Chl a, b and carotenoids towards higher concentrations. In this experiment, Ni-treatment led to a decreased Chl content and increased carotenoid content (Fig. 7). In this way, the current study shows that heavy metal concentrations previously regarded as rather harmless for multicellular organisms may have strong inhibitory effects. Regarding microalgae, Deleebeeck et al. (2009a, 2009b) developed a model with which the toxicity of Ni can be predicted dependently on water hardness.

Ceratophyllum tolerates and accumulates Cd most likely due to the upregulation of specific Cd-binding proteins, the phytochelatines (Kumar and Prasad, 2004; Mishra et al., 2009, Andresen et al., 2013) or detoxifying systems like antioxidants (Mishra et al., 2008). The decrease in PF2-detected H_2O_2 production after an initial peak (Fig. 8) may be due to an increase of catalase (CAT) activity, maybe together with a reduction of superoxide dismutase (SOD). Both scenarios, but also the opposite effects have been described as a response to Cd-treatment (Gallego et al., 1996; Mediouni et al., 2008; Sandalio et al., 2001; Srivastave and Telor, 1991). The stress symptoms measured by chlorophyll fluorescence did not correspond to the H_2O_2 production, as it was revealed by the spatial distribution of both signals, which did not correspond to each other (Fig. 9).

The inhibition was clearly higher in the Cd&Ni combination treatments than in the treatment with the same concentration with Ni alone. This was particularly surprising in view of the stimulatory effect of the low Cd concentration when applied alone, as discussed above.

Thus the elevated damage in the Cd&Ni treatments must have been due to a synergistic effect of Cd and Ni. The accumulation of Cd was higher in those plants that were cultivated in the CdNi-P nutrient solution than in the CdNi and the Cd-only treatment (Tab. 2, 4). At first glance this may seem contradictory to an earlier study on metal interaction, where the accumulation and the toxicity of Cd, Cu and Pb in cucumber was less when a ternary mixture of heavy metals was given instead of a single metal treatment (An et al., 2004).

Not one, but many heavy metals were over optimum for our model plant in the lake water and the simulations. The plants cultivated in the simulated lake water containing Cd, Ni and less P (soft water) showed the highest degree of damage of their photosystems. At the end of the treatment, the plants had a strongly reduced maximal fluorescence (Fig. 2), were not able to recover after the actinic light phase (Fig. 3) and had reduced pigment contents (Fig. 7). The inhibitory effect on photosynthesis of the two metals, in combination with phosphate limitation was higher than for the two metals alone (CdNi), for the real lake water (epi- and hypolimnion) and for simulations of the lake water containing more salts, or a combination of metals and salts (data not shown).

The results of the present study showed that also other components in the water influence metal availability. For example, pH (Fig. 1) may also be important. The pH in general influences the bioavailability of heavy metals and other ions. The effect is different in aqueous solutions, where metal toxicity often decreases with increasing pH while it is the opposite in soils (Plette et al., 1999). The pH of the epilimnion was slightly higher than in the hypolimnion of lake Ammelshain (Fig. 1). While the single heavy metal concentrations did not differ much between the depth levels (Tab. 2), the plants that were cultivated in the hypolimnion water accumulated more Cd and less Ni than in the epilimnion water (Tab. 4). Another factor influencing metal accumulation is the competition with other ions, and this seems to be very important for the case of lake Ammelshain. In hard waters the high(er) amounts of Ca and Mg ions protect aquatic organisms by competing for the available binding sites on the organism's surface. Especially the divalent metal ions (Cd, Zn, Ni, Pb) can be taken up by the cell via Ca transporters (e.g. Ca^{2+}-ATPase, Markich and Jeffree, 1994), emphasizing the use of Ca concentrations instead of total water hardness for water quality guidelines. High concentrations of Ca reduce heavy metal toxicity by preventing entrance into the cell just by competing for uptake. Consistently, aquatic moss species accumulated less Cd in harder water (applied as $CaCO_3$, Gagnon et al., 1998). On the other hand, green unicellular microalgae were protected against Ni toxicity solely by Mg, not Ca ions (Deleebeeck et al.,

2009a). The uptake mode of different metals into water plants varies though. Copper e.g. enters the plant via specific transporters where no competition with Ca and/or Mg ions takes place (see above). Concordantly, the increased water hardness did not have a protective effect on the Cu accumulation in *C. demersum* and other organisms (Markich et al., 2006, and citations within). Especially the comparison of the CdNi-P treatment in soft and hard water (e.g. (F_m-F_0/F_m) in Fig. 2) underlines the protective effect that must be due to the higher water hardness. These samples were hardly inhibited in the above mentioned parameters. Oligotrophic lakes are nutrient-poor, which mostly refers to phosphate limitation. Phosphate is needed in various cell components like phospholipids, nucleic acids and ATP, and as P_i also involved in the regulation of enzyme activity and metabolic pathways (Schachtman et al., 1998). The samples of the Control-P treatment suffered from the P-limitation (Fig. 6). An enhancement of heavy metal stress in combination with P-limitation has been shown. Kamaya and colleagues found Cu to be more toxic for the alga *Selenastrum capricornutum* under P-limitation (Kamaya et al., 2004). This would explain the disastrous inhibition of the CdNi-P (soft water) plants (e.g. Fig. 2) and the very slight inhibition of the CdNi-P (hard water) plants if we furthermore accept the protective role of Ca and Mg in the water. Therefore, our study clearly showed that in soft or moderate hard water lakes, especially when combined with low phosphate, plants may suffer already from slightly elevated heavy metal concentrations. This may be ecologically important for oligotrophic lakes in many parts of the world (e.g. many alpine lakes in Switzerland). Finally, it is known that dissolved organic matter (DOM) controls dissolved metals speciation (Florence, 1982). Bunluesin et al. (2007) showed that the addition of humic acid decreased the bioavailability of Cd and Zn due to complexation and significantly reduced toxicity of these metals to *C. demersum*. This has to be kept in mind when comparing our case study with other aqueous habitats.

5. Conclusions

Despite many simulations, the same inhibition of the lake water could not be achieved, pointing out the complex interactions between many abiotic factors influencing plant growth. Nevertheless, our experiments clearly show that heavy metals may have negative effects at much lower concentrations than normally tested in mechanistic studies, especially when previously unexpected synergistic effects, like those shown now for Cd&Ni, occur. This,

points out the need for further studies which inhibition mechanisms act in this very low concentration range. Further, the strongly detrimental effect of these low heavy metal concentrations indicates that in many more watersheds and lakes than believed so far changes in plant growth and ecosystem balance may be due to heavy metal toxicity stress. In view of these results the damage potential of environmental pollution by heavy metals and its underlying mechanisms have to be reconsidered.

Acknowledments

We thank Christopher Chang for making the contact to Bryan Dickinson who synthesised the PF2 dye. We would like to thank Michael Oberländer for providing us with the water samples and Melanie Gerigk for indispensible help with *C. demersum* stock cultures.

Figures

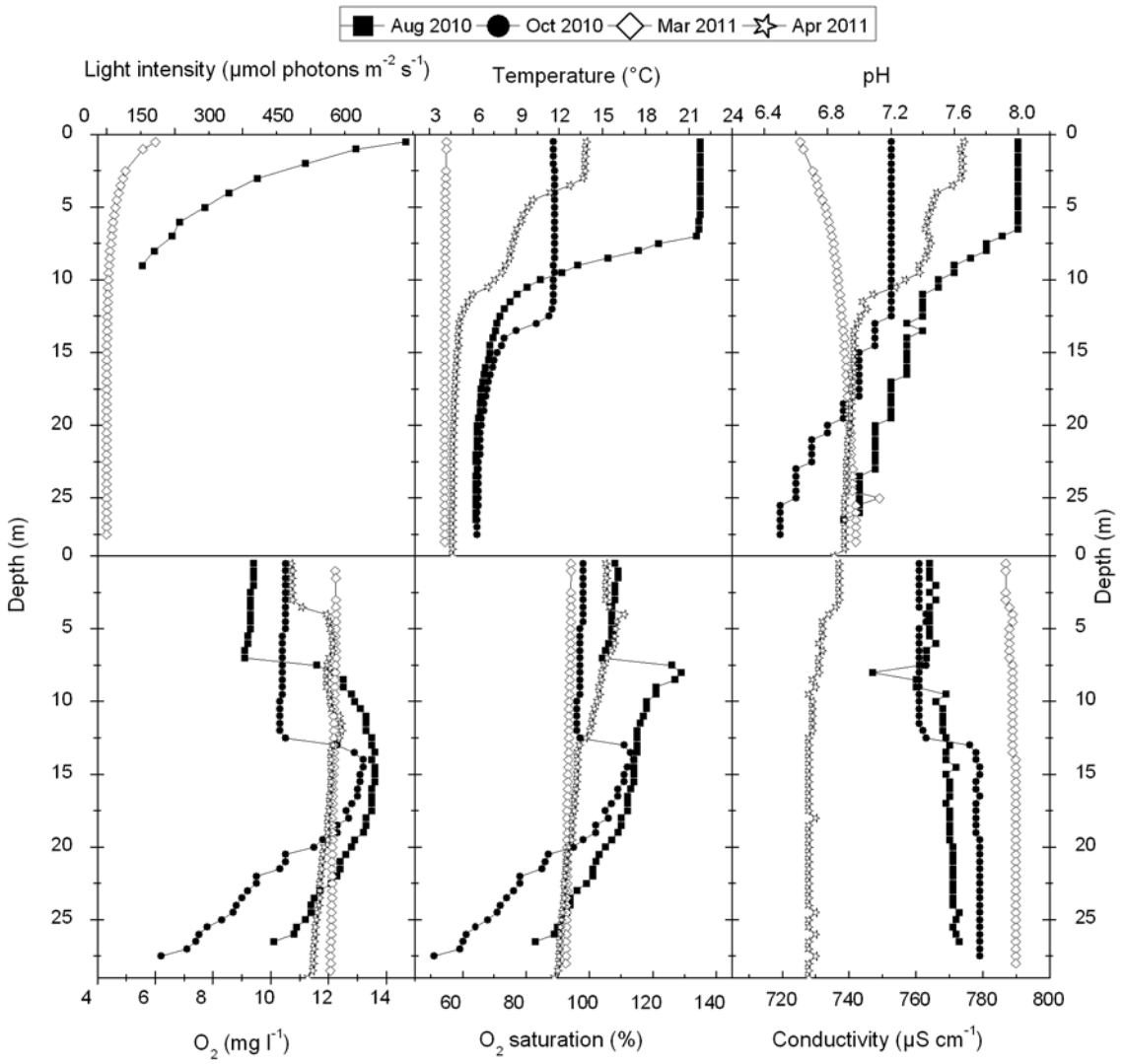

Figure 1. Limnological parameters of lake Ammelshain measured at 4 dates in 2010 and 2011. Light intensity, temperature, pH, oxygen content and oxygen saturation and conductivity were determined until the ground, except for the light intensity.

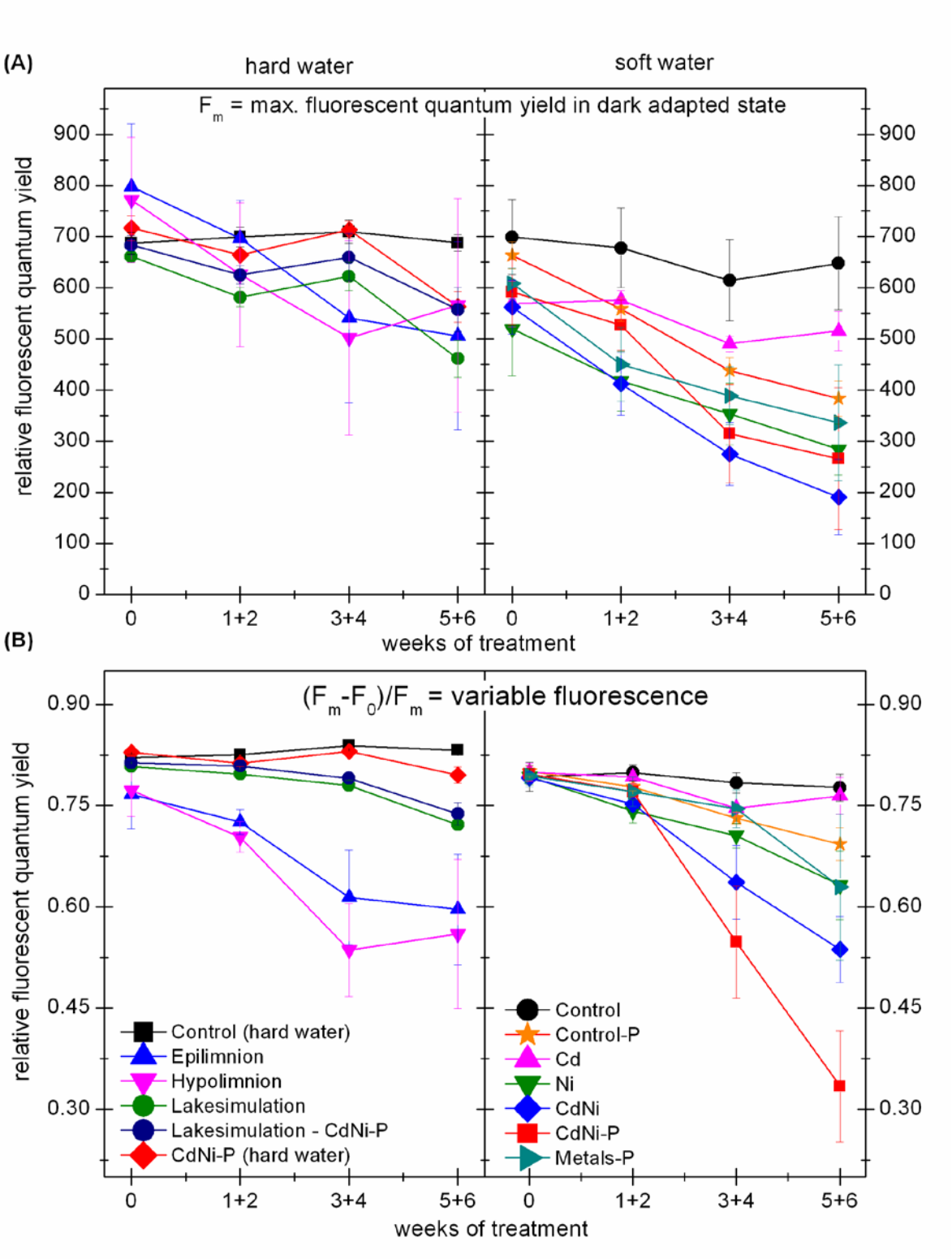

Figure 2. Changes in photosynthetic parameters during 6 weeks of treatment. Values are means from 6 (Control), 3 (Epi- and Hypolimnion, CdNi-P) or 2 (Control (hard water), Control-P, Cd, Ni, CdNi, CdNi-P (hard water), Metals-P, Lakesimulation, Lakesimulation – CdNi-P) experiments, error bars represent standard error of the mean. **(A)** F_m = Maximal

fluorescence quantum yield of dark adapted samples. **(B)** F_v/F_m = **(**F_m-F_0)/F_m) = Maximal photochemical quantum yield of the photosystem II reaction centres of dark adapted samples. Left: hard water samples; right: soft water samples.

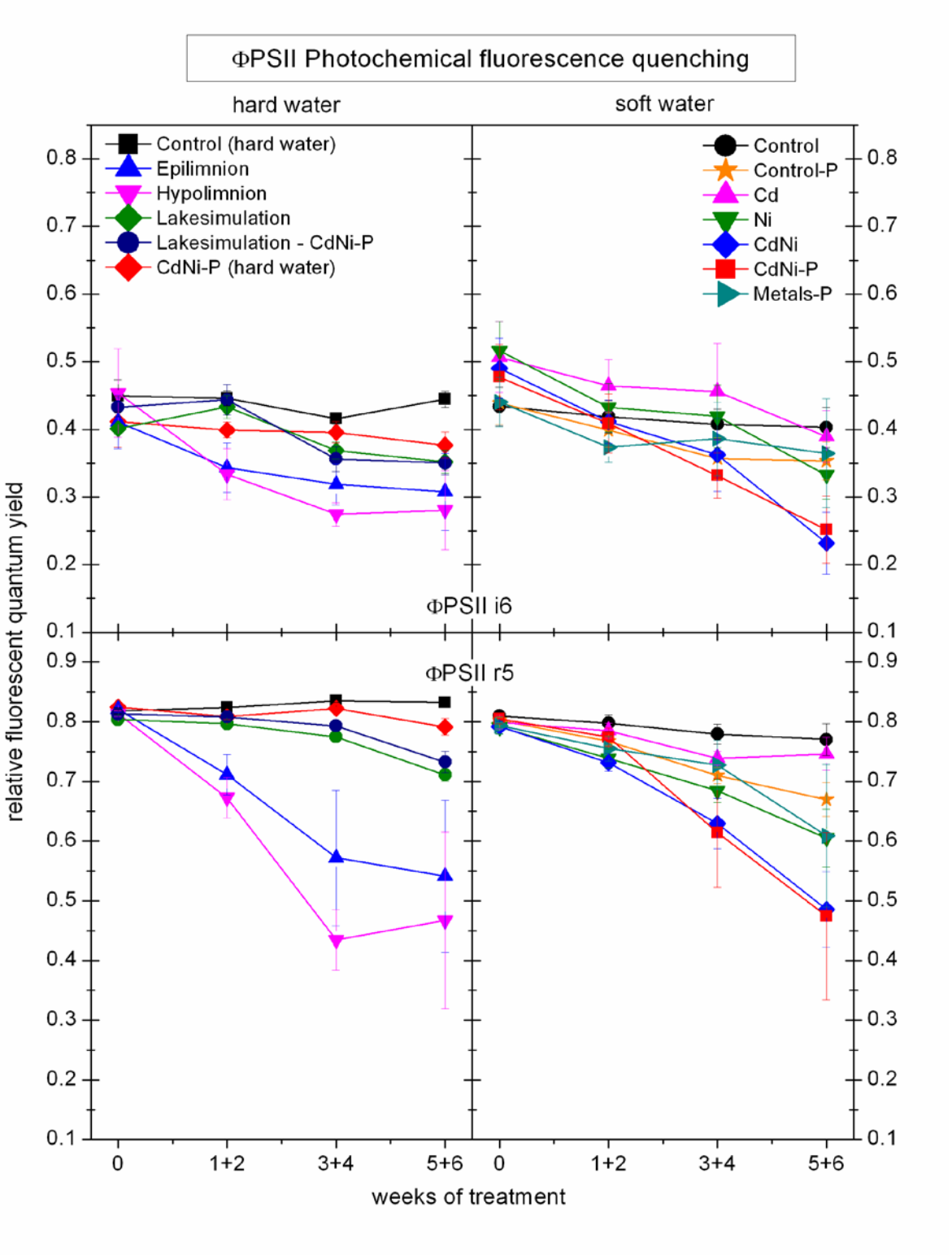

Figure 3. Effect of the different treatments on biophysics of photosynthesis. Values are means from 6 (Control), 3 (CdNi-P) or 2 (Epi- and Hypolimnion, Control (hard water) Control-P, Cd, Ni, CdNi, CdNi-P (hard water), Metals-P, Lakesimulation, Lakesimulation –

CdNi-P) experiments; error bars represent standard error of the mean. Left panel: hard water samples. Right panel: soft water samples Top row: Φ_{PSII} i6 = Capacity of electron flow at the end of the actinic light phase. Bottom row: Φ_{PSII} r5 = Capacity of electron flow at the end of the dark phase.

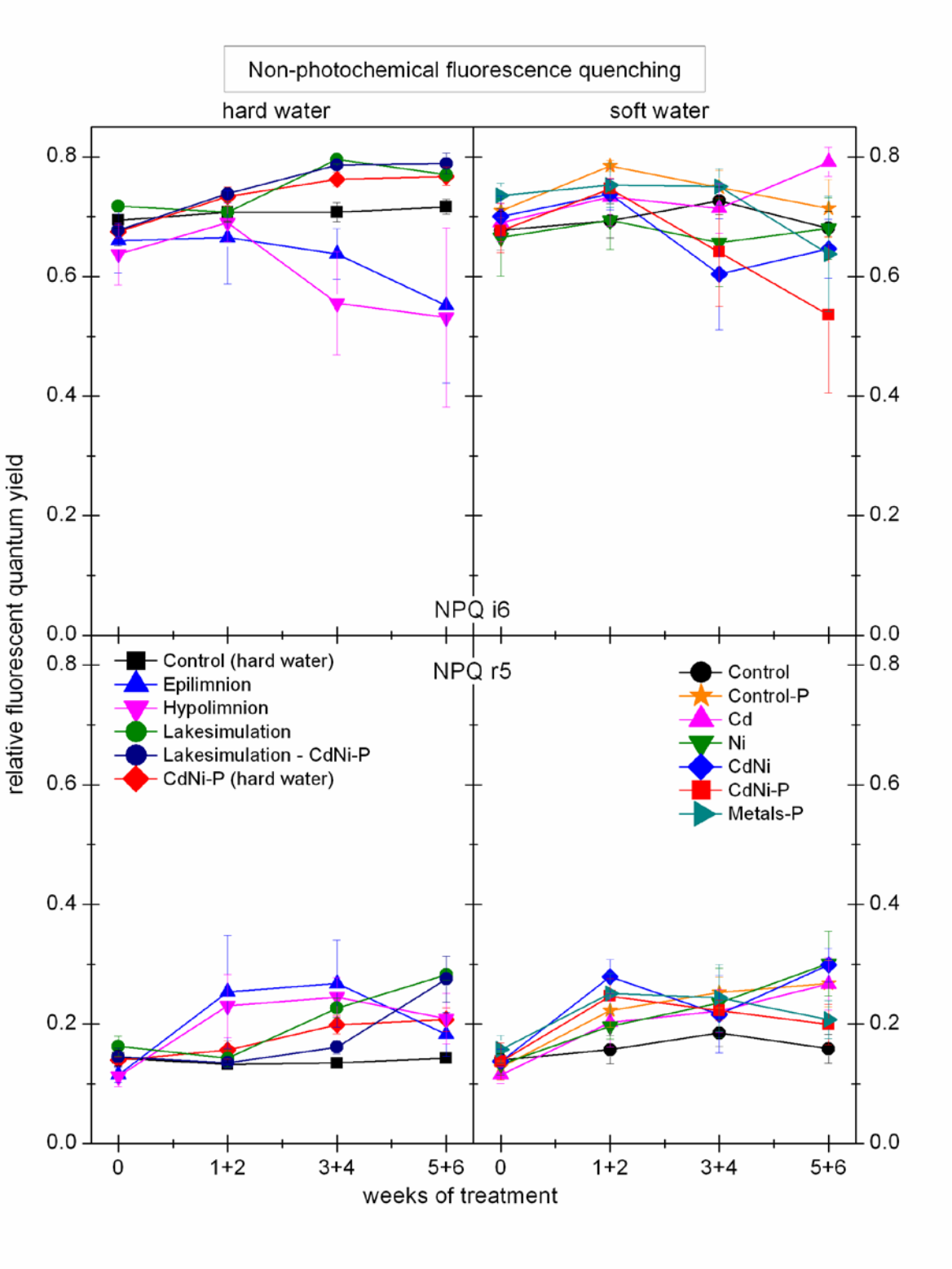

Figure 4. Effect of the different treatments on non-photochemical energy quenching measured as NPQ = $(F_m-F_{m'})/F_m$. Values are means from 6 (Control), 3 (CdNi-P) or 2 (Epi- and Hypolimnion, Control (hard water) Control-P, Cd, Ni, CdNi, CdNi-P (hard water), Metals-P, Lakesimulation, Lakesimulation – CdNi-P) experiments; error bars represent

standard error of the mean. Left panel: hard water samples Right panel: soft water samples Top row: NPQ i6 = non-photochemical energy quenching at the end of the actinic light phase. Bottom row: NPQ r5 = non-photochemical energy quenching at the end of the dark phase.

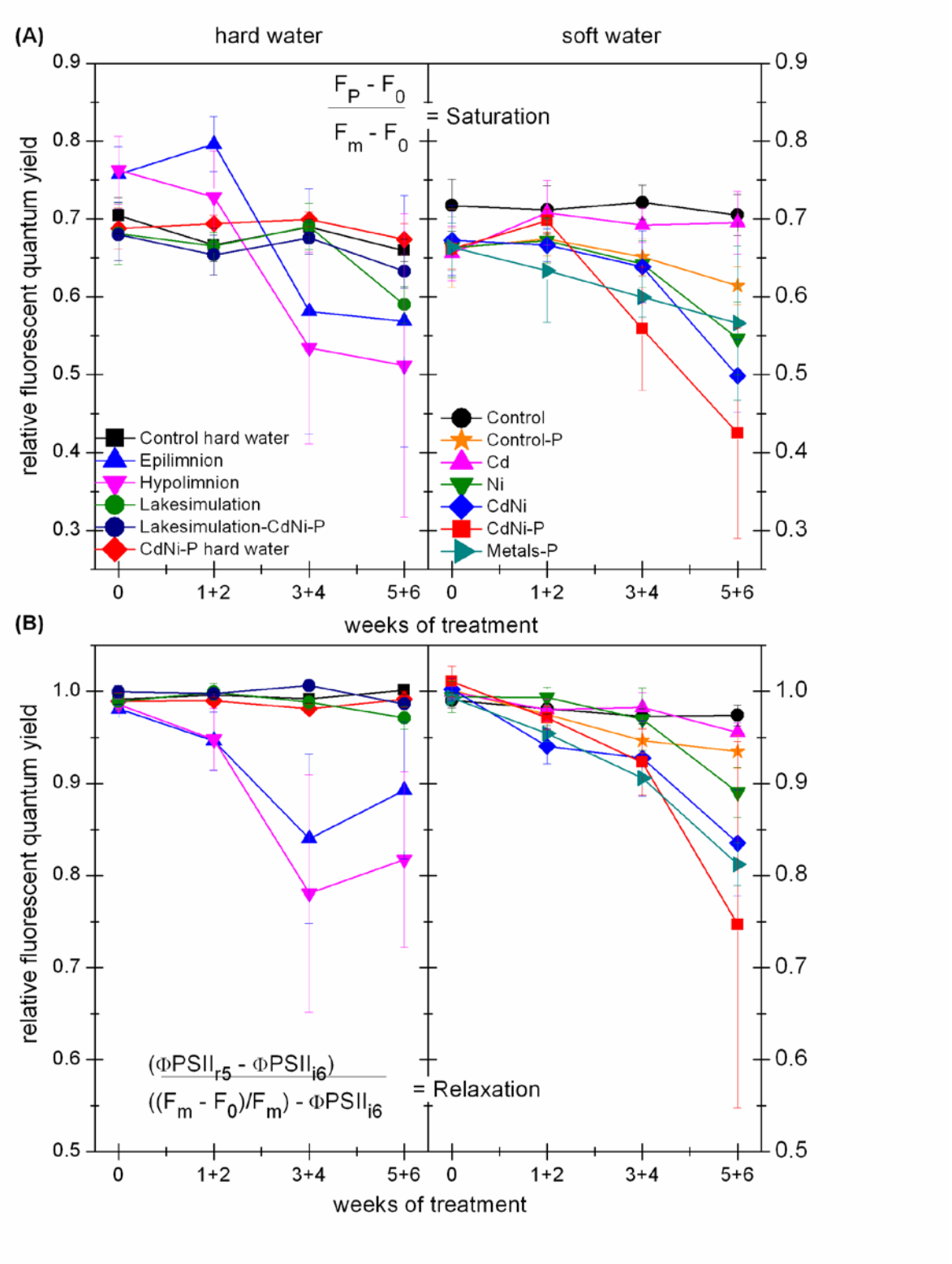

Figure 5. Effect of the different treatments on saturation and recovery abilities of PSII. (A) Saturation = $(F_p\text{-}F_0)/(F_m\text{-}F_0)$; displaying antennae to Chl ratio. Values are means from 6 (Control), 3 (Epi- and Hypolimnion, CdNi-P) or 2 (Control (hard water), Control-P, Cd, Ni, CdNi, CdNi-P (hard water), Metals-P. Lakesimulation, Lakesimulation – CdNi-P)

experiments; error bars represent standard error of the mean. (B) Relaxation = (Φ_{PSII} r5 - Φ_{PSII} i6)/((F_m-F_0)/F_m) - Φ_{PSII} i6); ability to recover the plastoquinon pool after actinic light phase. Values are means from 5 (Control), 3 (CdNi-P) or 2 (Epi- and Hypolimnion, Control (hard water), Control-P, Cd, Ni, CdNi, CdNi-P, Metals-P, Lakesimulation, Lakesimulation-CdNi-P) experiments; error bars represent standard error of the mean. Left: hard water samples; right: soft water samples.

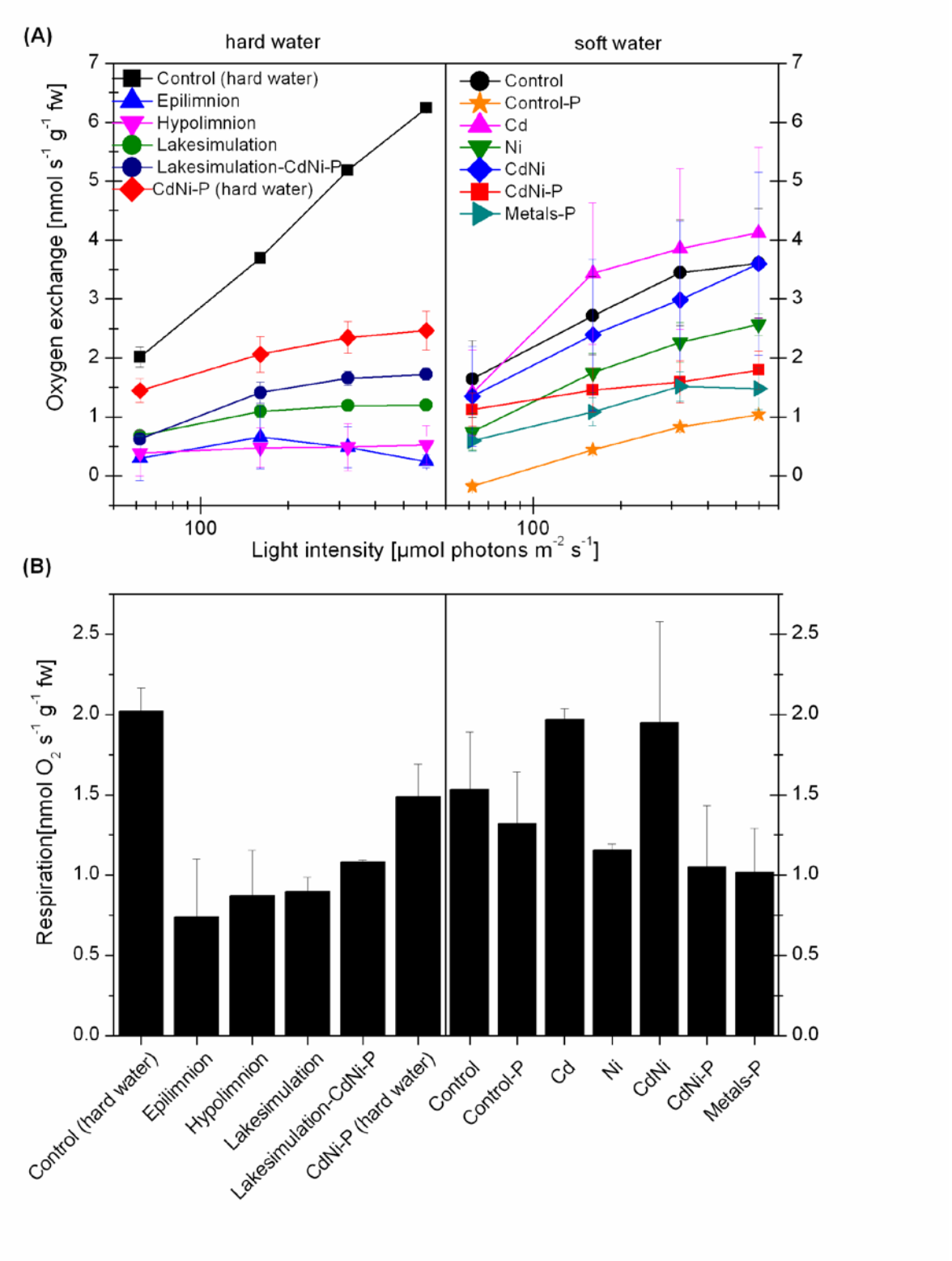

Figure 6. Effect on photosynthesis (A) and respiration (B) after 6 weeks of treatment duration. Left: hard water samples; right: soft water samples. Values are means from 6 (Control), 3 (Epi- and Hypolimnion, CdNi-P) or 2 (Control (hard water), Control-P, Cd, Ni,

CdNi, CdNi-P (hard water), Metals-P, Lakesimulation, Lakesimulation - CdNi-P) experiments; error bars represent standard error of the mean. FW: fresh weight.

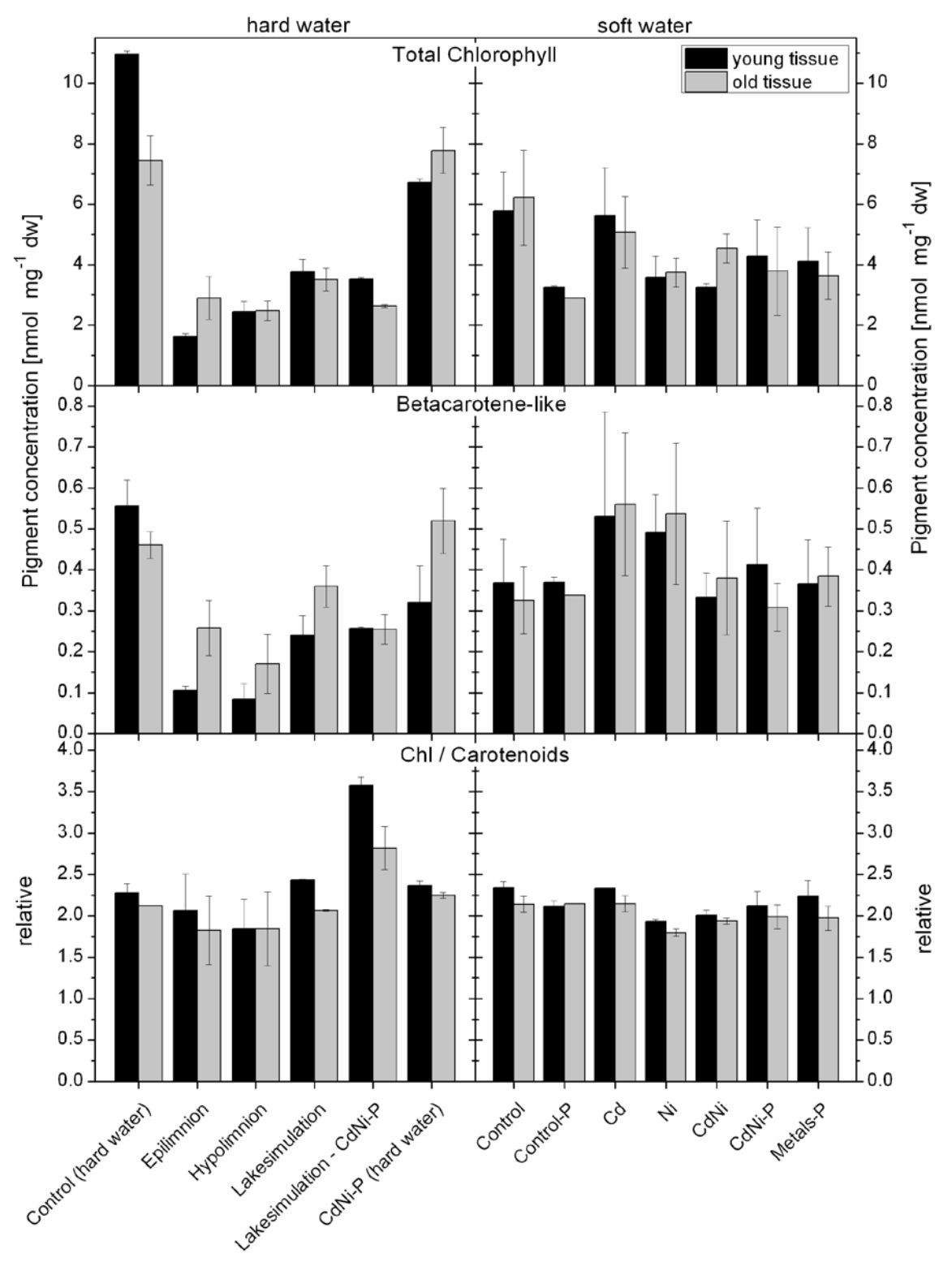

Figure 7. Pigment composition in young and old tissues after 6 weeks of treatment duration. Values are means from 6 (Control), 3 (Epi- and Hypolimnion, CdNi-P) or 2 (Control (hard water), Control-P, Cd, Ni, CdNi, CdNi-P (hard water), Metals-P, Lakesimulation,

Lakesimulation - CdNi-P) experiments; error bars represent standard error of the mean. DW: dry weight.

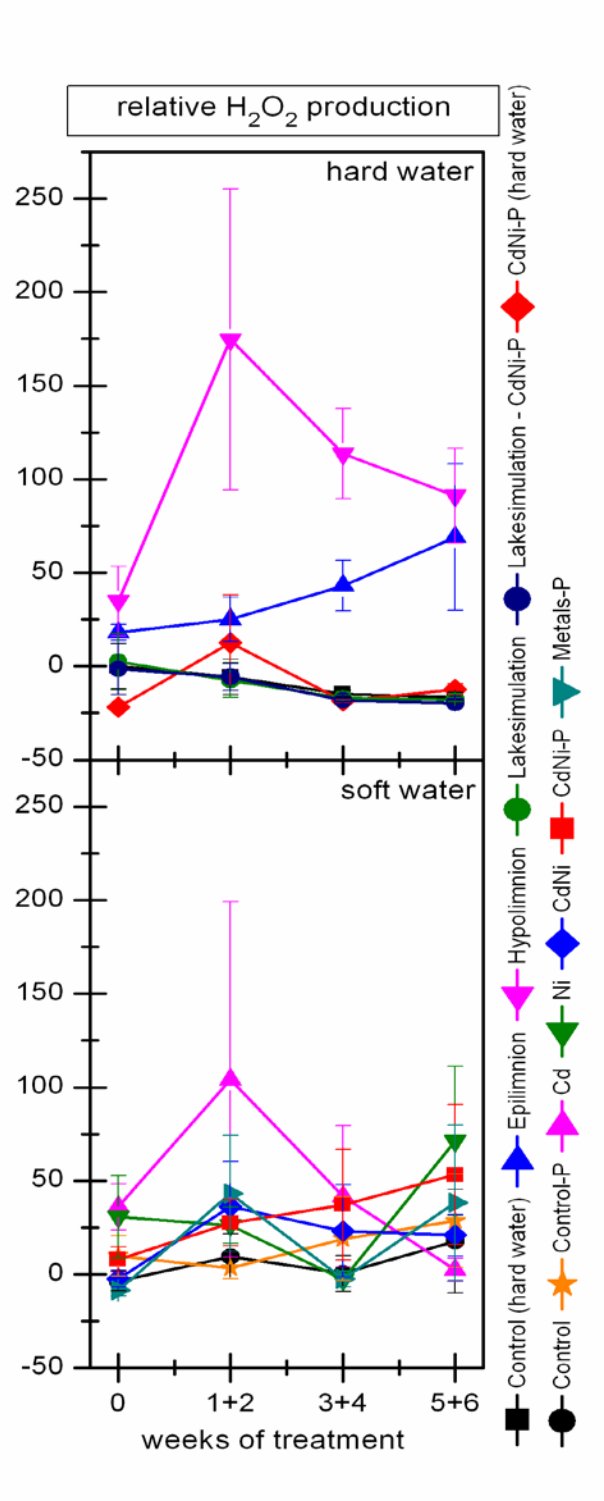

Figure 8. Effect of the treatments on relative H_2O_2 production. Values are means from 6 (Control), 3 (CdNi-P), or 2 (Epi- and Hypolimnion, Control (hard water), Control-P, Cd, Ni, CdNi, CdNi-P (hard water), Metals-P, Lakesimulation, Lakesimulation-CdNi-P) experiments, error bars represent standard error of the mean. Top: hard water samples; bottom: soft water samples.

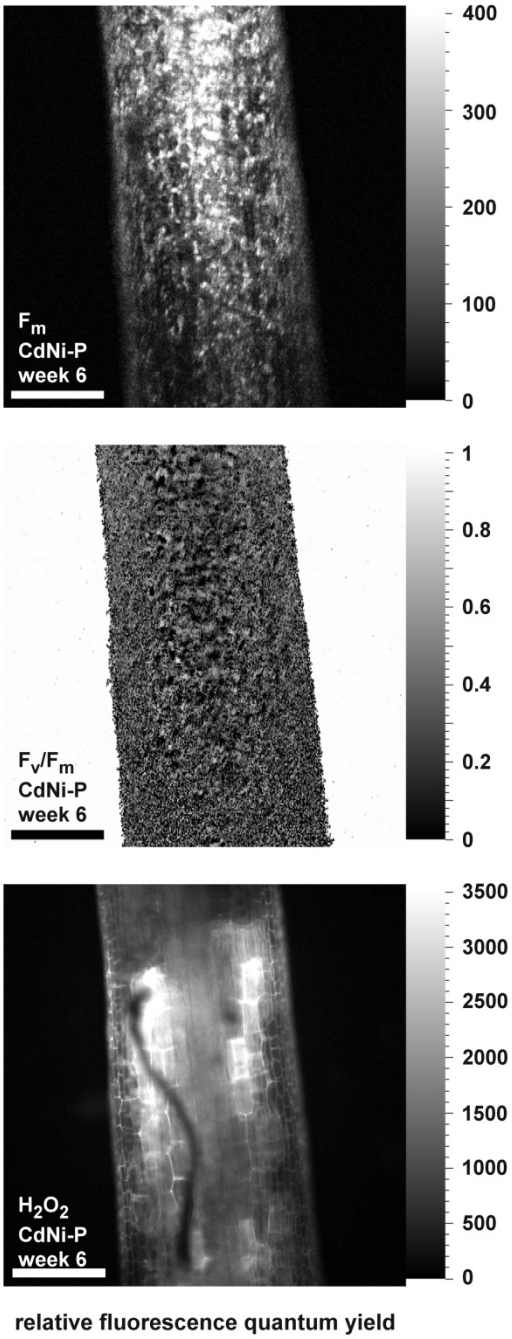

Figure 9. Fluorescence kinetic microscopy imaging after 6 weeks of CdNi-P treatment. F_m (top), $(F_m-F_0)/F_m$) (middle) and H_2O_2 production (bottom). Scale bar: 0.2 mm.

Tables

Table 1: Composition of the different test solutions.

Control (soft water)	SMNS (see text)
Cd	SMNS + 3nM Cd
Ni	SMNS + 300 nM Ni
CdNi	SMNS + 3 nM Cd + 300 nM Ni
CdNi-P	SMNS +3 nM Cd + 300 nM Ni, reduced P 75 nM
Metals-P	SMNS with 20 nM Cu, no Mo + 3 nM Cd + 300 nM Ni, reduced P 75 nM
Control (hard water)	SMNS + Ca + Cl + Mg + Na
CdNi-P (hard water)	SMNS +3 nM Cd + 300 nM Ni, reduced P 75 nM + Ca + Cl + Mg + Na
Lakewatersimulation	Simulation of the Lakewater samples (see table 2)
Lakewatersimulation – CdNi-P	Simulation of the Lakewater samples without Cd, Ni and P-stress (see table 2)
Epilimnion	Lake water samples from the epilimnion
Hypolimnion	Lake water samples from the hypolimnion

Table 2: Concentration of macro- and micronutrients in the different nutrient solutions.

Nutrient	Epilimnion	Hypolimnion	Lake Constance	Control nutrient solution	Lakewater simulation	Hard water simulation
	µM	µM	µM	µM	µM	µM
Na	1570 ± 212	1560 ± 233	226	60 [1]	1560 [1]	1560 [1]
Mg	8308 ± 70	835 ± 73	325	148 ± 4	825 ± 35	830 ± 12
K	120 ± 12.6	120 ± 11.7	35.8	120 [1]	120 [1]	120 [1]
Cl	980 ± 50	964 ± 38	192	88 [1]	900 [1]	900 [1]
Ca	2190 ± 71	2210 ± 62	1198	46 ± 1	2070	2030 ± 31
P	0.06 ± 0.01	0.059 ± 0.01	0.081	2.02 ± 0.48	0.04 ±0.0	0.73 ± 0.39
S	2740 ± 241	2780 ± 230	1091	560 ± 36	2940 [1]	2940 [1]
N (Nitrite+ Nitrate +Ammonia)	26.9 ± 2.2	26.9 ± 2.2	73.14	90 [1]	29.1 [1]	29.1 [1]
DOC [2]	270 ± 64	2708 ± 20	91.6	4000 [1]	26.8 [1]	26.8 [1]
	nM	nM	nM	nM	nM	nM
Cd	1.86 ± 0.39	1.98 ± 0.31	0.22 - 0.44	0.11 ±0.037	6.6 ± 0.3	0.1 ± 0.05
Cr	1.66 ± 0.2	1.70 ± 0.34	5.39 - 19.23	2.19 ± 0.1	1.3841 ± 0.2	1.4 ± 0.1
Cu	16.2 ± 2.6	16.8 ± 1.4	17.31	10.8 ± 1.5	15.90 ± 0.3	13 ± 1.1
Fe	520 ± 200	454 ± 231	91.3	76 ± 13 (200	171 ±12.1 (550 [1])	60 ± 1.7 (550 [1])
Mo	1.25 ± 0.05	1.09 ± 0.07	10.42	12.2 ± 0.86	0.68 ± 0.0	11 ± 0.32
Ni	270 ± 27	265 ± 26.1	12.1 - 17.04	17± 7.0	325 ± 11	28 ± 9.2
Zn	50.4 ± 19.5	62.6 ± 15.1	22.94	45 ±8.8	52 ± 5	57 ±2.7
pH	Varying;	Varying;	7.9	7.8	7.9 - 8.0	7.5 – 7.6

The data for lake Ammelshain (epi- and hypolimnion) originated from sampling at 4 points in 2010 and 2011). Values for lake Constance are shown as a comparison for an oligotrophic, medium hard lake with broad macrophyte flora (according to Zweckverband Bodensee-Wasserversorgung, annual mean values from 2010 & 2011). Control nutrient solution (SMNS) gives the composition of control treatment to which Cd, Ni and P stress were added (Cd, Ni, CdNi, CdNi-P). For the lake water simulation (Lake simulation), it was attempted to simulate the composition of epi- and hypolimnion with the previously measured data. The hard water simulation shows the composition with elevated Mg and Ca concentrations, which was used for hard water treatments (Control (hard water)) and to which Cd, Ni and P-stress were added (CdNi-P (hard water)).The values are averages from 2 to 18 measurements (± standard error of the mean).

1: nominal values

2: DOC includes all organic C compounds, i.e. not only those which are biologically available to the plant; only few of them are ligands for metals. In SMNS DOC originates from Hepes & EDDHA

Table 3: Instrumentation and operating conditions for the ICP-sfMS system (Element XR).

Parameters	
Cool argon flow	16 $L.min^{-1}$
Auxillary argon flow	0.8 $L.min^{-1}$
Shield argon flow	0.3 $L.min^{-1}$
Nebuliser argon flow	0.88 $L.min^{-1}$
Plasma power	1250 W
Low resolution (LR)	275$m.\Delta m^{-1}$
Medium resolution (MR)	4100$m.\Delta m^{-1}$
High resolution (HR)	10250 $m.\Delta m^{-1}$
Method	
Runs	6
Passes	1
Integration time	1 s (As & Rh* 1.85 s) 1.85 s)
Elements, nominal masses & resolution	
Mo	95 LR
Rh	103 LR
Cd	111 LR
W	184 LR
P	31 MR
S	32 MR
Cr	52 MR
Fe	56 MR
Ni	60 MR
Cu	63 MR
Zn	66 MR
Rh	103 MR
As	75 HR
Rh*	103 HR

Table 4: Accumulation of micro- and macronutrients in young and old tissues after 6 weeks of treatment.

	Cd	SE	Cu	S	Fe	SE	Mo	SE	Ni	SE	P	SE	S	SE	Zn	SE
Control young	1.6	0.7	37	11	48	12	1.45	0.65	28.3	6.1	2150	530	2940	528	690	146
Control old	1.2	0.4	27	6	58	17	1.48	0.61	27.5	8.3	1470	358	2520	446	723	181
Control-P young	0.3	0	19.	0.	16.1	0.1	0.46	0.09	18.6	0.6	1070	95	2090	74	340	34
Control-P old	0.4	0.1	14.	0.	45	13	0.67	0.13	15.8	1.8	547	21	1980	35	350	58
Cd young	23	2.0	41	18	185	90	6.43	2.06	20.6	1.1	2510	390	3370	310	358	64
Cd old	24	7	16	5	109	43	3.09	1.17	20.7	6.3	1690	600	2870	479	321	46
Ni young	0.7	0.2	23	9	49	10	2.18	0.67	1220	615	2060	244	3380	352	573	126
Ni old	0.7	0.3	23	5	74	13	3.06	0.93	1230	688	1380	326	2870	420	507	192
CdNi young	77	23	27	7	52	28	2.24	0.65	1120	561	2430	501	3560	349	598	118
CdNi old	69	24	17	4	58	7.7	2.94	0.81	1150	517	1500	300	3000	266	550	139
CdNi-P young	86.	20.	35	6	76	33	4.0	0.74	788	180	1670	213	3210	102	604	158
CdNi-P old	75	16	28	4	169	71.2	3.55	1.89	1070	352	1090	121	2930	163	537	67
Metals-P young	57	15	31	3	31.9	5.7	0.18	0.04	849	11	1180	176	2540	180	308	76
Metals-P old	62	25	35	2	48.4	3.7	0.41	0.25	942	320	1030	41	2390	10	371	135
Control (hard water) young	0.8	0.4	84	9	79	20	1.18	0.43	17	2.9	6120	340	7650	233	439	39
Control (hard water) old	0.7	0.3	32	2	64	2	2.31	0.44	17.8	0.5	2890	84	1050	440	853	8
CdNi-P (hard water) young	91	11	48	10	63.7	22	0.96	0.37	1010	490	2600	1040	7600	927	544	195
CdNi-P (hard water) old	151	64	45	3.	53	14	0.77	0.24	1430	507	1970	158	8550	2000	815	336
Epilimnion young	18	3.4	43.	5.	226	80	1.21	0.01	473	137	1460	470	5070	813	711	40
Epilimnion old	7.4	2.2	45	7	316	94	1.52	0.21	284	81	937	172	5360	648	662	114
Hypolimnion young	32	10	27	4.	187	83	1.0	0.0	280	72	1400	240	5020	856	800	90
Hypolimnion old	21	8	35	3.	430	140	1.79	0.0	214	67	935	208	5400	760	663	125
Lakesimulation young	65	1.6	32.	3.	45	4.6	0.41	0.01	751	3.6	1690	197	4930	255	347	12.1
Lakesimulation old	49	5.5	17.	0.	43	6.2	0.41	0.0	962	121	585	36	5710	390	306	37.6
Lakesimulation-CdNi-P	0.2	0.0	16	1.	65	15	0.45	0.06	40.6	0.3	956	84	3790	161	267	22.4
Lakesimulation-CdNi-P	0.3	0.0	15	0.	101	22	0.40	0.01	58.3	2.5	619	10	5580	243	328	3.7

The values are averages from 2 (Control (hard water), Control-P, Cd, Ni, CdNi, CdNi-P (hard water), Metals-P, Lakesimulation, Lakesimulation-CdNi-P), 3 (CdNi-P), 4 (Epilimnion, Hypolimnion) or 6 (Control) measurements. SE = standard error of the mean. Data in µg g-1 dw.

3. General Discussion

The thesis deals with the responses of the aquatic model plant *C. demersum* to heavy metals, from deficient via optimal to toxic concentrations, with special focus on copper. The whole range of plant responses from physiology to proteomics were studied using a large array of biophysical and biochemical methods. These experiments performed under environmentally relevant conditions, established the time and concentration thresholds of different previously proposed damage mechanisms, the sequence of occurrence of the events and the interdependence between different mechanisms, ultimately leading to either optimal growth or growth inhibition by deficiency or toxicity.

The maximum growth of the plant was observed in the narrow beneficial range between 10 nM and 20 nM Cu after six weeks of treatment in the high light (HL) as well as in the low light (LL) conditions which was the same concentration as used in the stock cultures. When the amount of Cu available to the plant was below or above this range, the stress responses of the plant caused by deficiency or toxicity were recorded with a large array of methods, during the six weeks experiment.

3.1 Copper deficiency

Copper deficiency was attained in the "0" nM Cu treatment from the first week which was associated with the reduction in growth and other physical stress symptoms, in both the HL (Thomas et al., 2013; Chapter 2.1 in thesis) and LL conditions (Chapter 2.2 in thesis), and were more pronounced in high irradiance. This was observed when the Cu limitation became significant below 5 nM in the growth pattern from the fourth week in HL while under LL conditions the decrease in growth was observed below 1 nM Cu concentration which further decreased towards the sixth week in both cases.

These results indicate that the plants try to cope up with the Cu deficiency by initially utilizing the internal reserve of Cu for their normal functions during the initial weeks. As the internal Cu decreased as observed from the metal accumulation, proteomic analysis (Chapter 2.2 in thesis) and metal distribution studies (Thomas et al., 2013; Chapter 2.1 in thesis), a deficiency of Cu occurred which was initially observed with a reduction in growth and ultimately leading to plant death. A clear evidence for the release of Cu out of the tissues and

into the nutrient solutions, when the Cu^{2+} concentration in the media was below the optimum range was observed from the metal analysis of the media prepared and that available to the plant (Thomas et al., 2013 Chapter 2.1 in thesis). This indicated the lack of effective copper transporters suitable to actively uptake Cu below the threshold concentration.

Former studies (Yu and Rengel, 1999) states that the light stress in addition to the Cu deficiency would increase the oxidative stress. This was confirmed by the comparison of the HL and LL studies where the HL experiment (Thomas et al., 2013; Chapter 2.1 in thesis) with greater light intensity showed higher Cu deficiency stress in the plants, than the LL experiment (Chapter 2.2 in thesis). The disruption of the carbon assimilation and/ or the damage to the photosynthate transport during Cu deficiency would have further increased the oxidative stress (Bowler et al., 1992) which would have been responsible for the negative growth rate in high light conditions (Thomas et al., 2013; Chapter 2.1 in thesis).

Even though the plant downregulates the Cu/Zn SOD and makes the Cu available for plastocyanin as in *Arabidopsis* (Abdel-Ghany and Pilon, 2008), in the case of *Ceratophyllum demersum*, there is no Cu available for the proper functioning of the plastocyanin, due to Cu deficiency. The Cu peak associated with plastocyanin (during Cu deficiency) decreased, indicating either a decrease in the plastocyanin or damage to the protein due to the removal of Cu from its active centre (Chapter 2.2 in thesis). Either of these situations, limited the electron flow between the photosystems under HL (Thomas et al., 2013; Chapter 2.1 in thesis) and LL conditions (Chapter 2.2 in thesis) while the photochemical yield of PSII was not inhibited. In addition to the malfunctioning of photosynthesis, a decrease in net photosynthetic oxygen release at deficient Cu concentrations was associated with decrease in starch production which further added to the growth reduction (Thomas et al., 2013; Chapter 2.1 in thesis).

The increase in peroxides at Cu deficiency could be the result of a dismutation of the superoxides into peroxides either by increased SOD activity or by induction of Zn SOD as there was an increased Zn accumulation at deficient Cu conditions from the metal distribution studies in HL (Thomas et al., 2013 Chapter 2.1 in thesis). The increase in Zn concentration was expected as earlier studies reported the compensatory absorption of micronutrients under deficiency stress (Del Rio et al., 1978; Dudev and Lim, 2013).

The distribution of the heavy metal(loid)s and the metal homeostasis in plants was studied using the technique of µXRF of frozen hydrated samples which involves no chemical fixation and potential alteration when compared to other techniques (Punshon et al., 2009). While Cu was mainly localized in the veins during Cu deficiency, with increase in time from

the second to the fourth week, its accumulation decreased in the “0” nM Cu treatment, which suggested a utilization of the internal reserve of Cu by the plant (Thomas et al., 2013; Chapter 2.1 in this thesis). The lack of efficient Cu transporters for active uptake of Cu below the threshold concentration, resulting in the release of Cu as observed from Aquaria Vs Barrel Cu study further added to the deficiency. While the Cu associated with the proteins decreased here, an increase in Zn accumulation was observed in the leaves from the metal distribution study and the increase in Zn peaks from the proteomic study. Here the Zn compartmentation was damaged. The additional accumulated Zn was sequestered to the epidermis (Thomas et al., 2013; Chapter 2.1 in thesis).

A sequence of events, interdependence and thresholds of various mechanisms of Cu deficiency stress in plants could be deduced from the time dependent studies (Thomas et al., 2013; Chapter 2.1 in thesis). A damage to plastocyanin from the second week due to lack of Cu resulted in inhibition of the light acclimated electron flow. The plants were unable to redistribute Cu in order to make best use of it. Still most of the Cu remained in the vein. The growth rate was reduced from 5 nM Cu after four weeks and the deficiency symptoms became prominent while the reserve Cu was used up by the plant. The reduction in the pigment content after the fifth week, further affected the light harvesting, photosynthesis and growth.

3.2 Copper toxicity

Ceratophyllum demersum in HL and LL conditions was able to tolerate Cu upto a threshold level of 10 nM Cu in the nutrient solution, when the internal plant Cu concentration was 20 ppm (suggested as optimal concentration from Thomas et al., 2013; Chapter 2.1 and 2.2 in thesis; Gupta, 1979; Stevenson, 1986). At higher Cu concentrations i.e. above the optimal concentration, there is overloading of the copper efflux system which caused the loss of control over internal copper. This was also evident from the proteomic analysis where the Cu peaks increased from the optimal range of Cu towards toxic Cu concentrations. This would indicate an increase in the Cu protein level or increased physiological copper loading of these proteins (less empty binding sites) which would result in an enhanced metabolic performance. Another possibility would be the incorporation of Cu at unphysiological sites of proteins which would lead to Cu toxicity (Chapter 2.2 in thesis).

Here the accumulation of Cu in the plants increased which was observed with a reduction in growth rate. The Cu toxicity thresholds strongly depend on the plant species. However, earlier studies (Gupta, 1979; Stevenson, 1986) and as also observed in the HL and LL studies, the toxicity effects become visible when the mature tissue concentration of Cu reaches above 20 ppm. The toxicity symptoms were visible with growth damage at Cu concentrations above 50 nM after six weeks of treatment in HL while under LL even though the optimum growth rate was never recorded, there was no toxicity symptoms observed at these concentrations. But once Cu concentration was above 200 nM, the plants were reported to suffer from toxic stress even in LL conditions from the first week of treatment until the plant died at 500 nM after four weeks. This was associated with a displacement of other essential ions including Zn, leading to Zn deficiency in addition to Cu stress (Thomas et al., 2013; Chapter 2.1 and 2.2 in thesis).

Plants, in their response to Cu stress, behave differently to the high and low irradiances of light, resembling sun and shade reactions which damage the photosynthesis process. During sun reaction, the light harvesting complex II (LHCII)- Chls are inaccessible to substitution and instead there is insertion of Cu into the Phe a of the PSII reaction centre (PSII RC) (Cedeno-Maldonado and Swader 1972; Küpper et al., 1996, 1998, 2002, 2009). In our study during HL conditions (Thomas *et al.*, 2013 Chapter 2.1 in thesis) the chlorophyll content in the young leaves decreased with increased Cu concentration. The reduction in light harvesting was caused by a decrease in pigments which would have been responsible for the decrease of the maximal Chl fluorescence yield in the young plant tissues. A decrease in the maximal quantum yield of the PSII RC in dark adapted state as explained before, could be a result of the insertion of Cu into the Phe a of the PSII RC. This was observed in the HL plants with greater F_m decrease than F_0 resulting in a decrease in F_v/F_m at high copper concentrations. These symptoms would resemble a “sun” reaction type of damage. A stronger decrease of Φ_{PSII} compared to F_v/F_m also indicates a secondary inhibition target which as suggested by Küpper et al., (2009) could be an inactivation of the electron transfer after PSII or due to the inhibition of the water splitting complex.

During shade reaction (Cedeno-Maldonado and Swader, 1972; Küpper et al. 1996, 1998, 2002, 2009), Cu substitutes Mg^{2+} in Chl molecules which are bound to the LHCII. In our LL study (Chapter 2.2 in thesis), damage to the LHC was indicated by a decrease of minimal and maximal quantum yield of in vivo Chl fluorescence (F_0 and F_m) towards toxic Cu concentrations resembling the shade reaction type of damage where the Chl a of the

LHCII was more accessible to Cu substitution forming Cu-Chl and thus leading to a decrease in the F_0 and F_m. A decrease in the fluorescent parameters, including F_v/F_m and Φ_{PSII} towards toxic copper concentrations along with a decrease of Chl a, further indicated the existence of non-functional photosynthetic units with >0 fluorescence emission, in contrast to earlier reports of "shade reaction" (e.g. Küpper et al., 1998, 2002).

The native form of LHC II is a trimer formed with basic monomer units in the presence of Mg. We could clearly separate the Mg peak corresponding to the trimer and monomer peak using size exclusion chromatopgraphy. Different heavy metal (Cu/Cd) toxicity in *Secale cereal* as measured with the help of Chl a fluorescence emission reported different effects on LHCII. When Cd enhanced the trimerization, Cu increased the complex aggregation (Janik et al., 2010). Cd affects the trimer protein by post-translational or gene expression modification (Janik et al., 2010) while Cu doesn't influence gene expression at all (Atienza et al., 2004). Conformational changes in the native form of LHCII (pigment-protein complex) as a result of Cu replacement have been reported earlier (Küpper et al., 1996, 2002; Janik et al., 2010). Unlike Mg-Chl, Cu-Chl does not have axial ligands (Boucher and Katz, 1967) for the Chl binding to the protein (Rebeiz and Belanger, 1984). Without Chl binding to the protein the correct LHCII folding cannot take place (Paulsen et al., 1993). This will ultimately lead not only to dissociation of the trimeric LHCII but finally result in denatured monomers. This was observed in the metalloproteomic analysis where during Cu toxicity, a decrease in the Mg trimer peak accompanied with an increase in the monomer peak, which overlaid the increased Cu peak, evidently states that Mg was replaced from the LHCII-trimer causing a conformational change in the pigment-protein complex forming monomers. This would affect the light harvesting and quenching mechanisms in the plant (Horton et al., 1996), resulting in damage to the photosynthesis. This is consistent with the decrease in NPQ and Chl a at the toxic Cu concentrations from the fifth week of treatment (Chapter 2.2 in thesis).

Damage to the photosynthetic apparatus as a result of Cu toxicity, transfers the excess energy to oxygen resulting in the formation of reactive oxygen species (ROS) (reviewed by Pinto et al., 2003). Unlike most earlier studies, using highly toxic Cu much above the environmentally relevant conditions to show fast effects (Tsay et al., 1995; Baryla et al., 2000), environmentally relevant but still toxic Cu concentrations resulted in a decrease of peroxides when compared to the deficient Cu concentrations in our study (Thomas et al., 2013; Chapter 2.1 in thesis). The activation of various anti-oxidative enzymes with Cu active centres including superoxide dismutase (SOD) and ascorbate peroxidise (APX) would have

been responsible for the quenching of the ROS (Srivastava et al., 2006). A similar decrease of peroxides was observed in the plants under Cd toxicity (Andresen et al., 2013b; Chapter 2.4 in thesis). This will be discussed later in context of the lake study.

PSII-mediated photochemistry in HL, was more vulnerable to Cu toxicity than the regulation of non-photochemical dissipation of excess energy (as the NPQ values remain unaffected by toxic copper concentrations for a longer period than the photochemical activities (F_v/F_m and Φ_{PSII})) (Thomas et al., 2013; Chapter 2.1 in thesis). An increase in photosynthesis observed at optimal Cu concentrations was associated with an increase in starch content. The damage to the photosynthesis at increased Cu conditions resulted in a continuous decrease of the starch content and was associated with a decrease in growth. (Thomas et al., 2013; Chapter 2.1 in thesis)

Plants developed certain mechanisms or strategies to combat metal stress like the synthesis of phytochelatins (PC) for heavy metal(loid) detoxification especially in non-hyperaccumulator plants. Our study suggest an induction of PCs from a lower nanomolar range of metal concentration as in the case with Cd at 20 nM Cd when compared to earlier experiments, which showed PC induction at 250 times higher Cd concentration (Mishra et al., 2009). One reason for this could be the use of Fe-EDTA component in the nutrient media which might unspecifically chelate the Cd ions (Hoagland and Arnon, 1950). Our study examined different PC species (including PC_2 to PC_6) in *Ceratophyllum demersum* rather than metal-PC-complexes (as had been done in earlier studies where the cell components got mixed during isolation of the PCs which made it less metal specific PC binding ability). The studies on Cd treated plant (Andresen et al., 2013a) revealed a switch like induction, with different Cd concentration thresholds for different PC species. An increase in Cd results in an overall increase of PC synthesis along with a change in the PC composition. This could indicate either that different PCs have different tasks (from homeostasis to detoxification) or for alleviating moderate toxicity PC_3 is formed and plants invests in synthesis of long chain PCs only when the critical need for survival arises (Andresen et al., 2013a; Chapter 2.3 in thesis). In the Cu treated plants, enhancement of PCs was observed only at Cu concentrations above 100 nM, i.e. PCs were induced only in plants with internal Cu concentration of 400 ppm and above to help in detoxification (Andresen et al., 2013a, Chapter 2.3 in thesis).

Copper requirement by the plant is different for individual physiological processes as observed in both the HL (Thomas et al., 2013; Chapter 2.1 in thesis) and LL (Chapter 2.2 in thesis) experiments. In *C. demersum*, photosynthesis was more sensitive to copper toxicity

than other mechanisms (F_v/F_m had highest value at 2 nM Cu and decreased with increasing Cu concentrations) or metabolism that limit growth (growth was maximum between 10 and 20 nM Cu). In *Nitzschia closterium*, Cu toxicity (0.47 µM) for 72 hrs inhibited the growth but did not affect photosynthesis (Lumsden and Florence, 1983). This made us to conclude that the relative Cu requirement and tolerance for growth and photosynthesis in some cases at least are different in higher plants vs. diatoms (Thomas et al., 2013; Chapter 2.1 in thesis).

In order to protect the more sensitive mesophyll from metal toxicity the Zn (Küpper et al., 1999) and Ni (Küpper et al., 2001) hyperaccumulators have developed a well known mechanism of metal sequestration into the epidermis. A similar mechanism was now observed in our Cu and Cd treatments on *Ceratophyllum demersum* at the optimal and low toxic or above optimal conditions while at toxic concentrations the metal sequestration was damaged (Thomas et al., 2013, Andresen et al., 2013a). At optimal Cu conditions, Cu was mainly localized in the veins while Zn was homogenously distributed throughout the leaves. µXRF studies suggested a two phase response to Cu toxicity by the plant (Thomas et al., 2013; Chapter 2.1 in thesis), where initially the excess Cu (200 nM Cu) was sequestered from the veins to the mesophyll and epidermis as a defense mechanism during the second week and after the fourth week the export from the veins broke down. This was associated with an inhibition to the Zn uptake, affecting the Zn nutrition and further accelerates leaf damage in addition to the Cu toxicity which ultimately led to the death of the plant. From the results obtained by Elisa Andresen in the Cd treated plants (Andresen et al, 2013a), increased Cd concentration led to enhanced sequestration of Cd into the epidermis and vein, with the highest amount of Cd found in the vein at 200 nM Cd. Here Zn was redistributed and localized mainly in the vein.

From the time dependent studies, we could deduce a sequence of events, interdependence and thresholds of various mechanisms of Cu toxicity stress in plants In HL conditions, at toxic Cu concentrations, PSII RC damage was significant from the second week which was associated with a decrease in chlorophyll and other pigments. A sequestration of Cu from vein to the mesophyll affected photosynthesis by inhibiting PSII RC and hampering the light harvesting which led to a gradual decrease in growth. A further decrease in chlorophyll pigments was observed in the fourth week accompanied by inhibition of electron transport after PSII in addition to the PSII RC inhibition. A damage to the transport mechanism responsible for sequestration of Cu to epidermis resulted in accumulation of Cu in veins while Zn uptake was inhibited. A negative growth rate at 200 nM Cu was associated

with highest Cu accumulations and lowest starch content due to lack of photosynthesis. In LL conditions during Cu toxicity, damage to LHCII was the initial event to be reported from the fluorescence measurement (Chapter 2.2 in thesis) after third week followed by decrease in Chl a after fifth week. Cu replacing Mg in the chlorophyll of the LHCII, led to the denaturation of the LHCII trimer into monomers. This was responsible for the decrease in NPQ and photosynthesis breakdown with increase in Cu-Chl. There was increased starch and Cu accumulation while Zn uptake had been inhibited.

3.3 Lake Study

Ceratophyllum demersum was cultivated in water samples taken from oligotrophic lake in Germany, Lake Ammelshain and systematic simulations of the lake water, to study whether heavy metal concentrations were responsible for the nearly complete lack of submerged macrophytes in the lake. The responses of the *Ceratophyllum* to Cd and Ni toxicity were also studied with soft and hard water conditions.

The Cd only treatment, which would have resulted in toxic stress effects on the plant, interestingly yielded positive results as observed by healthy control plants with no visible symptoms of stress. This response of the plant was earlier reported by Ornes and Sajan (1993) at 89 nM Cd even though the study used chelating agents which would have reduced the bioavailability of Cd. Another study where Cd showed a positive effect was reported in the Zn-limited cultures of the diatom *Thalassiosira weissfloggi* where a specific Cd-carbonic anhydrase (Cd-CA) was expressed (Lane and Morel, 2000). The scenario reported earlier was rather unlikely to take place in Lake Ammelshain in *Ceratophyllum* as the lake had even more Zn than the control medium, and the Zn accumulation in the plant was similar in Cd treated and control plants. Earlier studies have already reported the role of Cd in the metabolic functioning of the plant (Lane and Morel, 2000). Studies on *Noccaea caerulescens* (formerly known as *T. caerulescens*) (Liu et al., 2008) further shows the need of further study on the beneficial effects of Cd on *Ceratophyllum* whether it enhances the activity of CA or leads to expression of Cd-CA.

Earlier studies on Ni and Cd were performed at several higher concentrations than in our study, reaching several hundreds of micromolar concentrations and performed only seldom with aquatic macrophytes and multicellular algae (Li and Xiong, 2004). In one such

study, authors found that Ni treatment with concentrations above 9 mg l^{-1} (= 150 µM) were toxic to the duckweed, and when above 1 mg l^{-1} (=17 µM) towards higher concentrations, there was a gradual decrease in contents of Chl a, b and carotenoids with a reduction in the multiplication rate (Singh et al., 2011). In our study, a decrease in the Chl content and an increase in the carotenoid content were already observed by Ni treatment in the nanomolar range. The current study, in this way, shows that heavy metal concentrations which were previously regarded as rather harmless for multicellular organisms may have strong toxic and inhibitory effects.

The nanomolar Ni stress directly inhibited photochemistry. This was clear from the Ni only treatment which led to reduced photosynthetic activity. The low maximal fluorescence was associated with reduced Chl content. This could be responsible for the low NPQ in light phase as less excited energy was available from the reaction centre to be dissipated as heat. An increase in NPQ in the dark phase at the end of treatment indicated damage to the relaxation by the NPQ mechanism. The F_v/F_m reduction further indicates damage to the PSII core (Andresen et al., 2013b; Chapter 2.4 in thesis).

Various studies suggest that *Ceratophyllum* tolerates and accumulates Cd most likely by the upregulation of the Cd binding protein phytochelatins (Kumar and Prasad, 2004; Mishra et al., 2009, Andresen et al., 2013a) or by antioxidants which detoxify the ROS or inhibit / reduce their production (Mishra et al., 2008). The decrease in H_2O_2 detected in our study could be due to the increase in catalase activity, probably together with a decrease in the superoxide dismutase activity. Both of these activities but also their opposite scenarios have been reported from earlier studies on Cd (Gallego et al., 1996; Mediouni et al., 2008; Sandalio et al., 2001; Srivastave and Telor, 1991). The stress symptoms measured with the spatial distribution of signals from both H_2O_2 production and chlorophyll fluorescence however did not correspond to each other in our experiment (Andresen et al., 2013b; Chapter 2.4 in thesis).

The high metal bioaccumulation factor at extremely low concentrations has been a common feature of aquatic organisms (McGeer et al., 2003). The earlier studies which suggested *Ceratophyllum* for phytoremediation, due to its hyperaccumulation properties at low Cd concentration (Bunluesin et al., 2004), have been questioned in the lake simulation studies. Here the low Cd concentrations when combined with Ni reported an increased inhibition when compared to the Ni alone treatment at the same concentration (Andresen et al., 2013b Chapter 2.4 in thesis). This combinatory elevated damage indicates a synergistic effect of Cd and Ni. Adding to these results there was an increased accumulation of Cd in

plants cultivated in the CdNi-P nutrient solution than in the CdNi and Cd only treatment, even though earlier studies on cucumber reported that the accumulation and toxicity of Cd, Cu and Pb was less when a trio combination of heavy metals were given instead of single metal treatment (An et al., 2004). Further, a higher degree of photosynthesis damage by the two metals in combination with phosphate limitation was reported in our study than for the two metals alone in the real lake water, or the lake water simulations containing more salts or a combination of metals and salts.

Additional factors influencing the metal bioavailability have been suggested in our study. While metal toxicity decreases with increase in pH in aqueous solutions an opposite effect was reported in soils (Plette et al., 1999). Even though single metal concentrations did not differ much in the depth levels, the plants were found to accumulate more Cd and less Ni in the hypolimnion (hypolimnion water in Lake Ammelshain had slightly lower pH than epilimnion water) water than the epilimnion water. The higher amounts of Ca and Mg ions as in the case with hard water was found to be an additional factor influencing the metal toxicity, where they compete with the available sites on the organism's surface and thereby protecting the aquatic organisms (Allen and Janssen 2006). The divalent metal ions (including Cd, Zn, Ni, Pb) can be taken up by the cell via Ca transporters (e.g. Ca^{2+}-ATPase, Markich and Jeffree, 1994). During heavy metal toxicity, high Ca concentrations by competing for uptake into the cell, prevent the entrance of the heavy metals as observed in the Cd accumulation studies in aquatic moss in hard water (applied as $CaCO_3$, Gagnon et al., 1998). While in green unicellular microalgae the protective mechanism from Ni toxicity by competition was solely by Mg (Deleebeeck et al., 2009a). On the other hand *Ceratophyllum* and other organisms could not be protected from Cu toxicity with water hardness as Cu enters the plant via specific transporters where no Ca and/ or Mg ions can play a role (Markich et al., 2006, and citations within).

Phosphate (an essential element involved in plant metabolism) limitation is a major problem in oligotrophic lakes. In our Control-P treatment the plants suffered from P-limitation. Our study showed that heavy metal toxicity was enhanced when in combination with P-limitation. A similar report where Cu was found to be more toxic in P-limitation has been reported in the alga *Selenastrum capricornutum* (Kamaya et al., 2004). The disastrous inhibition in the plants with CdNi-P treatment in soft water compared to slight inhibition in hard water as in the case with F_v/F_m parameter could further explain the protective role of Ca and Mg in the water. Our study clearly states that in soft or moderate hard water lakes, plants

could already suffer from slightly elevated heavy metal concentrations, especially when combined with P-limitation. This is ecologically relevant, especially for the oligotrophic lakes having low nutrient content (which mainly refers to low P) in many parts of the world. Some other factors which affect the bioavailability of heavy metals include the dissolved organic matter (DOM) which controls dissolved metals speciation (Florence, 1982) and the addition of humic acid in some studies which decreased the bioavailability of Cd and Zn due to complexation (Bunluesin et al., 2007), significantly reducing the toxicity of these metals to *C. demersum*.

3.4 Topics for future research

The thesis was able to provide new insights into the mechanism of plant response to Cu stress at environmentally relevant conditions.

Preliminary proteomic study showed changes in level of various Cu proteins in a differential way under Cu deficiency and Cu excess, however, only one of the Cu proteins in the membrane fractions could be identified in the present study. The identification of other Cu containing as well as Cu responsive proteins would provide further understanding to the mechanism and targets of Cu stress, adding to the biochemical and biophysical insights from the study. Additionally, the proteomic study with Cd would give comparative insights on the specific responses of Cd, a redox inert metal with Cu, a redox active metal.

These specific proteins would be the molecular targets for future study. The unknown Cu proteins could be purified, characterized and cloned. This will help us to genetically modify these proteins which would be able to resist the Cu deficiency or toxicity mechanisms in the plant.

We could then transfer this knowledge of the proteomics and mechanistic response towards Cu stress to various crop plants including Soybean and Barley which are very relevant for human nutrition.

4. References

Abdel-Ghany, S.E., Müller-Moulé, P., Niyogi, K.K., Pilon, M., Shikanai T., 2005. Two P-type ATPases are required for copper delivery in *Arabidopsis thaliana* chloroplasts. Plant Cell. 17, 1233-1251.

Abdel-Ghany, S.E., Pilon, M., 2008. MicroRNA-mediated systemic down- regulation of copper protein expression in response to low copper availability in *Arabidopsis*. J Biol Chem. 283, 15932–15945.

Adriano, D.C., 2001. Trace elements in the terrestrial environments: biogeochemistry, bioavailability and risk of metals. Springer-Verlag, New York-Heidelberg-Tokyo.

Aguilera, F., McDougall, C., Degnan, B.M., 2013. Origin, evolution and classification of type-3 copper proteins: lineage-specific gene expansions and losses across the Metazoa. BMC Evol. Bio. 13, 96-108.

Allen, H.E., and C.R. Janssen. 2006. Incorporating bioavailability into criteria for metals. In: Twardowska, I., Allen, H.E., Haggblom, M.M., Stefaniak, S. (Eds.), Viable Methods of Soil and Water Pollution Monitoring. Protection and Remediation, Springer, Dordrecht, pp. 93–105.

Alloway, B.J. and Tills, A.R. (1984). Copper deficiency in world crops. Outlook Agric. 13, 32-42.

An, Y.J., Kim, Y.M., Kwon, T.I., Jeong, S.W., 2004. Combined effect of copper, cadmium, and lead upon *Cucumis sativus* growth and bioaccumulation. Sci. Total Environ. 326, 85-93.

Ahmed, S.I., A. Sabo, A., Maleka, D.D., 2011. Trace metals' contamination of stream water and irrigated crop at Naraguta-Jos, Nigeria. ATBU J. E. T. 4, 49-56.

Andresen, E., Lohscheider, J., Setlikova, E., Adamska, I., Simek, M., Küpper, H., 2010. Acclimation of *Trichodesmium erythraeum* ISM101 to high and low irradiance analysed on the physiological, biophysical and biochemical level. New Phytol. 185, 173-188.

Andresen, E., Küpper, H., 2013. Cadmium Toxicity in Plants, in: Sigel, A., Sigel, H., Sigel, R.K.O. (Eds.), Cadmium: From Toxicity to Essentiality, Metal Ions in Life Sciences, Volume 11, Springer Business Media, Dordrecht, pp. 395-413.

Andresen, E., Mattusch, J., Wellenreuther, G., Thomas, G., Abad, U.A., Küpper, H., 2013a. Different strategies of cadmium detoxification in the submerged macrophyte *Ceratophyllum demersum* L. Metallomics 5(10), 1377-1386.

Andresen E., Opitz, J., Thomas, G., Stärk, H.J., Dienemann, H., Jenemann, K., Dickinson, B.C., Küpper, H., 2013b. Effects of Cd & Ni toxicity to *Ceratophyllum demersum* under environmentally relevant conditions in soft & hard water including a German lake. Aqua Tox. 142-143, 387-402.

Andrés-Colás N., Perea-García A, Mayo de Andrés S, Garcia-Molina A, E, Rodríguez-Navarro S., Pérez-Amador MA., Puig S., and Peñarrubia L., 2013. Comparison of global responses to mild deficiency and excess copper levels in Arabidopsis seedlings. Metallomics. DOI : 10.1039/C3MT00025G

Aravind, P., Prasad, M.N.V., 2004. Carbonic anhydrase impairment in cadmium-treated *Ceratophyllum demersum* L. (free floating freshwater macrophyte): toxicity reversal by zinc. J. Anal. At. Spectrom. 19, 52-57.

Atienza, S.G., Faccioli, P., Perrotta, G., Dalfino, G., Zschiesche, W., Humbeck, K., Stanca, M., Cattivelli, L., 2004. Large scale analysis of transcripts abundance in barley subjected to several single and combined abiotic stress conditions. Plant Sci.167, 1359-1365.

Ayala, M.B., Sandmann. G., 1988. Activities of Cu-containing proteins in Cu-depleted pea leaves. Physiologia Plantarum, 72: 801-806.

Baccini, P., 1985. Metal transport and metal/biota interactions in lakes. Environ. Technol. Lett. 6, 327-334.

Bachor, A., Nawrocki, A., Evert, J., 2012. Schadstoffuntersuchungen in Oberflächengewässern Mecklenburg-Vorpommerns im Zeitraum 2007-2011, Schadstoffe zur Bewertung des chemischen Zustands gemäß Oberflächengewässerverordnung (OGewV), Herausgeber: Landesamt für Umwelt, Naturschutz und Geologie Mecklenburg-Vorpommern

Baker, N.R., 2008. Chlorophyll fluorescence: a probe of photosynthesis in vivo. Annu. Rev. Plant Biol. 59, 89-113.

Baker, A.J.M., McGrath, S.P., Reeves, R.D., Smith, J.A.C., 2000. Metal hyperaccumulator plants: A review of the ecology and physiology of a biological resource for phytoremidiation of metal-polluted soils, In: Terry, N., Bañuelos, G.S. (Eds.),

Phytoremediation of Contaminated Soil and Water. CRC Press, Boca Raton, pp. 85–107.

Baszynski, T., Wajda, L., Krol, M., Wolinska, D., Krupa, Z., Tukendorf, A., 1980. Photosynthetic activities of cadmium treated tomato plants *Lycopersicon esculentum* cultivar Moneymaker. Physiol. Plant 48, 365-370

Baryla, A., Laborde, C., Montillet, J.L., Triantaphylidès, C., Chagvardieff, P., 2000. Evaluation of lipid peroxidation as a toxicity bioassay for plants exposed to copper. Environ. Pollut. 109, 131-135

Baszynski, T., Ruszkowska, M., Krol, M., Tukendorf, A., Wolinska, D., 1978. The effect of copper deficiency on the photosynthetic apparatus of higher plants. Zeitschrift für Pflanzenphysiologie 89, 207-216.

Benavides, M.P., Gallego, S.M., Tomaro, M.L., 2005. Cadmium toxicity in plants. Braz. J. Plant Physiol. 17, 21-34.

Bernhard, S., 2010. Bewertung stehender Gewässer nach EU-WRRL unter besonderer Berücksichtigung von pH-Wert -Änderungen am Beispiel des Autobahnsees Ammelshain und der Kiesgrube Naunhof. Masterarbeit, Universität Rostock, Rostock, Germany.

Best E.P.H., 1977. Seasonal changes in mineral and organic components of *Ceratophyllum demersum* and *Elodea canadensis*. Aquat. Bot. 3,337-348.

Best E.P.H., Visser H.W.C., 1987. Seasonal growth of the submerged macrophyte *Ceratophyllum demersum* L. in mesotrophic Lake Vechten in relation to insolation, temperature and reserve carbohydrates. Hydrobiologia. 148(3): 231-243

Blüm, V., Stretzke, E., Kreuzberg, K., 1994. CEBAS-aquarack project - the mini-module as tool in artificial ecosystem research. Acta Astronautica 33, 167-177.

Boucher, L.J., Katz, J.J., 1967. Aggregation of metalloporphyrins. J. Am. Chem. Soc. 89, 4703-4708.

Bowler, C., Van Montagu, M., Inze, D., 1992. Superoxide dismutase and stress tolerance. *Annual Rev. of Plant Physiol. and Plant Mol. Biol.* 43, 83-116.

Boyd, R.S., Martens, S.N., 1994. Nickel hyperaccumulated by *Thlaspi montanum* var. *montanum* is acutely toxic to an insect herbivore. Oikos 70, 21-25.

Bunluesin, S., Kruatrachue, M., Pokethitiyook, P., Lanza, G.R., Upatham, E.S., Soonthornsarathool, V., 2004. Plant screening and comparison of *Ceratophyllum*

demersum and *Hydrilla verticillata* for cadmium accumulation. Bull. Environ. Contam. Toxicol. 73, 591-598.

Bunluesin, S., Pokethitiyook, P., Lanza, G.R., Tyson, J.F., Kruatrachue, M., Xing, B., Upatham, S., 2007. Influences of cadmium and zinc interaction and humic acid on metal accumulation in *Ceratophyllum demersum*. Water, Air, Soil Pollut. 180, 225-235.

Bussler, W., 1981. Physiological functions and utilization of copper. In: Loneragan, J.F., Robson, A.D., Graham, R.D. (Eds.), Copper in soils and plants. Academic Press, pp. 213−234,

Cakmak, I., Marschner, H., 1993. Effect of zinc nutritional status on activities of superoxide radical and hydrogen peroxide scavenging enzymes in bean. Plant and Soil. 156, 127-130.

Cedeno-Maldonado, A., Swader, J.A., Heath, R.L**.,** 1972. The cupric ion as an inhibitor of photosynthetic electron transport in isolated chloroplasts. Plant Physiol. 50, 698-701.

Chang, C.M.Y., Pralle, A., Isacoff, E.Y., Chang, C.J., 2004. A selective, cell-permeable optical probe for hydrogen peroxide in living cells. J Am Chem Soc. 126, 15392-15393.

Chen, C., Huang, D., Liu, J., 2009. Functions and toxicity of nickel in plants: Recent advances and future prospects. Clean: Soil, Air, Water 37, 304-313.

Clemens, S., 2001. Molecular mechanisms of plant metal tolerance and homeostasis Planta 212, 475-486.

Clemens, S., 2006. Toxic metal accumulation, response to exposure and mechanisms of tolerance in plants. Biochimie 88, 1707-1719.

Cobbett, C., Goldsbrough, P., 2002. Phytochelatins and metallothioneins: roles in heavy metal detoxification and homeostasis. Annu. Rev. Plant Biol. 52, 159-182.

Deleebeeck, N.M.E., De Schamphelaere, K.A.C., Janssen, C.R., 2009a. Effects of Mg(2+) and H(+) on the toxicity of Ni(2+) to the unicellular green alga *Pseudokirchneriella subcapitata*: Model development and validation with surface waters. Sci. Total Environ. 407, 1901-1914.

Deleebeeck, N.M.E., De Laender, F., Chepurnov, V.A., Vyverman, W., Janssen, C.R., De Schamphelaere, K.A.C., 2009b. A single bioavailability model can accurately

predict Ni toxicity to green microalgae in soft and hard surface waters. Water Res. 43, 1935-1947.

Delhaize E, Lonergan JF, Webb J (1985). Development of three copper metalloenzymes in clover leaves. Plant Physiol. 78, 4-7.

Delhaize E, Dilworth MJ, Webb J (1986). The effects of copper nutrition and developmental state on the biosynthesis of diamine oxidase in clover leaves. Plant Physiol. 82:1126-1131

Del Rio, L.A., Sevilla, F., Gomez, M., Yanez, J., Lopez-George, J., 1978. Superoxide dismutase: an enzyme system for the study of micronutrient interaction in plants. Planta. 140, 221-225.

De Nolf, W., Janssens, K., 2010. Micro X-ray diffraction and fluorescence tomography for the study of multilayered automotive paints. Surface Interface Anal. 42, 411-418.

Dickinson, B.C., Huynh, C., Chang, C.J., 2010. A palette of fluorescent probes with varying emission colors for imaging hydrogen peroxide signaling in living cells. J. Am. Chem. Soc. 132**,** 5906-5915.

Dong, J., Wu, F., Zhang, G., 2006. Influence of cadmium on antioxidant capacity and four microelement concentrations in tomato seedlings (*Lycopersicon esculentum*). Chemosphere. 64, 1659-1666.

Droppa, M., Masojidek, J., Rózsa, Z., Wolak, A., Horváth, L.I., Farkas, T., Horváth, G., 1987. Characteristics of Cu deficiency-induced inhibition of photosynthetic electron transport in spinach chloroplasts. Biochim. Biophys. Acta. 891, 75-84.

Dudev, T., Lim, C., 2013. Competition among Metal Ions for Protein Binding Sites: Determinants of Metal Ion Selectivity in Proteins. Chem. Rev, DOI: 10.1021/CR4004665.

Ellis, R.J., 1979. The most abundant protein in the world. Trends Biochem. Sci., 4, 241-244.

European Commission, 2012. Proposal for a directive of the European parliament and of the council amending Directive 2000/60/EC and 2008/105/EC as regards priority substances in the field of water policy. http://ec.europa.eu/environment/water/water-dangersub/pdf/com_2011_876.pdf

Fagioni, M., D'Amici, G.M., Timperio, A.M., Zolla, L., 2009. Proteomic analysis of multiprotein complexes in the thylakoid membrane upon cadmium treatment. J. Proteome Res. 8, 310-326.

Fergusson, JE., Hayes, R.W., Yong, T.S., Thiew, S.H., 1980. Heavy metal pollution by traffic in Christchurch, New Zealand: Lead and cadmium content of dust, soil and plant samples. New Zea. J. Sci. 23, 293-310.

Festa, R.A., Thiele, D.J., 2011. Copper: An essential metal in biology. Curr Biol. 21, R877–R883.

Florence, T.M., 1982. The speciation of trace elements in waters. Talanta. 29, 345-364.

Fordham-Skelton, AP., Wilson, J.R., Groom, Q., Robinson, N.J., 1997. Accumulation of metallothionein transcripts in response to iron, copper and zinc: Metallothionein and metal-chelate reductase. Acta Physiol. Plant. 19, 451-457.

Foyer, C.H., Descourivieres, P., Kunert, K.J., 1994. Protection against oxygen radicals: an important defence mechanism studied in transgenic plants. Plant, Cell and Environ. 17, 507-523

Frank, R., Braun, H.E., Ishida, K., Suda, P., 1976. Persistent organic and inorganic pesticide residues in orchard soils and vineyards of southern Ontario. Can. J. Soil. Sci. 56, 463-484.

Frausto da Silva, J.J.R., Williams, R.J.P., 2001. The Biological Chemistry of the Elements: The Inorganic Chemistry of Life. Oxford University Press, Oxford.

Frey, B., Keller, C., Zierold, K., Schulin, R. 2000. Distribution of Zn in functionally different leaf epidermal cells of the hyperaccumulator *Thlaspi caerulescens*. Plant Cell Envi. 23, 675-687.

Fukuda, N., Hokura, A., Kitajima, N., Terada, Y., Saito, H., Abe, T., Nakai, I., 2008. Micro X-ray fluorescence imaging and micro X-ray absorption spectroscopy of cadmium hyper-accumulating plant, *Arabidopsis halleri* ssp. *gemmifera*, using high-energy synchrotron radiation. J. Anal. At. Spectrom. 23, 1068-1075.

Gagnon, C., Vaillancourt, G., Pazdernik, L., 1998. Influence of water hardness on accumulation and elimination of cadmium in two aquatic moss under laboratory conditions. Arch. Environ. Contam. Toxicol. 34, 12-20.

Gallego, S.M., Benavides, M.P., Tomaro, M.L., 1996. Effect of heavy metal ion excess on sunflower leaves: Evidence for involvement of oxidative stress. Plant Sci. 121, 151-159.

Garab, G., Cseh, Z., Kovacs, L., Rajagopal, S., Varkonyi, Z., Wentworth, M., Mustardy, L., Der, A., Ruban, A., Papp, E., Holzenburg, A., Horton, P., 2002. Light-induced

trimer to monomer transition in the main light-harvesting antenna complex of plants: thermo-optic mechanism. Biochemistry, 41: 15121-15129.

Genty, B., Briantais, J., Baker, N.R., 1989. The relationship between the quantum yield of photosynthetic electron-transport and quenching of chlorophyll fluorescence. Biochim. Biophys. Acta., 990, 87-92.

Gill, S.S., Tuteja, N., 2011. Cadmium stress tolerance in crop plants. Probing the role of sulfur. Plant Signal Behav. 6, 215–222.

Gimeno-Garcia, E., Andreu, V., Boluda, R., 1996. Heavy metals incidence in the application of inorganic fertilizers and pesticides to rice farming soils. Environ. Pollut. 92, 19-25.

Gupta, P., Chandra, P., 1996. Response of cadmium to *Ceratophyllum demersum* L., a rootless submerged plant. Waste Management 16, 335-337.

Gupta, U.C., 1979. Copper in agricultural crops, In: Nriagu, J.O. (Eds.), Copper in the environment. Part I: Ecological Cycling. John Wiley & Sons, New York, pp. 255-288.

Grill, E., Winnacker,E.-L., Zenk, M.H., 1985 Phytochelatins: The principal heavy-metal complexing peptides of higher plants. Science 203, 674-676.

Grill, E., Winnacker, E.-L., Zenk, M.H., 1987 Phytochelatins, a class of heavy-metal-binding peptides from plants, are functionally analogous to metallothioneins, PNAS, 84, 439-443.

Hall, J.L., 2002. Cellular mechanisms for heavy metal detoxification and tolerance. J. Exp. Bot. 53, 1-11.

Halliwell, B., Gutteridge, J.M.C., 1984. Oxygen toxicity, oxygen radicals, transition metals and disease. J Biol Chem. 219, 1–14.

Hasan, S.A., Fariduddin, Q., Ali, B., Hayat, S., Ahmad, A., 2009. Cadmium: Toxicity and tolerance in plants. J. Environ. Biol. 30, 165-174.

Henze, W. and Umland F., 1987. Speciation of Cadmium and Copper in Lettuce Leaves. Trace Element in Med. Biol. 4, 501-507.

Hoagland, D.R., Arnon, D.I., 1950. The water-culture method for growing plants without soil. Calif. Agric. Exp. Sation Circ. 347, 1-32.

Horton P., Ruban, A.V., Walters, R.G., 1996. Regulation of light harvesting in green plants. Annu. Rev. Plant Physiol. Plant Mol. Biol. 47, 655–684.

Horton, P., Ruban, A. V., 2005. Molecular design of the photosystem II light harvesting antenna: photosynthesis and photoprotection. J. Exp. Bot. 56, 365–-373.

Huguet, S., Bert, V., Laboudigue, A., Bartès, V., Isaure, M.P., Llorens, I., Schat, H., Sarret, G., 2012. Cd speciation and localization in the hyperaccumulator *Arabidopsis halleri*. Environ. Exp. Bot. 82, 54-65.

Huguet, S., Soussou, S., Cleyet-Marel, J.C. Trcera, N., Isaure, M.P., 2013. Rhizostabilization of a mine tailing highly contaminated: Previous study of a Cd localization and speciation in *Anthyllis vulneraria*. E3S Web of Conferences, 19008, 1-4.

Isaure, M.P., Fayard, B., Sarret, G., Pairis, S., Bourguignon, J., 2006. Localization and chemical forms of cadmium in plant samples by combining analytical electron microscopy and X-ray spectromicroscopy. Spectrochimi. Acta, Part B 61, 1242-1252.

Jacobson, A.R., Dousset, S., Guichard, N., Baveye, P., Andreux, F., 2005. Diuron mobility through vineyard soils contaminated with copper. Environ Pollut. 138(2), 250-259.

Janik, E., Maksymiec, W., Mazur, R., Garstka, M., Gruszecki, W.I., 2010. Structural and functional modifications of the major light-harvesting complex II in cadmium or copper-treated *Secale cereale.* Plant and Cell Physiol. 51, 1330–1340.

Jiang, R.F., Ma, D.Y., Zhao, F.J., McGrath, S.P., 2005. Cadmium hyperaccumulation protects *Thlaspi caerulescens* from feeding damage by thrips (*Frankliniella occidentalis*). New Phytol. 167, 805-814.

Kabata-Pendias, A., Pendias, H., 1984. Trace elements in Soils and Plants, Boca Raton, CRC Press, Florida.

Kamaya, Y., Takada, T., Suzuki, K., 2004. Effect of medium phosphate levels on the sensitivity of *Selenastrum capricornutum* to chemicals. Bull. Environ. Contam. Toxicol. 73, 995-1000.

Keskinkan, O., Goksu, M.Z.L., Basibuyuk, M. and Forster, C.F. 2004. Heavy metal adsorption properties of a submerged aquatic plant (*Ceratophyllum demersum)*. Bioresource Technol. 92, 197-200.

Kholodova, V.P., Ivanova, E.M., Kuznetsov, V.V., 2011. Initial steps of copper detoxification: outside and inside of the plant cell In: Sherameti, I. Varma, A. (Eds.) Detoxification of Heavy Metals. Springer-Verlag, Berlin, pp. 143-167.

Kim, S.A., Punshon, T. Lanzirotti, A., Li, L., Alonso, J.M., Ecker, J.R., Kaplan, J., Guerinot, M.L., 2006. Localization of iron in *Arabidopsis* seed requires the vacuolar membrane transporter VIT1. Science 314, 1295-1298.

Komárek, M., Balík, J., Chrastný, V., Száková, J., 2009. Distribution and fractionation of copper in contaminated hop field soils. Fres. Environ. Bul. 18, 1319-1323

Komárek, M., Cadková, E., Chrastný, V., Bordas, F., Bollinger, J.C., 2010. Contamination of vineyard soils with fungicides: a review of environmental and toxicological aspects. Environ Int. 36, 138-151.

Kowalewska, G., Falkowski, L., Hoffmann, S.K., Szczepaniak, L.S., 1987. Replacement of magnesium by copper II in the chlorophyll porphyrin ring of planktonic algae. Acta Physiol. Plant 9, 43-52.

Kowalewska, G., Hoffmann, S.K., 1989. Identification of the copper porphyrin complex formed in cultures of blue-green alga *Anabeana variabilis*. Acta Physiol. Plant 11, 39-50.

Kowalewska, G., Lotocka, M., Latala, A., 1992. Formation of the copper-chlorophyll complexes in cells of phytoplankton from the Baltic Sea. Pol. Arch. Hydrobiol. 39, 41-49.

Kühlbrandt, W., Wang, D.N., Fujiyoshi, Y., 1994. Atomic model of plant lightharvesting complex by electron crystallography. Nature 367, 614–21.

Kumar, G.P., Prasad, M.N.V., 2004. Cadmium toxicity to *Ceratophyllum demersum* L.: Morphological symptoms, membrane damage, and ion leakage. Bull. Environ. Contam. Toxicol. 72, 1038-1045.

Kuper J., Llamas A., Hecht H.J., Mendel R.R., Schwarz G. 2004. Structure of the molybdopterin-bound Cnx1G domain links molybdenum and copper metabolism. Nature. 430, 803-806.

Küpper, H., Küpper, F., Spiller, M., 1996. Environmental relevance of heavy metal substituted chlorophylls using the example of submersed water plants. J. Exp. Bot. 47, 259-266.

Küpper, H., Küpper, F.C., Spiller, M., 1998. In situ detection of heavy metal substituted chlorophylls in water plants. Photosynth. Res. 58, 123-133.

Küpper, H., Setlik, I., Trtilek, M., Nedbal, L., 2000a. A microscope for two-dimensional measurements of in vivo chlorophyll fluorescence kinetics using pulsed

measuring light, continuous actinic light and saturating flashes. Photosynthetica 38, 553-570.

Küpper, H., Spiller, M., Küpper, F.C., 2000b. Photometric method for the quantification of chlorophylls and their derivatives in complex mixtures: Fitting with Gauss-peak spectra. Anal. Biochem. 286, 247-256.

Küpper, H., Lombi, E., Zhao, F.J., Wieshammer, G., McGrath, S.P., 2001. Cellular compartmentation of nickel in the hyperaccumulators *Alyssum lesbiacum, Alyssum bertolonii* and *Thlaspi goesingense*. J. Exp. Bot. 52, 2291-2300.

Küpper, H., Dedic, R., Svoboda, A., Hala, J., Kroneck, P.M.H., 2002. Kinetics and efficiency of excitation energy transfer from chlorophylls, their heavy metal-substituted derivatives, and pheophytins to singlet oxygen. Biochim. Biophys. Acta 1572, 107-113.

Küpper, H., Šetlík, I., Spiller, M., Küpper, F.C., Prášil, O., 2002. Heavy metal-induced inhibition of photosynthesis: targets of in vivo heavy metal chlorophyll formation. J. Phycol. 38, 429-441.

Küpper, H., Kroneck, P.M.H**.,** 2005. Heavy metal uptake by plants and cyanobacteria, In: Sigel, A., Sigel, H., Sigel, R.K.O. (Eds.), Metal Ions in Biological Systems, Marcel Dekker, New York, pp. 97-142.

Küpper, H., Küpper, F.C., Spiller, M., 2006. [Heavy metal]-chlorophylls formed in vivo during heavy metal stress and degradation products formed during digestion, extraction and storage of plant material. Eur. J. Phycol. 41, 395-403.

Küpper, H., Aravind, P., Leitenmaier, B., Trtílek, M., Šetlík, I., 2007a. Cadmium-induced inhibition of photosynthesis and long-term acclimation to Cd-stress in the Cd hyperaccumulator *Thlaspi caerulescens*. New Phytol. 175**,** 655-674.

Küpper, H., Seibert, S., Aravind, P., 2007b. A fast, sensitive and inexpensive alternative to analytical pigment HPLC: quantification of chlorophylls and carotenoids in crude extracts by fitting with Gauss-Peak-Spectra. Anal. Chem**.** 79, 7611-7627.

Küpper, H., Šetlík, I., Seibert, S., Prášil, O., Šetlikova, E., Strittmatter, M., Levitan, O., Lohscheider, J., Adamska, I., Berman-Frank, I., 2008. Iron limitation in the marine cyanobacterium *Trichodesmium* reveals new insights into regulation of photosynthesis and nitrogen fixation. New Phytol. 179, 784-798.

Küpper, H., Kochian, L.V., 2010. Transcriptional regulation of metal transport genes and mineral nutrition during acclimation to cadmium and zinc in the Cd/Zn

hyperaccumulator *Thlaspi caerulescens* (Ganges population). New Phytol. 185, 114-129.

Küpper, H., Leitenmaier, B., 2013. Cadmium-accumulating plants, in Sigel, A., Sigel, H., Sigel, R.K.O. (Eds.), Cadmium: From Toxicity to Essentiality. Springer Science + Business Media B.V., Dordrecht, pp. 12. 373-393.

Küpper, H., Lombi, E., Zhao, F.J., McGrath, S.P., 2000. Cellular compartmentation of cadmium and zinc in relation to other elements in the hyperaccumulator *Arabidopsis halleri*, Planta, , 212, 75-84.

Küpper, H., Lombi, E., Zhao, F.J., Wieshammer,G., McGrath, S.P., 2001. Cellular compartmentation of nickel in the hyperaccumulator *Alyssum lesbiacum, Alyssum bertolonii* and *Thlaspi goesingense*. J. Exp. Bot. 52, 2991-2300.

Küpper, H., Mijovilovich, A., Götz, B., Küpper, F.C., Wolfram, M.W., 2009. Complexation and toxicity of copper in higher plants (I): Characterisation of copper accumulation, speciation and toxicity in *Crassula helmsii* as a new copper hyperaccumulator. Plant physiol. 151, 702-714.

Küpper, H., Parameswaran, A., Leitenmaier, B., Trtilek, M.Setlik, I., 2007. Cadmium-induced inhibition of photosynthesis and long-term acclimation to cadmium stress in the hyperaccumulator *Thlaspi caerulescens*. New Phytol. 175, 655-674.

Küpper, H., Zhao, F.J., McGrath, S.P., 1999. Cellular compartmentation of zinc in leaves of the hyperaccumulator *Thlaspi caerulescens*. Plant Physiol. 119, 305-311.

Lagriffoul, A., Mocquot, B., Mench, M., Vangronsveld, J., 1998. Cadmium toxicity effects on growth, mineral and chlorophyll contents, and activities of stress related enzymes in young maize plants (*Zea mays* L.). Plant Soil 200, 241-250.

Lane, T.W., Morel, F.M.M., 2000. A biological function for cadmium in marine diatoms. Proc. Natl. Acad. Sci. U.S.A. 97, 4627-4631.

Li, T., Xiong, Z., 2004. A novel response of wild-type duckweed (*Lemna paucicostata* Hegelm.) to heavy metals. Environ. Toxicol. 19, 95-102.

Li, W., Zhang, M., Shu H., 2005. Distribution and fractionation of copper in soils of apple orchards. Environ Sci Pollut Res Int. 12(3), 168-172.

Lidon, F.C., Henriques, F.S., 1991. Limiting step in photosynthesis of rice plants treated with varying copper levels. Plant Physiol. 138, 115-118.

Lipman, C.B., McKinney, G., 1931. Proof of the essential nature of copper for higher green plants. Plant Physiol. 6, 593-599.

Lippert, A.R., Van de Bittner, G.C., Chang, C.J., 2011. Boronate oxidation as a bioorthogonal reaction approach for studying the chemistry of hydrogen peroxide in living systems. Acc. Chem. Res. 44, 793-804.

Liu, M.-Q., Yanai, J., Jiang, R.-F., Zhang, F., McGrath, S.P., Zhao, F.-J., 2008. Does cadmium play a physiological role in the hyperaccumulator *Thlaspi caerulescens*? Chemosphere. 71, 1276-1283.

Loland, J.O., Singh, B.R., Copper contamination of soil and vegetation in coffee orchards after long-term use of Cu fungicides. Nut. Cycl. Agroeco. 69 (3), 203-211.

Loneragan, J.F., Delhaize, E., Webb, J., 1982 Enzymic diagnosis of copper deficiency in subterranean clover. I. Relationship of ascorbate oxidase activity in leaves to plant copper status. *Aust J Agric Res* 33: 967-979

Lonergan JF., Delhaize E., Webb J. 1985. Development of three copper metalloenzymes in clover leaves. *Plant Physiology* 78, 4-7.

Luciński, R., Jackowski, G., 2006. The structure, functions and degradation of pigment-binding proteins of photosystem II. *Acta Biochim. Pol.* 53:693-708.

Lumsden, B.R., Florence, T.M., 1983. A new algal assay procedure for the determination of the toxicity of copper species in seawater. Envirno. Technol. Lett. 4, 271-276.

Luna, C.M., González, C.A., Trippi, V.S., 1994. Oxidative damage caused by excess of copper in oat leaves. Plant Cell Physiol. 35, 11-15.

Mantovi, P., Bonazzi, G., Maestri, E., Marmiroli, N., 2003. Accumulation of copper and zinc from liquid manure in agricultural soils and crop plants. Plant Soil 250, 249-257.

Markich, S., King, A., Wilson, S., 2006. Non-effect of water hardness on the accumulation and toxicity of copper in a freshwater macrophyte (*Ceratophyllum demersum*): How useful are hardness-modified copper guidelines for protecting freshwater biota? Chemosphere. 65, 1791-1800.

Marschner, H., 1995. Mineral Nutrition of Higher Plants. Academic Press, London.

Mattar, S., Scharf, B., Kent, S.B.H., Rodewald, K., Oesterhelt, D., Engelhard, M:, 1994. The primary structure of halocyanin, an archaeal blue copper protein, predicts a lipid anchor for membrane fixation. J Biolg Chem. 269(21), 14939–14945.

Maxwell, K., Johnson, G.N., 2000. Chlorophyll fluorescence- a practical guide. J. Exp. Bot 51**,** 659-668.

Martens, S.N., Boyd, R.S., 1994. The ecological significance of nickel hyperaccumulation: a plant chemical defense. Oecologia. 98, 379-384.

McGeer, J.C., Brix, K.V., Skeaff, J.M., DeForest, D.K., Brigham, S.I., Adams, W.J., Green, A., 2003. Inverse relationship between bioconcentration factor and exposure concentration for metals: Implications for hazard assessment of metals in the aquatic environment. Environ. Toxicol. Chem. 22, 1017-1037

McKenna, I.M. Chaney, R.L., Williams, F.M., 1993. The effects of cadmium and zinc interactions on the accumulation and tissue distribution of zinc and cadmium in lettuce and spinach. Environ. Pollut. 79, 113-120.

McLaughlin, M.J., Parker, D.R., Clarke, J.M., 1999. Metals and micronutrients – food safety issues. Field Crops Research 60, 143-163.

Mediouni, C., Houlne, G., Chaboute, M.-E., Ghorbel, M.H., Jemal, F., 2008. Cadmium and copper genotoxicity in plants, In: Abdelly, C., Öztürk, M., Ashraf, M., Grignon, C. (Eds.), Biosaline agriculture and high salinity tolerance. Birkhäuser Verlag AG, Basel, pp. 325-333.

Milner, M.J., Kochian, L.V., 2008. Investigating heavy-metal hyperaccumulation using *Thlaspi caerulescens* as a model system. Ann. Bot. 102, 3-13.

Mishra S., Srivastava S., Tripathi RD., Trivedi PK. (2008). Thiol metabolism and antioxidant systems complement each other during arsenate detoxification in *Ceratophyllum demersum* L. Aqua. Toxicol. 86:205-215.

Mishra S., Tripathi RD., Srivastava S., Dwivedi S., Trivedi PK., Dhankher OP., Khare A. (2009) Thiol metabolism play significant role during cadmium detoxification by *Ceratophyllum demersum* L.Bioresource technology 100:2155-2161.

Moore, J.W., Ramamoorthy, S., 1984. Heavy metals in natural waters-Applied monitoring and impact assessment. Springer-Verlag, New York, pp. 268.

Nerissian, A.M., Immoos, C., Hill, M.G., Hart, P.J., Williams, G., Herrmann, R.G., Valentine, J.S., 1998.Uclacyanins, stellacyanins and plantacyanins are distinct subfamilies of phytocyanins: Plant-specific mononuclear blue copper proteins. Protein Science 7, 1915-1929.

Nixdorf, B., Hemm, M., Hoffmann, A., Richter, P., 2008 Dokumentation über Zustand und Entwicklung der wichtigsten Seen Deutschlands. Teil 8: Hessen, Thüringen und Sachsen. In: Abschlussbericht F&E Vorhaben FKZ 299 24 274 im Auftrag des Umweltbundesamtes. Germany.

Ornes, W.H., Sajwan, K.S., 1993. Cadmium accumulation and bioavailability in coontail (*Ceratophyllum demersum L.*) plants. Water, Air, Soil Pollut. 69, 291-300.

Ouzounidou, G., Eleftheriou, E.P., Karataglis, S., 1992. Ecophysiological and ultrastructural effects of copper in *Thlaspi ochroleucum* (Cruciferae). Can. J. Bot. 70, 947-957.

Paulsen, H., Finkenzeller, B., Kühlein, N., 1993. Pigments induce folding of light-harvesting chlorophyll a/b-binding protein. Eur. J. Biochem. 215, 809-816.

Palms, J.M., Yanez, J., Gomez, M., Del Rio, L.A., 1990. Copper-binding proteins and copper tolerance in *Pisum sativum L*. Plants 181, 487-495.

Perfus-Barbeoch, L., Leonhart, N., Vavasseur, A., Forestier, C., 2002. Heavy metal toxicity: cadmium permeates through calcium channels and disturbs the plant water status. Plant J. 32, 539-548.

Petri, M., 2006. Water quality of Lake Constance, In: Knepper, T.P. (Ed.), The Rhine. Springer Verlag, Berlin, pp. 127-138.

Piccini, D.F., Malavolta, E., 1992. Effect of nickel on two common bean cultivars. J. Plant Nutr. 15, 2343-3250.

Pilon, M., Abdel-Ghany, S.E., Cohu, C.M., Ye, H., 2006. Copper cofactor delivery in plant cells. Curr. Opin. Plant Biol. 9, 256-263.

Pinto, E., Teresa, C.S., Maria, A.S., Oswaldo, K.O., David, M., Colepicolo, P., 2003. Heavy metal induced oxidative stress in algae. J. Phycol. 6, 1008–1018.

Plette, A.C.C., Nederlof, M.M., Temminghoff, W.J.M., van Riemsdijk, W.H., 1999. Bioavailability of heavy metals in terrestrial and aquatic systems: A quantitative approach. Environ. Toxicol. Chem. 18, 1882-1890.

Puig, S., Andres-Colas, N., Garcia-Molina, A., 2007. Copper and iron homeostasis in *Arabidopsis*: responses to metal deficiencies, interactions and biotechnological applications. Plant Cell Envi. 30, 271-290.

Punshon,T. Guerinot, M. L., Lanzirotti, A., 2009. Using synchrotron X-ray fluorescence microprobes in the study of metal homeostasis in plants. Ann. Bot.,103, 665-672.

Quartacci, M.F., Pinzino, C., Sgherri, C.L.M., Dalla, V.F., 2000. Growth in excess copper induces changes in the lipid composition and fluidity of the PSII enriched membrane in wheat. Physiol. Plant. 108, 87-93.

Rao, K.V.M., Sresty, T.V.S., 2000. Antioxidative parameters in the seedlings of pigeonpea (*Cajanus cajan* L. Millspaugh) in response to Zn and Ni stresses. Plant Sci. 157, 113-128.

Rea, P.A., 2012, Phytochelatin synthase: of a protease a peptide polymerase made. Physiol. Plant. 145, 154-164.

Rebeiz, C.A., Belanger, F.C., 1984. Chloroplast Biogenesis 46: Calculation of Net Spectral Shifts Induced by Axial Ligand Coordination in Metalated Tetrapyrroles Spectrochim. Acta. 40A, 793-806.

Rubino, J.T., Franz, K.J., 2012. Coordination chemistry of copper proteins: How nature handles a toxic cargo for essential function. J. Inorg. Biochem. 107, 129-143.

Sadi, B.B.M., Vonderheide, A.P., Gong, J.-M., Schroeder, J.I., Shann, J.R., Caruso, J.A., 2008. An HPLC-ICP-MS technique for determination of cadmium-phytochelatins in genetically modified *Arabidopsis thaliana*. J. Chromatogr. B. Analt. Technol. Biomed. Life Sci., 861, 123-129.

Salam, Z.A., 2001. Diagnosis of copper deficiency through growth, Nutrient uptake and some biochemical reactions in P*isum sativum L. Pak. J. Boil. Sciences.* 4(11): 1299-1302.

Sandalio, L.M., Dalurzo, H.C., Gomez, M., Romero-Puertas, M.C., Del Rio, L.A., 2001. Cadmium-induced changes in the growth and oxidative metabolism of pea plants. J. Exp. Bot. 52, 2115-2126.

Sadmann, G., Böger P., 1980. Copper-mediated lipid peroxidation processes in photosynthetic membranes. Plant Physiol. 66, 797-800.

Schachtman, D.P., Reid, R.J., Ayling, S.M., 1998. Phosphorus uptake by plants: From soil to cell. Plant Physiol. 116, 447-453.

Schlekat, C.E., Van Genderen, E., De Schamphelaere, K.A.C., Antunes, P.M.C., Rogevich, E.C., Stubblefield, W.A., 2010. Cross-species extrapolation of chronic nickel Biotic Ligand Models. Sci. Total Environ. 408, 6148-6157.

Schramel O, Michalke B, Kettrup A., 2000. Study of the copper distribution in contaminated soils of hop fields by single and sequential extraction procedures. Sci Total Environ. 263, 11-22.

Senesi, G.S., Baldassarre, G., Senesi, N., Radina, B., 1999. Trace element inputs into soils by anthropogenic activities and implications for human health. Chemosphere 39, 343-377.

Singh, A., Malodia, P., Kachhawaha, M., Ansari, N., Jain, S.K., Khatri, P.K., 2011. Effect of EDTA, phosphate, pH and metal species on cadmium and nickel uptake by aquatic macrophyte *Spirodela Polyrhiza*. Asian J. Water, Environ. Pollut. 8, 51-60.

Skjelkvåle, B.L., Andersen, T., Fjeld, E., Mannio, J., Wilander, A., Johansson, K., Jensen, J.P., Moiseenko, T., 2001. Heavy metal surveys in nordic lakes; concentration, geographic patterns and relation to critical limits. Ambio. 30, 2-10.

Solé, V.A., Papillon, E., Cotte, M., Walter, P., Susini, J**.,** 2007. A multiplatform code for the analysis of energy-dispersive X-ray fluorescence spectra. Spectrochim. Acta B. 62, 63-68.

Solomon, E.I., Baldwin, M.J., Lowery, M.D., 1992. Electronic structures of active sites in copper proteins: contributions to reactivity. Chem Rev. 92, 521–542.

Solomon, E.I., Sundaram, U.M., Machonkin, T.E., 1996. Multicopper oxidases and oxygenases. Chem Rev. 96, 2563–2605.

Sommer, A.L., 1931. Copper as an essential element for plant growth. Plant Physiol. 6, 339-345.

Srivastave, A., Telor, E., 1991. Effect of some environmental pollutants on the superoxide-dismutase activity in *Lemna*. Free Radic. Res. Comm. 12-13, 601-607.

Srivastava S., Mishra S., Tripathi R.D., Dwivedi S., Gupta D.K., 2006 Copper-induced oxidative stress and responses of antioxidants and phytochelatins in *Hydrilla verticillata* (L.f.) Royle. Aquat. Toxicol. 80, 405-415.

Stankovic, Z., Pajevic, S. and Vuckovic, M., 2000. Concentrations of trace metals in dominant aquatic plants of the Lake Provala (Vojvodina, Yugoslavia). Biologia Plantarum (Prague). 43 (4), 583-585.

Stevenson, F.J., 1986. Cycles of soil- Carbon. nitrogen, phosphorous sulphur, micronutrients. John Wiley & Sons, New York, pp. 380

Tarvainen, T., Lahermo, P., Mannio, J., 1997. Sources of trace metals in streams and headwater lakes in Finland. Water, Air Soil Pollut. 94, 1-32.

Thomas G, Stärk HJ, Wellenreuther G, Dickinson BC and Küpper H. (2013) Effects of nanomolar copper on water plants-Comparison of biochemical and biophysical mechanisms of deficiency and sublethal toxicity under environmentally relevant conditions. Aquat. Toxicol. 140-141, 27-36.

Tian, S., Lu., L., Labavitch, J.M., Yang, X., He, Z., Hu, H., Sarangi, R., Newville, M., Commisso, J., Brown, P., 2011. Cellular sequestration of cadmium in the hyperaccumulator plant species *Sedum alfredii*. Plant Physiol. 157, 1914-1925.

Tian, S., Lu, L., Yang, X.-E., Labavitch, J.M., Huang, Y.Y., Brown, P., 2009. Stem and leaf sequestration of zinc at the cellular level in the hyperaccumulator *Sedum alfredii*. New Phytol. 182, 116-126.

Tsay, C.C., Wang, L.W., Chen, Y.R., 1995. Plant response to Cu toxicity. Taiwana 40, 173-181.

Vallee, B.L., Wacker, W.E.C., 1970. Metal-protein interactions. In H Neurath, (ed.), The Proteins. Vol 5. Academic Press, New York, pp 25-60.

Van Camp, W., Capiau, K., Van Montagu, M., Inze, D., Slooten, L. 1996. Enhancement of oxidative stress tolerance in transgenic tobacco plants overproducing Fe-superoxide dismutase in chloroplasts. Plant Physiol. 112, 1703-1714.

Vatamaniuk, O.K., Bucher, E.A., Ward, J.T., Rea, P.A., 2001. A new pathway for heavy metal detoxification in animals. J. Biol. Chem. 276, 20817-20820.

Vaughan, D., DeKock, P.C., Ord, B.G., 1982. The nature and localisation of superoxide dismutase in fronds of *Lemna gibba L.* and the effect of copper and zinc defciency on its activity. Physiol. Plantar. 54, 253-257.

Vogel-Mikus, K., Regvar, M., Mesjasz-Przbylowicz, J., Pryzbylowicz, W.J., Simcic, J., Pelicon, P., Budnar, M., 2008. Spatial distribution of cadmium in leaves of metal hyperaccumulating *Thlaspi praecox* using micro-PIXE, New Phytol. 179, 712-721.

Wang, C., Wang, L.Y., Sun, Q., 2010. Response of phytochelatins and their relationship with cadmium toxicity in a floating macrophyte *Pistia stratiotes L*. at environmentally relevant concentrations. Water Environ. Res. 82, 147-154.

Welch, R.M., Norvell, W.A., Schaefer, S.C., Shaff J.E., Kochian, L.V., 1993. Induction of iron(III) and copper(II) reduction in pea (*Pisum sativum L*.) roots by Fe and Cu status: Does the root-cell plasmalemma Fe(III)-chelate reductase perform a general role in regulating cation uptake. Plant 190, 555-561.

Wetzel, R.G., 2001. Limnology: Lake and River Ecosystems, third ed. Academic Press, San Diego.

Wink, M., 1993. The plant vacuole: a multifunctional compartment, J. Exp. Bot., 44, 231-246.

Yamamoto, H.Y., Tatsuyama, K., Uchiwa, T., 1985. Fungal flora of soil polluted with copper. Soil Biol. Biochem. 17, 785-790.

Yamasaki, H., Pilon, M., Shikanai, T., 2008 How do plants respond to copper deficiency? Plant Signal. Behav. 4, 231-232.

Yruela, I., 2005. Copper in plants. Brazilian J. Plant Physiol. 17,145-146

Yruela, I., 2009. Copper in plants: acquisition, transport and interactions. Funct. Plant Biol. 36, 409-430.

Yu, Q., Osborne, L.D., Rengel, Z., 1998. Micronutrient deficiency changes activities of superoxide dismutase and ascorbate peroxidase in tobacco plants. J. Plant Nutrition. 21, 1427-1437.

Yu Q, Rengel Z. 1999.Micronutrient deficiency in plant growth and activities of superoxide dismutases in narrow-leafed lupins. Annals of Bot. 83, 175-182.

Zhang, G., Fukami, M., Sekimoto, H., 2002 Influence of cadmium on mineral concentrations and yield components in wheat genotypes differing in Cd tolerance at seedling stage. Field Crops Res. 77, 93-98.

Zhang, M., He, Z., Calvert, D.V., Stoffella, P.J., Yang, X**.,** 2003. Surface runoff losses of copper and zinc in sandy soils. J. Environ. Qual. 32, 909-915.

Zhang, J., Kirkham, M.B., 1994. Drought-stress-induced changes in activities of superoxide dismutase, catalase, and peroxidase in wheat species. Plant. Cell Physiol. 35, 785-791.

Zhao, F., McGrath, S.P., Crosland, A.R., 1994. Comparison of three wet digestion methods for the determination of plant sulphur by inductively coupled plasma atomic emission spectrometry (ICP-AES). Commun. Soil Sci. Plant Anal. 25, 407-418.

5. Appendix

5.1 Author contributions (Eigenabgrenzung)

George Thomas has written this text using only the resources mentioned in the text and the references section (4). The contribution of the author to the specific chapters has been mentioned below.

Chapter 2.1. Effects of nanomolar copper on water plants - comparison of biochemical and biophysical mechanisms of deficiency and sublethal toxicity under environmentally relevant conditions

The experiments were planned together with Hendrik Küpper. The plants were taken from the stock cultures which were maintained by me and other lab members and later cultivated in the experiment aquaria by GT. All the methods and data analysis of the experiment were performed by GT, except for the metal analysis via ICPMS that was done by Hans-Joachim Stärk, and the µXRF measurements where most of the data analysis was done by Gerd Wellenreuther. The first version of the manuscript was written by GT and revised by all others.

Chapter 2.2. Effects of nanomolar copper on water plants in low irradiance – a metalloproteomic and physiological study

The experiment was planned together with HK. The plants were taken from the stock cultures which were maintained by me and other lab members, and later cultivated in the experiment aquaria by GT. The preparation of samples for metalloproteomics was done with Elisa Andresen following a protocol from HK, the size exclusion chromatography coupled to ICP-MS and UV-Vis spectroscopy was performed by Jürgen Mattusch. The other methods and data analyses were performed by GT partly assisted by Stefan Strungaru. The first version of the manuscript was written by GT, revision was done by HK.

Chapter 2.3. Different strategies of cadmium detoxification in the submerged macrophyte Ceratophyllum demersum L.

The experiments were planned mostly by EA together with HK. The plants were taken from the stock cultures which were maintained by myself and other lab members, and later cultivated in the experiment aquaria by EA and GT for the Cd treatment and Cu treatments. The extractions of the PCs were performed by EA for the Cd experiments and by GT for the

Cu experiments. Measurements of the PCs and the standards were done by JM and Uriel Arroyo-Abad. Analyses of the obtained date were done by JM, UAA and EA. The µXRF samples were prepared by HK and EA, who also measured them together with GW. The µXRF data analysis was performed by GW with input from EA and HK. The first version of the manuscript was written by EA, revisions were done mostly by HK. The Cu section in the manuscript was written by GT and further revised by others.

Chapter 2.4. Effects of Cd & Ni toxicity to Ceratophyllum demersum under environmentally relevant conditions in soft & hard water including a German lake.

The project was initiated by Kerstin Jenemann. The experiments were planned by HK, EA and GT. The lake samples were collected with help of KJ, Holger Dienemann and Michael Oberländer. The first two replicates of the experiment were performed by GT followed by EA (3 replicates) and Judith Opitz (2 replicates). The plants were taken from the stock cultures which were maintained by HK and lab members and later cultivated by JO, EA and GT for the experiment. All the methods and data analysis of the experiment were performed by JO, EA and GT except the metal analysis using the ICPMS by HJS. The first version of the manuscript was written by EA, revisions were done by all authors.

5.2 Acknowledgements

I owe my sincere gratitude to Prof. Dr. Hendrik Küpper who had been my guide and support for the work at the University of Konstanz. I am greatly obliged to him for his constant support and help, right from his invitation to Germany via IAESTE (DAAD) and my gratitude to him will still have miles to go. Apart from guiding me in my thesis he made sure that I did have a good publication record. Keeping my financial situation in safe hands, he always made sure that I am constantly updated with the latest in research through conferences in different parts of the world.

I need to mention the warmth and the comfortable atmosphere in the group which my lab members maintain. Dr. Barbara Leitenmaier who helped me cross the hard times of my work during my initial years in the lab and filling me with motivation throughout my thesis period. My friend and co-worker Elisa never compromised on calming me down with her time and mental support each time I needed them the most. Dr. Mishra was a big support for me to clear my scientific basics and for regular motivation at each step of my PhD.

I would thankfully remember Prof. Dr. Peter Kroneck for his critical comments and remarks for my work. Never could I stop learning from his experience in academics and non academics which are much beyond textbooks or lectures.

I also remember my co-supervisor Prof. Dr. Eva Freisinger, who always welcomed me with open hands for discussion even in the midst of her priorities and schedules. I donot forget our collaborators in Leipzig, Dr. Jürgen Mattusch and Dr. Hans-Joachim Stärk who stood by us at all times focused on the success of the project. I remember Gerd Wellenreuther who was involved in the µXRF measurements at the Desy in Hamburg where he arranged beam time and helped me with the data recordings and analysis even in the middle of the nights.

My motivation would have dried out without my dear friend Anns and all my near and dear ones, who always made sure that I never lost focus. I remember my family in India with my parents and my sister, who were always with a bunch of support at all times. Last but not the least I thank my almighty God for his grace and blessings without which this thesis wouldn‘t have been a reality.